# Antiproliferative Effect of the Chinese Medicinal Herb, *Centipeda Minima*

SU, Miaoxian

A Thesis Submitted in Partial Fulfilment of

the Requirements for the

Degree of Doctor of Philosophy

in

Biology

**The Chinese University of Hong Kong**

**August 2009**





ProQuest LLC.
789 East Eisenhower Parkway
P.O. Box 1346
Ann Arbor, MI 48106 - 1346

## Thesis Committees:

| | |
|---|---|
| Prof. Hau Yin CHUNG | Supervisor |
| Prof. Peter Chi Keung CHEUNG | Committee Member |
| Prof. Yum Shing WONG | Committee Member |
| Prof. David K.Y. LEI | External Examiner |

## Declaration of Originality

The work contained in this thesis is the original research performed by the author at the Department of Biology, The Chinese University of Hong Kong. No part of the work described in this thesis has already been or is being currently submitted for any such degree, diploma or other qualification.

## Acknowledgements

During the past three years of my graduate study, many people, too many to mention have help and support me to go to the end.

Firstly, I would like to express my sincere gratitude to my supervisor, Prof. Hau Yin Chung, for his advice, support, understanding, and patience. Thank you for him to provide me the chance to entering the biology world. I would also like to thank the other members of my committee, Prof. Peter Chi Keung Cheung and Prof. Yum Shing Wong for their professional suggestion of my research project. Thank you for Prof. David K.Y. Lei for being my external examiner and for his thoughtful advice. Deeply appreciation goes out to Prof. Li Yaolan from Jinan University. I would not have considered a graduate career in biological research without whose motivation and encouragement. And also thanks for her sustained support and expert suggestion. A very special thanks also goes out to Prof. Vincent Eng Choon Ooi for his academic advice and kindly help.

Besides, I must also acknowledge to Ms. Sze Nee Lim, for her great technical support and assistant in the past three years. Acknowledgements also go out to Ms. Jessie Lee, Mr. Freddie Kwok and Mr. Wilson Lau for their kindly technical support.

I would also like to thank the labmates in Prof. Chung's lab and friends in the Biology department. They enriched my life in the graduate study.

Finally, I would like to express my deep appreciation to my parents for the support, encouragement and understanding they provided me through my entire life.

## Abstract

*Centipeda minima* (L.) A. Br. (Compositae), a Chinese medicinal herb, is used to treat nasopharyngeal carcinoma (NPC) in the Chinese folk. However, there is a paucity of information on its anticancer activities. In particular, both of its anti-NPC potential and the potent constituents remain elusive.

In this study, the *n*-hexane fraction of *C. minima* showed broad spectrum of inhibitory effects on five human cancer cell lines, including the breast carcinoma MCF7 cells, the prostate carcinoma PC-3 cells, the hepatocellular carcinoma Hep G2 cells, the nasopharyngeal cancer CNE cells and the acute promyelocytic leukemia HL-60 cells, with $IC_{50}$ values ranging from 6.1 to 47.3 μg/mL. Bioactivity-guided separation of the *n*-hexane fraction using the CNE cells as the cellular system led to the isolation of a sesquiterpene lactone, 2β-(isobutyryloxy)florilenalin (IF), which contained the bioactive α-methylene-γ-lactone ring. IF significantly induced CNE cell death with an $IC_{50}$ value of 3.1 μg/mL. Despite this potency, its effect on the normal Hs68 cells was much weaker, with an $IC_{50}$ value larger than 50 μg/mL. Its inhibitory effect on the CNE cells ascribed to apoptotic induction as evidenced by the cumulation of sub-G1 cell population, DNA fragmentation and nuclear condensation, caspase-3 activation and poly (ADP-ribose) polymerase (PARP) cleavage. Mechanistic study showed that both extrinsic and intrinsic apoptotic pathways were activated. In the extrinsic pathway, IF activated caspase-8, which further induced the activation of caspase-3 and caspase-7. In the intrinsic pathway, IF regulated the expressions of Bcl-2 family proteins, followed by depletion of mitochondrial membrane potential ($\Delta\Psi m$), the release of cytochrome *c* to cytosol, the activation of caspase-9 and other downstream caspases, and finally the induction of apoptosis.

Both volatile oils prepared by supercritical fluid extraction (SFE) and steam distillation (SD) were evaluated for their anti-NPC potential. Results showed that SFE oil was much stronger than that of SD oil. SFE oil significantly inhibited the

growth of CNE cells by dysfunctioning the mitochondria and activating caspases. Gas chromatography-mass spectrometry analysis revealed that the responsible principals in the SFE oil were likely homologues of sesquiterpene lactones.

Bioactivity-guided isolation of SFE oil led to the identification of another sesquiterpene lactone, 6-*O*-angeloylprenolin, containing the bioactive α, β-unsaturated cyclopentenone. MTT results showed that CNE cells were more susceptible to 6-*O*-angeloylenolin than the normal Hs68 cells. Besides, the inhibitory effect of 6-*O*-angeloylenolin on the CNE cells was slightly stronger than that of cisplatin, the positive control, albeit statistical insignificance.

Mechanistic investigation showed that 6-*O*-angeloylenolin caused cell cycle arrest at S and G2/M phases and induced apoptosis in CNE cells. For the cell cycle arrest, a sharp decrease was found in the expressions of cyclin D1, cyclin D3, cdc25c, and p-cdc25c, with concomitant decrease in CDK4, cyclin A, cyclin E, p-Rb(Ser780), $p21^{Waf1/Cip1}$, cdc2 and p-cdc2. For the induction of apoptosis, externalization of phosphatidylserine and depletion of $\Delta\Psi m$ prior to the detection of sub-G1 peak were found. Other apoptotic features including the presence of apoptotic bodies, the activation of caspase-3 activity and the cleavage of PARP were observed. Activation of caspase-8 and caspase-10 was detected. Besides, 6-*O*-angeloylenolin induced the release of cytochrome *c* and AIF to cytosol. The former formed apoptosome with caspase-9, further activated the downstream caspase-3 and caspase-7 and cleaved PARP, while the latter was translocated into the nucleus and caused large-scale DNA fragmentation. Failure of the pan-caspase inhibitor, z-VAD-fmk, to interrupt the apoptotic induction by 6-*O*-angeloylenolin suggested that caspase-independent pathway was involved. 6-*O*-Angeloylenolin was able to activate Akt, ERK and JNK pathways. But only with the addition of JNK inhibitor (SP600125), significant suppression of the 6-*O*-angeloylenolin-induced apoptosis was observed, suggesting the involvement of the JNK pathway in the apoptotic pathway. Taken together, this study provided a better mechanistic insight into the potential application of

6-*O*-angeloylenolin as a candidate for NPC treatment.

Overall, this study revealed that two sesquiterpene lactones, including IF and 6-*O*-angeloylenolin were found to be responsible for the potent anti-NPC effect of *C. minima*. This study reiterates the notion that Chinese medicinal herbs traditionally applied to cancer treatment may be good sources of anticancer drug discovery, and sesquiterpene lactone may be a group of noteworthy lead compounds displaying anti-NPC potential.

# 摘要

中草藥鵝不食草在民間用於治療鼻咽癌，但鮮有關於該草的抗癌活性報導。特別地，該草的抗鼻咽癌活性及其活性成分仍有待進一步闡述。

本課題的研究結果表明，從鵝不食草的乙醇提取物萃取得到的正己烷組分能顯著地抑制多種人類腫瘤細胞（包括：乳癌 MCF7 細胞，前列腺癌 PC-3 細胞，肝癌 Hep G2 細胞，鼻咽癌 CNE 細胞，白血病 HL-60 細胞）的增殖，其半數抑制濃度($IC_{50}$)為 6.1 至 47.3 μg/mL。採用 CNE 細胞作為研究模型，活性追蹤分離正己烷組分得到一個含有活性基團 α-亞甲基-γ-內酯環的倍半萜內酯 2β-(isobutyryloxy)florilenalin (IF)。IF 能夠高效，選擇性地抑制 CNE 細胞的增殖，其半數抑制濃度為 3.1 μg/mL。相反，IF 對正常 Hs68 細胞的作用則較弱，其半數抑制濃度大於 50 μg/mL。關於機制的研究表明，IF 通過觸發外源性和內源性的細胞凋亡通路從而抑制 CNE 細胞的生長。在外源性通路，IF 活化 caspase-8，進而活化下游的 caspase-3 和 caspase-7。在內源性通路，IF 通過調整 Bcl-2 家族蛋白的表達，誘導線粒體跨膜電位(ΔΨm)的消散及線粒體內細胞色素 C (cytochrome *c*)的釋放，進而活化 caspase-9 以及下游的 caspases，最終誘導凋亡。

本課題還研究了分別用超臨界萃取法(SFE)和水蒸氣蒸餾法(SD)提取的鵝不食草揮發油的抗鼻咽癌活性。研究結果表明，SFE 揮發油比 SD 揮發油更能有效地抑制 CNE 細胞的生長。機制研究發現，SFE 揮發油通過阻礙線粒體的功能和活化 caspases 進而誘導 CNE 細胞的凋亡。氣相-質譜聯用(GC-MS)分析揭示 SFE 揮發油的活性成分很可能是倍半萜內酯化合物。

活性追蹤分離 SFE 揮發油得到另一個含有活性基團 α, β-不飽和環戊烯酮的

倍半萜內酯，6-*O*-angeloylprenolin。6-*O*-angeloylprenolin 能夠選擇性地抑制 CNE 細胞的生長。此外，6-*O*-angeloylprenolin 的活性與陽性對照物順鉑(cisplatin)的活性相當。

機理研究表明，6-*O*-angeloylprenolin 通過下調多種細胞週期素(cyclins)及其相應的細胞週期蛋白依賴性激酶(CDKs)，並啟動 $p21^{Waf1/Cip1}$ 和 Rb 等腫瘤抑制因數從而誘導 CNE 細胞阻滯於 S 和 G2/M 期，繼而引發細胞凋亡。此外，6-*O*-angeloylprenolin 觸發磷脂醯絲氨酸外翻，$\Delta\Psi m$ 消散，伴隨凋亡體出現，caspase 活化以及 PARP 裂解。caspase-8 和 caspase-10 的活化提示外源性凋亡通路的啟動。另一方面，6-*O*-angeloylenolin 通過調整 Bcl-2 家族蛋白的表達，從而誘導 cytochrome *c* 及 AIF 的釋放，並最終導致 caspase 依賴性和非依賴性細胞凋亡的發生。Caspase 的廣泛抑制劑 z-VAD-fmk，不能夠阻止 6-*O*-angeloylprenolin 誘導的細胞凋亡，進一步提示 caspase 非依賴性細胞凋亡通路的啟動。上游機制的研究發現：6-*O*-angeloylenolin 啟動了促分裂素原活化蛋白酶(MAPKs)中的 JNK 和 ERK，並啟動了 Akt 信號通路。JNK 的特異性抑制劑 SP600125，能夠顯著地抑制 6-*O*-angeloylenolin 誘導的 CNE 細胞凋亡，提示 JNK 在 6-*O*-angeloylenolin 觸發的細胞凋亡中扮演重要角色。

本研究表明兩個倍半萜內酯化合物，即：IF 和 6-*O*-angeloylenolin，是鵝不食草中的主要活性成分。此外，本研究結果提示傳統用於治療癌症的中草藥具有很好的開發成為抗癌藥物的潛力；並且，倍半萜內酯化合物可能含有抗鼻咽癌的先導化合物。

# List of Abbreviations

| | |
|---|---|
| AIF | Apoptosis inducing factor |
| BrdU | 5-Bromo-2'-deoxyuridine |
| CDK | Cyclin-dependent kinase |
| DAPI | 4',6-Diamidino-2-phenylindole |
| EBV | Epstein-Barr virus |
| EI-MS | Electron ionization-mass spectrometry |
| ERK | Extracellular signal-regulated kinase |
| FBS | Fetal bovine serum |
| GC-MS | Gas chromatography-mass spectrometry |
| $IC_{50}$ | 50% Inhibition concentration value |
| IF | 2β-(Isobutyryloxy)-florilenalin |
| JC-1 | 5,5',6,6'-Tetrachloro-1,1',3,3'-tetraethylbenzimidazolcarbocyanine iodide |
| JNK | c-Jun N-terminal kinase |
| MAPK | Mitogen-activated protein kinase |
| MMP | Mitochondrial membrane potential ($\Delta\Psi m$) |
| MTT | 3-(4,5-Dmethylthiazol-2-yl)-2,5-diphenyl tetrazolium bromide) |
| nd | Not determined |
| NMR | Nuclear magnetic resonance |
| NPC | Nasopharyngeal carcinoma |
| PARP | Poly (ADP-Ribose) polymerase |
| PBS | Phosphate buffered saline |
| PI | Propidium iodide |
| PS | phosphatidylserine |
| PVDF | Polyvinylidene fluoride |
| Rb | Retinoblastoma protein |
| SAPK | Stress-activated protein kinase |
| SD | Steam distillation |

| | |
|---|---|
| SDS | Sodium dodecyl sulfate |
| SFE | Supercritical fluid extraction |
| SLs | Sesquiterpene lactones |
| TBST | Tris-buffered saline tween-20 |
| TLC | Thin layer chromatography |
| + | Positive result |
| − | Negative result |

# List of Figures

# List of Tables

# Table of Contents

# Chapter 1: Introduction

## 1.1 Cancer

Cancer, an unusual growth of cells resulted from multiple changes in gene expression leading to dysregulated balance of cell proliferation and cell death, is regarded as a complex family of diseases (Ruddon, 2007). Generally, there are three steps involved in cancer development. The first step is initiation involving a mutation of DNA which does not undergo DNA repair. The second one is promotion, in which mutated cells are promoted to uncontrolled growth and proliferation. The last one is metastasis, in which cancerous cells invade the nearby tissues and migrate to other tissues via circulatory or transport systems. Cancer is proposed to be characterized by six essential alterations in cell physiology (Hanahan and Weinberg, 2000), namely, self-sufficiency in growth signals, insensitivity to growth-inhibitory signals, evasion of apoptosis, limitless replicative potential, sustained angiogenesis, and tissue invasion and metastasis.

According to the World Health Organization (WHO), a number of common risk factors including unhealthy lifestyle, exposure to occupational or environmental carcinogens, radiation, and some virus infections have been involved in cancer development. Although cancer may occur at any age, it is usually considered as a disease of aging (Ruddon, 2007). With increasing life expectancy of the world population nowadays, the worldwide cancer incidence is inevitably augmented. It is estimated that the total number of deaths caused by cancer will rise from 6 million in the year 2000 to over 16 million in the year 2050 (Schwartsmann et al., 2002). Cancer thus still remains a major challenge worldwide.

Currently, there are three conventional cancer therapeutic strategies including surgery, radiotherapy and chemotherapy. The adoption of strategy varies by geographic area, tumor type, as well as tumor stage. Actually, chemotherapy is the most rapidly developing field in cancer treatment due to it is essential both as a treatment in its own and as an adjuvant to localized treatment (Atkinson et al., 2008).

However, side effects such as nausea, anemia, weakening of the immune system, diarrhea, vomiting and hair loss, and the development of resistance are often encountered in the classical chemotherapeutic drugs (Verweij and de Jonge, 2000).

## 1.2 Apoptosis

Apoptosis, a highly conserved evolutionary program, is the intrinsic death motion of cells involved in regulating many physiological and pathological processes (Fulda, 2009). Defects in the physiological pathways for apoptosis have a role in many diseases including cancer (Reed, 2002). In fact, evasion of apoptosis is one of the characteristics of cancer.

Morphologically, apoptosis is characterized by chromatin condensation, nuclear fragmentation, cell shrinkage and plasma membrane 'blebbing' (Reed, 2002). A family of proteases known as "caspases" is responsible for such morphological changes. Basically, there are two apoptotic pathways involved in the activation of caspases, namely the extrinsic pathway and intrinsic pathway (Fulda, 2009). The extrinsic pathway operates through the ligation of cell-surface death receptors to activate the activator caspases, such as caspase-8 and caspase-10, which then cleave and activate the downstream effector caspases, such as caspase-3 and caspase-7. The intrinsic pathway is tightly controlled by the Bcl-2 family proteins which regulate the mitochondrial membrane integrity. Disruption of mitochondrial membrane releases the mitochondrial proteins such as cytochrome *c*, which then forms the apoptosome by recruiting Apaf-1, and caspase-9, thereby initiating the apoptotic caspase cascade (Wang, 2001). Besides, there would be a crosstalk between the extrinsic and intrinsic pathways through the truncation of Bid by caspase-8. In this case, caspase-8 triggers the proteolytic processing of Bid, a unique BH3-only proapoptotic protein, into truncated forms of tBid, which further translocates to mitochondria and induces the intrinsic pathway. Bid thus bridges the extrinsic and intrinsic pathways to amplify the execution signal and exacerbate the pace of cell demise (Yi et al., 2003).

More recently, caspase-independent apoptotic pathway has been proposed. In

addition to cytochrome *c*, mitochondria also release several other proteins, including AIF, Endo G, as well as IAP antagonists SMAC/Diablo and OMI/HtrA2 (Reed, 2003). Notably, AIF has been identified as the principal factor in the caspase-independent signaling pathway. After released to cytosol, AIF translocates to the nucleus, where it affects a long-range disruption of nuclear chromatin but not oligonucleosomal level DNA fragmentation (Cregan et al., 2004). Figure 1.1 showed a scheme of the apoptotic signaling pathways.

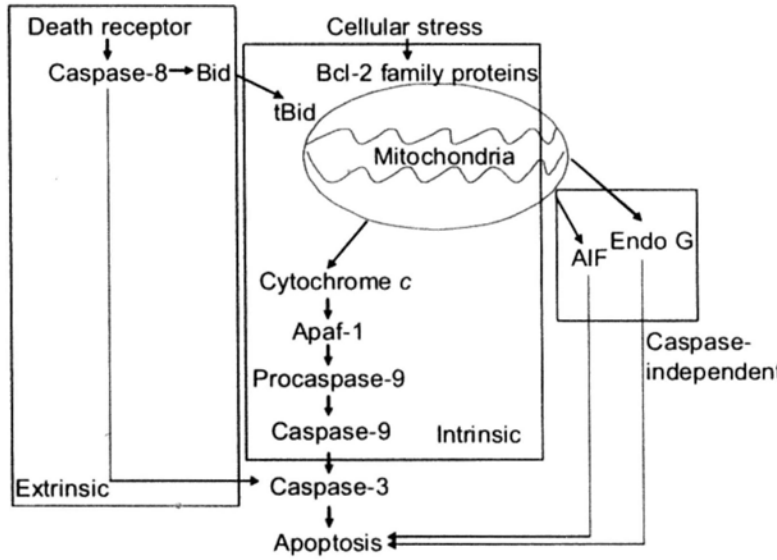


**Figure 1.1.** Apoptotic signaling pathways

## 1.3 Chinese medicinal herbs as sources of anticancer agents

Throughout human history, plants have been an indispensable source of natural products for medicine including cancer drugs. Due to the physiological functions by serving either as protective agents against various pathogens or growth regulatory molecules, secondary metabolites are potential anticancer drugs (Kintzios, 2004). Most of the new clinical applications of plant secondary metabolites and their derivatives over the last century have focused on combating cancer (Balunas and Kinghorn, 2005). Among them, taxol (paclitaxel), taxotere (docetaxel), vincristine, navelbine, etoposide, teniposide, topotecan and irinotecan are the most well-known plant-derived anticancer drugs approved by US FDA (Mukherjee et al., 2001). Figure 1.2 showed the chemical structures of these eight well-known anticancer drugs.

Chinese medicinal herbs have cumulated long-term folk experience due to their practices by the Chinese and other Asian people. More recently, Chinese medicinal herbs have received more attention as an alternative therapy worldwide. Some monographs of anticancer herbs summarized that more than four hundred Chinese medicinal herbs have anticancer property (Anonymous, 1986; Cheng and Li, 1998; Zhang, 2000) which may serve as leads for the discovery of novel anticancer agents.

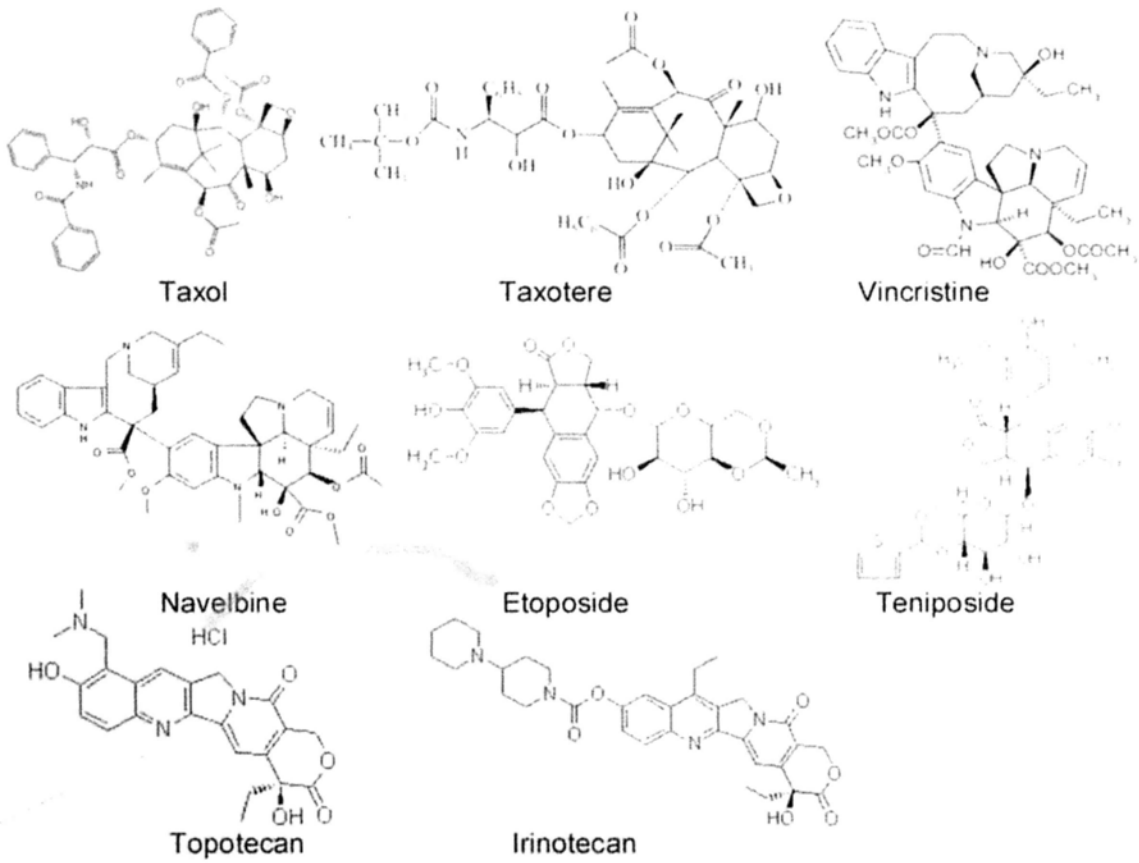


**Figure 1.2.** Chemical structures of the most well-known plant-derived anticancer drugs approved by US FDA

Campbell and coauthors (2002) screened a panel of 71 aqueous extracts used in traditional Chinese medicine against five breast cancer cell lines. Results showed that 21% of the extracts (15 of 71) showed significant growth inhibition on at least four of the five cell lines studied. Besides, six of seven studied herbs induced high molecular weight DNA fragmentation, an early marker of apoptosis. This team further chose 12 of the active herbs to evaluate their antiproliferative effects on a panel of human and murine cancer cell lines (Shoemaker et al., 2005). Their results showed that all

aqueous extracts exhibited growth inhibitory activity on some or all of the cancer cell lines, but only two showed activity against the normal mammary epithelial cells. These results indicated that many of the herbs used in traditional Chinese medicine for the treatment of cancer have significant growth inhibitory effects on cancer cells *in vitro*.

In another study, 24 Chinese medicinal herbs traditionally used as anticancer or anti-inflammatory drugs in clinics in China were screened for the anti-angiogenesis activity (Wang et al., 2004). Results indicated that the aqueous extracts of *Berberis paraspecta*, *Catharanthus roseus*, *Coptis chinensis*, *Taxus chinensis*, *Scutellaria barbata*, *Polygonum cuspidatum* and *Scrophularia ningpoensis* had strong anti-angiogenesis activity. Among the active herbs, *Catharanthus roseus* and *Taxus chinensis* were reported to contain anti-tumor compounds, vincristine and taxol, respectively, while *Polygonum cuspidatum* had resveratrol which was revealed as an inhibitor of angiogenesis.

Paoletta and coauthors (2008) conducted a random Forest screening of the phytochemical constituents of 240 herbs used in traditional Chinese medicine to identify potential inhibitors of the human aromatase enzyme (CYP19), which is produced to high levels particularly in those areas in and around tumor sites in breast tissue. Molecular modeling/docking studies indicated that three of the compounds, namely, myricetin, liquiritigenin and gossypetin, would likely form stable complexes with the enzyme. Subsequent experimental assay confirmed the virtual screening results and revealed that liquiritigenin showed about a 10-fold increase in potency over the first generation aromatase inhibitor, aminoglutethimide.

A number of investigations have been conducted to understand the underlying mode of actions by which Chinese medicinal herbs take the anticancer effects. Up till now, several mechanisms have been postulated such as induction of cell cycle arrest, induction of apoptosis, regulation of the immune system, reversion of multidrug resistance (MDR), induction of cell differentiation to normal cell and inhibition of angiogenesis (Liang and Zhong, 2006). Among the possible mechanisms, induction of apoptosis and cell cycle arrest has attracted the most interest.

The Chinese medicinal herbs could induce apoptosis through different pathways depending upon herbs and cell types involved. In most studies, caspase-dependent pathways including either intrinsic or extrinsic or both were found to be responsible for their actions. However, caspase-independent pathway was also found to play important role in some cases.

The cell cycle, which is sequentially divided into G0/G1, S, G2, and M phases, is a set of events responsible for cell duplication (Pucci et al., 2000). Either phase could be halted by regulating the expression of cyclins, cyclin-dependent protein kinases (CDKs) and/or CDK inhibitors and further led to the death of the cells. Chinese medicinal herbs could induce the arrest of either phase depending on herbs and cell types.

### 1.4 *Centipeda minima*

*Centipeda minima* (L.) A. Br. (Compositae) (鵝不食草) is an annual plant distributed in the high humidity geographic locations throughout China, Korea, Japan, India, Malaysia and Oceania (Shi and Fu, 1983). There are six *Centipeda* species found, but only *C. minima* grows in China (Shi and Fu, 1983). The whole plant which is harvested during its anthesis in both summer and autumn has pharmaceutical application in China (Lin and Shi, 2005). Based on the record in the Pharmacopoeia of China (Lin and Shi, 2005), the dried plant is used to treat nasal allergies, rhinitis and sinusitis, cough and headache. Some Chinese medicinal preparations clinically used in the treatment of nasal allergies, rhinitis and sinusitis contain *C. minima* as the major ingredient in China. In addition, it is used in the Chinese folk medicine to treat nasopharyngeal carcinoma (NPC) (Cheng and Li, 1998; Zhang, 2000).

#### 1.4.1 Chemical constituents of *C. minima*

Terpenoids including monoterpenoides, sesquiterpenoids and triterpenoids are the major chemical constituents of *C. minima*. It is reported that 12 sesquiterpenoids have been isolated from *C. minima* (Table 1.1 and Figure 1.3), all of which were

sesquiterpene lactones (SLs) of guaianolide- or pseudoguaianolide-type (Bohlmann and Chen, 1984; Wu et al., 1985; Iwakami et al., 1992; Taylor and Towers, 1998; Liang et al., 2007a). All the lactones contain a biological active functional group of SLs, such as α-methylene-γ-lactone ring (Compounds 1, 2, 7, 8, 9, and 10) or α, β-unsaturated cyclopentenone ring (Compounds 3, 4, 5, 6, 11, and 12). Besides, flavonoids, thymol derivatives, and other chemical classes have been isolated from this plant. To date, more than 40 compounds have been isolated from *C. minima*.

Additionally, Tan et al. (2006) analyzed the volatile components in *C. minima* from two sources by gas chromatography-mass spectrometry (GC-MS). The most abundant components were found to be myrtenol, *trans*-chrysanthemyl acetate, myrtenyl acetate, hexadecanoic acid and thymol.

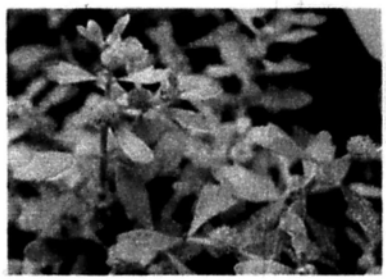

**Figure 1.3.** *Centipeda minima*

(Figure from http://www.nature.sdu.edu.cn/artemisia/pics/000870.jpg)

**Table 1.1.** Sesquiterpene lactones isolated from *Cenpeda minima*

| No. | Name | Reference |
|---|---|---|
| 1. | Arnicolide C | Bohlmann and Chen, 1984 |
| 2. | 6-*O*-angeloylprenolin | Bohlmann and Chen, 1984 |
| 3. | Helenalin | Bohlmann and Chen, 1984 |
| 4. | Florilenalin isoburate | Bohlmann and Chen, 1984 |
| 5. | Florilenalin isovalerate | Bohlmann and Chen, 1984 |
| 6. | Florilenalin angelate | Bohlmann and Chen, 1984 |
| 7 | 11,13-dihydrohelenalin | Wu et al., 1985 |
| 8. | Arnicolide B | Iwakami et al., 1992 |
| 9. | Microhelenin B | Iwakami et al., 1992 |
| 10. | Arnicolide D | Taylor and Towers, 1998 |
| 11 | 4,5β-dihydroxy-2β-(isobutyryloxy)-10βH-guai-11 (13)-en-12,8β-olide | Liang et al., 2007a |
| 12 | Pulchellin-2α-*O*-tiglate | Liang et al., 2007a |
| 13 | 4-hydroxy-1βH-guaia-9,11(13)-dien-12,8α-olide | Liang et al., 2007a |

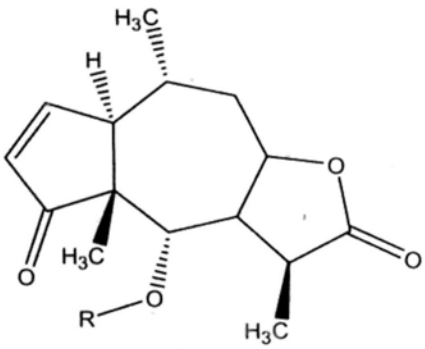

1: R=CO-CH(CH$_3$)$_2$
2: R=CO-C(CH$_3$)=CH-CH$_3$
7: R=CO-CH=C(CH$_3$)$_2$
8: R=CO-C(CH$_3$)$_3$
9: R=CO-CH(CH$_3$)-CH$_2$-CH$_3$
10: R=CO-C(CH$_3$)=CH$_2$

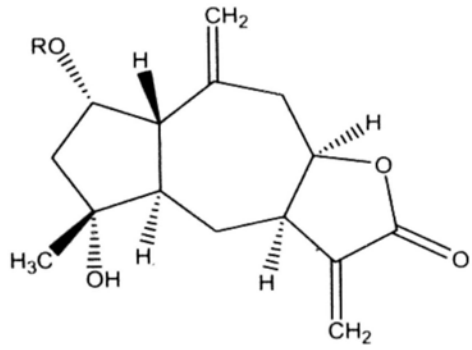

4: R=CO-CH(CH$_3$)$_2$
5: R=CO-CH(CH)(CH$_3$)$_2$
6: R=CO-C(CH$_3$)=CH-CH$_3$

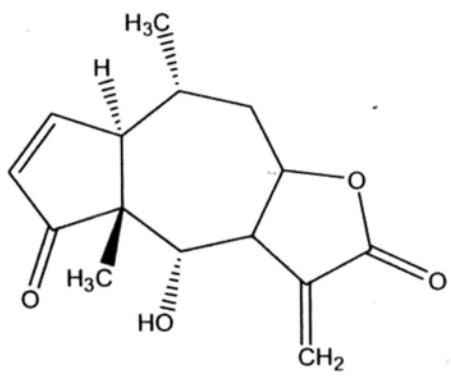

3

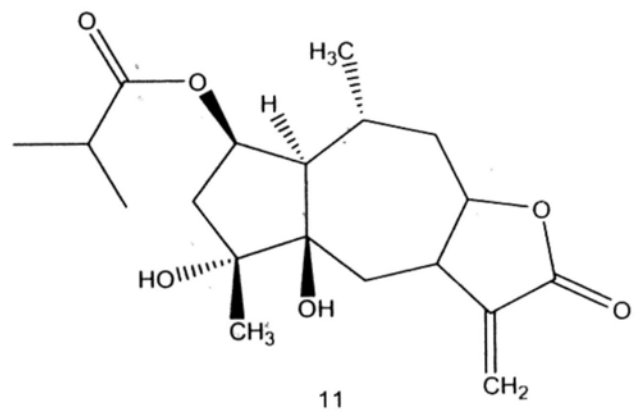

11

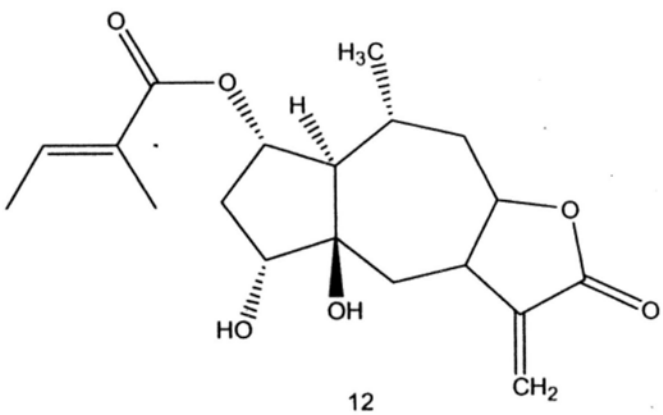

12

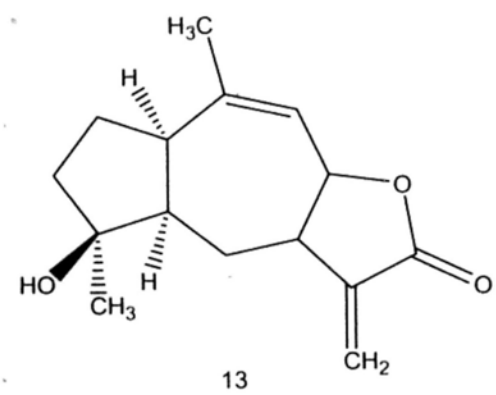

13

**Figure 1.4.** Chemical structures of sesquiterpene lactones isolated from *Centipeda minima*

### 1.4.2 Biological activity of *C. minima*

Recent pharmacological interest has focused on the anti-bacteria and anti-allergy effects of *C. minima*. However, other biological activities of the plant, such as anticancer and anti-inflammation, have drawn the attention of many researchers.

#### 1.4.2.1 Anti-bacterial and anti-protozoal activity

Li and coauthors (2003) reported that the decoction of the herb was able to eliminate R plasmids from *Pseudomonas aeruginosa*. The elimination rate of R plasmids in 24 h, 48 h and 72 h were 0.7%, 4.7% and 46.3%, respectively.

Three SLs, namely arnicolide C, D and 6-*O*-angeloylprenolin, isolated from this plant were found to have anti-bacteria effect on *Bacillus subtilis* (Taylor and Towers, 1998). The former two SLs showed similar activities with MIC (Minimum inhibitory concentration) values of 150 μg/mL. However, the latter showed a less effect with an MIC value of 300 μg/mL. Additionally, it was reported that 6-*O*-angeloylprenolin showed antigiardial activity with $IC_{50}$ value of 16.1 μM, and was similarly active against *Entamoeba histolytica* and *Plasmodium falciparum* with $IC_{50}$ value between 4.5 and 9 and 9.42 μM, respectively (Yu et al., 1994).

Liang and coauthors reported that two triterpenoids including taraxasterol acetate and taraxasterol, and some thymol derivatives isolated from the plant displayed potential anti-bacterial activities (Liang et al., 2007b and 2007c). It was found that taraxasterol acetate showed effect against *Salmonella typhimurium* and *Salmonella paratyphi*-A comparable to that of the positive control, e.g. cefradine and gentamycin. Taraxasterol could inhibit the growth of *Staphylococcus aureus*, *Escherichia coli* and *Salmonella typhimurium* with MIC values of 50 μg/mL (Liang et al., 2007b). Some thymol derivatives exerted anti-bacterial properties with MIC values as low as 6.25 μg/mL. 10-hydroxy-8,9-dioxyisopropylidene-thymol was found to be effective against *Bacillus subtilis*. 8,9,10-trihydroxythymol showed effect against *Salmonella typhimurium*, and 8-hydroxy-9,10-diisobutyryloxythymol had effect against *Staphylococcus aureus*, *Shigella flexneri*, and *Salmonella paratyphi*-B (Liang et al.,

2007c).

### 1.4.2.2 Anti-allergy activity

The ether, methanol and aqueous extracts of *C. minima* were found to have anti-allergy activity in passive cutaneous anaphylaxis (PCA) test (Wu et al., 1985). Three flavonoids including quercetin-3,3'-dimethyl ether, quercetin-3-methyl ether and apigenin, and two SLs including arnicolide C and 6-*O*-senecioylplenolin were isolated as inhibitors to induce histamine release from mast cells.

One of the most common traditional uses of this plant is to treat nasal allergies. An allergic rhinitis guinea pig model induced by ragweed pollen was established to investigate the mechanism of this traditional use (Yu et al., 2001; Liu et al., 2005). Results showed that there were a large number of lysosomes in the nasal epithelium with organelles vacuolated and nucleus deformed, and there was also infiltration of eosinophils and mast cells in the connective tissue in the positive control group. However, in the treatment group exposed to the volatile oil of *C. minima*, the pathological changes aforementioned were significantly reduced.

### 1.4.2.3 Anticancer activity

Lee and Lin (1988) adopted the *Salmonella*/microsomal system in the presence of picrolonic acid or benzo[a]pyrene to test the anti-mutagenic activities of extracts of 36 commonly used anticancer crude drugs from Chinese herbs. They reported that the hot water extract of *C. minima* had a moderate anti-mutagenic activity against benzo[a]pyrene.

Recently specific inhibitors of the FPTase (farnesyl protein tranferase) were suggested to develop effective anticancer agents. The methanolic extract of the aerial parts of the plant was found to show inhibitory effect on FPTase (Oh et al., 2006). Bioactivity-guided isolation led to the identification of 6-*O*-angeloylenolin which demonstrated a dose-dependent inhibition on FPTase.

Also, 6-*O*-angeloylenolin was found to inhibit the growth of the human leukemia HL-60 cells and the solid cancer growth in Lewis lung cancer xenograft models (Li et al., 2008). It is showed to induce apoptosis in HL-60 cells by inhibiting NF-κB activation, modulating Bcl-2 gene family expression and destructing mitochondrial

function.

#### 1.4.2.4 Anti-inflammatory activity

Qin and coauthors (2001 and 2005a) adopted carrageenan intrapleural injection induced rats model to study the anti-inflammatory effect of the volatile oil of the herb and its mode of action. Results showed that the volatile oil could significantly inhibit the acute inflammatory on mice by inhibiting the release of the PGE2 of the inflammatory tissue, the increase of NO, C-neactveprotein (CRP) and proinflammatory cytokines such as TNF-α.

The team (2005b) also reported that the volatile oil had a protective effect on acute lung injury in rats in the acute lung animal models. The oil was able to suppress lung edema and high numbers of neutrophils, decrease the expression of CD54 in the bronchial epithelium tissue.

#### 1.4.2.5 Inhibitory effect on platelet activating factor (PAF)

In the test of the inhibitory effect on platelet activating factor (PAF) binding to platelets, the aqueous extract of the plant showed significant effect (Iwakami et al., 1992). Active compounds were further found to be four SLs including 6-*O*-angeloylplenolin, 6-*O*-senecioylpenolin, microhelein B and arnicolide B, with $IC_{50}$ values ranging from 0.25 to 6.7 μM.

#### 1.4.2.6 Liver protective effect

Qian and coauthors (2004) reported that the decoction of the herb had significant hepatoprotective action. It significantly decreased the elevated serum ALT level in liver damage mice induced by $CCl_4$, APAP and D-GalN+LPS.

### 1.5 Objectives

Despite increasing efforts have been made to combat cancer, it is still the second killer only after cardiovascular disease in most countries (Ruddon, 2007). Chinese medicinal herbs have been serving as valuable sources to discover novel anticancer agents. Therefore, six Chinese medicinal herbs which were traditionally used in the treatment of cancer in China were selected for screening for their antiproliferative

effects against five different human cancer cell lines *in vitro*. Among the selected herbs, *Centipeda minima* was found to exert the most potent activity. Despite its potency to the cancer cells, there is a paucity of information of its anticancer properties of *C. minima*. Besides, the active constituent(s) responsible for its action remain elusive. Accordingly, the main objectives of this study are (1) to search for the active principal(s) in *C. minima*, (2) to purify and characterize the active principal(s) from the herb, and (3) to investigate their molecular mechanisms involved in their anticancer actions.

# Chapter 2: *In vitro* antiproliferative effects of selected Chinese medicinal herbs

## 2.1. Introduction

Cancer, an unusual growth of cells resulted from multiple changes in gene expression leading to dysregulated balance of cell proliferation and cell death, is regarded as a complex family of diseases (Ruddon, 2007). Although significant developments in detection, diagnosis and treatment of cancer have been achieved in the past decades, it still remains one of the major causes of morbidity and mortality worldwide (Varmus, 2006). Therefore, more efforts to prevent and cure cancer are needed.

Plants have been an important source in cancer drug discovery. In fact, most of the new clinical applications of plant secondary metabolites and their derivatives over the last century have focused on combating cancer (Balunas and Kinghorn, 2005). In particular, Chinese medicinal herbs are good sources of such secondary metabolites (Lee, 2004). Some monographs on anticancer herbs summarized more than four hundred Chinese medicinal herbs having anticancer property (Cheng and Li, 1998; Zhang, 2000; Bo et al., 2002), which may serve as leads for the discovery of novel anticancer agents.

In the course of our search for such novel agents, six medicinal herbs *Nervilia fordii* (Hance) Schltr., *Centipeda minima*, *Kaempferia galanga* L., *Lobelia chinensis* Lour., *Blumea laciniata* (Roxb.) DC. and *Elephantopus scaber* L., were chosen, based on their folk use to treat cancer in China (Table 2.1) (Anonymous, 1986; Cheng and Li, 1998; Zhang, 2000). In the present study, a rational screening scheme for antiproliferative effects of extracts and fractions prepared from the six aforementioned herbs on five human cancer cell lines *in vitro* was carried out.

## 2.2. Materials and methods

### 2.2.1. Plant materials

All the medicinal herbs were collected from Baiyun Mountain, Guangzhou, China,

and were authenticated by Mr Zhenqiu Mai, a senior herbalist at the Chinese Medicinal Material Company, Guangzhou, China. Voucher specimens were deposited at the Department of Biology, the Chinese University of Hong Kong with accession numbers from 06111201 to 06111206.

### 2.2.2. Cell lines and cell culture

MCF7 (human breast carcinoma cell), PC-3 (human prostate carcinoma cell), Hep G2 (human hepatocellular carcinoma cell), HL-60 (human acute promyelocytic leukemia cell), and Hs68 (human normal skin fibroblast cell) were obtained from the American Type Culture Collection (Rockville, MD). CNE (human nasopharyngeal carcinoma epithelial cell) was purchased from the Cell Bank Type Culture Collection of the Chinese Academy of Sciences (Shanghai, China). Cells were maintained in either EMEM, F12K, RPMI-1640 or DMEM media (Gibco, Rockville, MD), supplemented with 10% FBS and 1% penicillin-streptomycin. The medium for MCF7 cells contained 0.01 mg/mL bovine insulin. All cell cultures were incubated at 37°C in a 95% humidified atmosphere supplied with 5% $CO_2$.

### 2.2.3. Extraction and fractionation of the medicinal herbs

All medicinal herbs were pulverized with a Multi mill (Kenwood, UK). For aqueous extracts, dried herb (10 g) was decocted twice with 100 mL distilled water for 2 h, and filtered through a No. 2 filter paper (Whatman, England). The filtrate was then lyophilized. Similarly, for ethanolic extracts, dried herb (100 g) was immersed twice in 1000 mL 95% ethanol for 3 days. The supernatants were filtered, concentrated *in vacuo*, and lyophilized. Since the ethanolic extracts were found to be more active than their corresponding aqueous ones, they were subjected to further investigation. Briefly, the ethanolic extract (1 g) was suspended in distilled water (40 mL) and partitioned sequentially with *n*-hexane (40 mL × 5), ethyl acetate (40 mL × 5) and *n*-butanol (40 mL × 5). The residue was also collected. The solvent fractions were further concentrated *in vacuo*.

### 2.2.4. Thin layer chromatography (TLC) analysis of the active fractions

TLC analysis, using various chromogenic reagents (Satyajit et al., 2006), was carried out on the active fractions of the herbs, namely the *n*-hexane and/or ethyl acetate fractions. In brief, the *n*-hexane and ethyl acetate fractions were developed on silica gel $GF_{254}$ plates (0.2 mm, Merck, Germany) with a solvent system of *n*-hexane-ethyl acetate (8:2, v:v). Vanillin-$H_2SO_4$, phosphomolybdic acid, $FeCl_3$-ethanol, Dragendorff's reagent and ninhydrin reagent were used as the chromogenic reagents.

### 2.2.5. MTT assay

The 3-(4,5-dimethylthiazol-2-yl)-2,5-diphenyl tetrazolium bromide (MTT) assay was employed to evaluate the antiproliverative effects of the samples (Mosmann, 1983). Briefly, different concentrations of samples were added to the cells after 24 h incubation in a 96-well microtiter plate (NUNC, Denmark). Except for HL-60 cells, samples were added immediately after the cells were seeded. After incubation for 72 h, 20 μL of the MTT (Sigma, St. Louis, MO) solution [5 mg/mL in phosphate buffered saline (PBS)] was added to each well. The cells were further incubated for another 4 h. Excess medium was removed and replaced by 150 μL of DMSO in each well to dissolve the formazan crystals. Optical densities were determined by a microplate spectrophotometer (SPECTRAmax 250, Molecular Devices, Minnesota) at 570 nm.

### 2.2.6. Statistical analysis

All results were expressed as mean ± SD from three independent experiments. Statistical analysis was performed using a two-tailed Student's *t*-test. Difference with $p < 0.05$ (*) was considered statistically significant.

## 2.3. Results

### 2.3.1. Antiproliferative effect of extracts and fractions of the Chinese medicinal herbs

Since most of the medicinal herbs are traditionally administered as an aqueous

decoction, aqueous extracts of the herbs were prepared. In addition, ethanolic extracts were also prepared. As shown in Table 2.2, none of the aqueous extracts showed an antiproliferative effect on the cancer cells at the concentration of 250 μg/mL, except that of *C. minima* on the PC-3, Hep G2 and HL-60 cells. At the same time, the ethanolic extracts showed activities to different extents. Among them, the ethanolic extract of *C. minima* showed the strongest activity with $IC_{50}$ values from 25.4 to 71.4 μg/mL. These results suggested that the active constituents in the herbs were more soluble in ethanol. On the other hand, the ethanolic extracts had weak effects on the proliferation of the human normal skin fibroblast Hs68 cells. All of them had $IC_{50}$ values of larger than 500 μg/mL, except that of *C. minima* with $IC_{50}$ value of 194.2 μg/mL.

Subsequently, solvents of different polarities (*n*-hexane, ethyl acetate, *n*-butanol) were employed to fractionate the active ethanolic extracts that had $IC_{50}$ values of less than 125 μg/mL, and the obtained fractions were further tested for their antiproliferative activities on the susceptible cancer cell lines (Figure 2.1). As shown in Table 2.2, the bioactive fractions of the ethanolic extracts of the herbs were mostly found in the *n*-hexane and/or the ethyl acetate fractions with $IC_{50}$ values of less than 100 μg/mL. Among the active fractions, the *n*-hexane fraction of *C. minima* was the most potent with $IC_{50}$ values ranging from 6.1 to 47.3 μg/mL. Also, the active fractions showed weak antiproliferative effects on normal Hs68 cells.

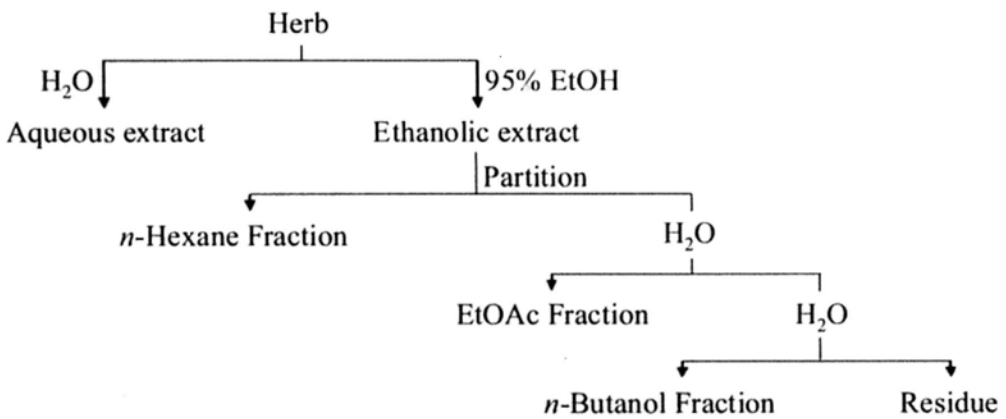


**Figure 2.1.** Flowchart of extraction and fractionation of the Chinese medicinal herbs

### 2.3.2 Thin layer chromatography (TLC) analysis of the active fractions in herbs

In order to characterize the active constituents in the herbs, TLC analysis of both the *n*-hexane and ethyl acetate fractions was carried out. All active fractions showed red and/or blue spots when treated with the vanillin-sulfuric acid reagent, suggesting the presence of terpenes (Table 2.3). Further confirmation was evidenced by the presence of blue spots in most of the fractions when phosphomolybdic acid reagent was employed. On the other hand, most fractions were positive to the $FeCl_3$-ethanol reagent, indicating the presence of phenolic compounds, except for both the *n*-hexane and the ethyl acetate fractions of *L. chinensis* and the *n*-hexane fraction of *B. laciniata*. Negative results were obtained for all the fractions when both Dragendorff's reagent and ninhydrin were applied, which suggested the absence of nitrogen-containing compounds. In short, results from the TLC analysis suggested that terpenes and/or phenolic compounds were likely to be the principal chemical classes in the herbs.

**Table 2.1.** Selected Chinese medicinal herbs used in the present study

| Herb species (Chinese name/Family) | Part used | Folk application related to cancer treatment | Voucher specimen no. | Extraction yield (%) | |
|---|---|---|---|---|---|
| | | | | A | E |
| *Nervilia fordii* (Hance) Schltr. (青天葵/Orchidaceae) | Whole plant | To treat nasopharyngeal carcinoma (Anonymou, 1986; Cheng and Li, 1998) | 06111201 | 13.8 | 1.4 |
| *Centipeda minima* (鵝不食草/Compositae) | Whole plant | To treat nasopharyngeal carcinoma (Cheng and Li, 1998; Zhang, 2000) | 06111202 | 15.6 | 2.4 |
| *Kaempferia galanga* L. (山柰/Zingiberaceae) | Rhizome | To treat stomach carcinoma (Cheng and Li, 1998) | 06111203 | 34.9 | 1.8 |
| *Lobelia chinensis* Lour. (半邊蓮/Campanulaceae) | Whole plant | To treat stomach carcinoma (Anonymou, 1986) | 06111204 | 8.2 | 2.0 |
| *Blumea laciniata* (Roxb.) DC. (六耳鈴/Compositae) | Whole plant | Have effects on detumescence and detoxification (Anonymou, 1986) | 06111206 | 10.0 | 2.6 |
| *Elephantopus scaber* L. (地膽草/Compositae) | Root | To treat different kinds of cancers (Anonymou, 1986; Zhang, 2000) | 06111207 | 17.3 | 6.0 |

A = Aqueous extract; E = Ethanolic extract

**Table 2.2.** Antiproliferative activity of the extracts and fractions from the selected Chinese medicinal herbs

| Herb | Sample | Cancer cell | | | | | Normal cell |
|---|---|---|---|---|---|---|---|
| | | MCF7 | PC-3 | Hep G2 | CNE | HL-60 | Hs68 |
| *N. fordii* | Aqueous | >250 | >250 | >250 | >250 | >250 | >500 |
| | Ethanol | 110.3 | 125.4 | 205.7 | 171.8 | 120.8 | >500 |
| | *n*-Hexane | >100 | nd | nd | nd | 38.5 | 145.3 |
| | EtOAc | 80.1 | nd | nd | nd | 86.5 | nd |
| | *n*-Butanol | 61.4 | nd | nd | nd | >100 | nd |
| | Residue | >100 | nd | nd | nd | >100 | nd |
| *C. minima* | Aqueous | >250 | 180.4 | 233.1 | >250 | 186.6 | >500 |
| | Ethanol | 30.5 | 45.9 | 71.4 | 25.4 | 48.5 | 194.2 |
| | *n*-Hexane | 15.7 | 12.5 | 47.3 | 21.2 | 6.1 | 95.5 |
| | EtOAc | 16.1 | 14.6 | 56.2 | 35.9 | 8.3 | 119.4 |
| | *n*-Butanol | 95.6 | >100 | >100 | 82.8 | 76.8 | nd |
| | Residue | >100 | >100 | >100 | >100 | >100 | nd |
| *K. galanga* | Aqueous | >250 | >250 | >250 | >250 | >250 | >500 |
| | Ethanol | >250 | 113.1 | 165.0 | 103.4 | 93.8 | >500 |
| | *n*-Hexane | nd | 82.3 | nd | 93.1 | 51.8 | 313.3 |
| | EtOAc | nd | >100 | nd | >100 | 12.2 | 298.6 |
| | *n*-Butanol | nd | >100 | nd | >100 | 76.1 | nd |
| | Residue | nd | >100 | nd | >100 | >100 | nd |
| *L. chinensis* | Aqueous | >250 | >250 | >250 | >250 | >250 | >500 |
| | Ethanol | 68.1 | 223.9 | >250 | >250 | >250 | >500 |
| | *n*-Hexane | 100.0 | nd | nd | nd | nd | nd |
| | EtOAc | >100 | nd | nd | nd | nd | nd |
| | *n*-Butanol | >100 | nd | nd | nd | nd | nd |
| | Residue | >100 | nd | nd | nd | nd | nd |

(to be continued)

| | | | | | | | |
|---|---|---|---|---|---|---|---|
| *B. laciniata* | Aqueous | >250 | >250 | >250 | >250 | >250 | >500 |
| | Ethanol | 175.0 | 128.5 | 121.4 | 124.8 | 52.3 | >500 |
| | *n*-Hexane | nd | nd | >100 | 53.4 | 24.3 | 216.2 |
| | EtOAc | nd | nd | >100 | >100 | 77.9 | nd |
| | *n*-Butanol | nd | nd | >100 | >100 | 76.1 | nd |
| | Residue | nd | nd | >100 | >100 | >100 | nd |
| *E. scaber* | Aqueous | >250 | >250 | >250 | >250 | >250 | >500 |
| | Ethanol | 158.3 | 52.0 | >250 | 60.8 | 25.9 | >500 |
| | *n*-Hexane | nd | 52.8 | nd | 54.4 | 27.2 | 229.9 |
| | EtOAc | nd | 21.8 | nd | 19.5 | 10.9 | 145.6 |
| | *n*-Butanol | nd | >100 | nd | >100 | >100 | nd |
| | Residue | nd | >100 | nd | >100 | >100 | nd |

Data are expressed as $IC_{50}$ values (μg/mL); nd: not determined.

**Table 2.3.** Results of TLC analysis from different active fractions

| Herb | Fraction | Chromogenic reagent [a] | | | | |
|---|---|---|---|---|---|---|
| | | A | B | C | D | E |
| *N. fordii* | *n*-Hexane | + | + | + | – | – |
| | EtOAc | + | – | + | – | – |
| *C. minima* | *n*-Hexane | + | + | + | – | – |
| | EtOAc | + | + | + | – | – |
| *K. galanga* | *n*-Hexane | + | + | + | – | – |
| | EtOAc | + | – | + | – | – |
| *L. chinensis* | *n*-Hexane | + | + | – | – | – |
| | EtOAc | + | – | – | – | – |
| *B. laciniata* | *n*-Hexane | + | + | – | – | – |
| | EtOAc | + | + | + | – | – |
| *E. scaber* | *n*-Hexane | + | + | + | – | – |
| | EtOAc | + | + | + | – | – |

[a] A: Vanillin-$H_2SO_4$, a universal spray, many terpenes give red and blue colors; B: Phosphomolybdic acid, for terpenes detection; C: $FeCl_3$-ethanol, for phenolic compounds detection; D: Dragendorff's reagent, for alkaloid detection; E: Ninhydrin, for amino acids, amines and alkaloid detection.

+: positive result; –: negative result.

## 2.4. Discussion

In this study, six Chinese medicinal herbs traditionally used to treat cancer in China were screened for their antiproliferative activities on five human cancer cell lines. Most of their aqueous extracts showed weak or no activity on the cancer cells ($IC_{50}$ > 250 μg/ml), whereas most of the ethanolic extracts showed antiproliferative activities on the same cancer cells ($IC_{50}$ < 250 μg/ml) (Table 2.2). Apparently, the potent constituents in the herbs are more soluble in ethanol. Also, all ethanolic extracts had little effect on the proliferation of the normal Hs68 cells, but strong antiproliferative effect on the cancer cells, suggesting that the ethanolic extracts induced different responses in cancer and normal cells. At present, the successful screening of effective anticancer agents depends on the properties of the natural bioactive agents that can induce selectivity on cancer cells over the normal cells (Mukherjee et al., 2001). Our study provided evidence that the ethanolic extracts prepared from the six Chinese medicinal herbs exhibited selective antiproliferative activity on the cancer cells.

In order to further investigate the constituents responsible for the antiproliferative activity in the herbs, their active ethanolic extracts were partitioned into four fractions of different polarities. MTT assay carried out on each one of them found *n*-hexane and/or ethyl acetate fractions were very active ($IC_{50}$ < 100 μg/ml) suggesting low polarity components were to be focused. TLC analysis of the fractions further suggested the principal active components in the herbs might be terpenes and/or phenolic compounds. Terpenes which possessed anticancer activity have been widely reported (Ikezoe et al., 2003; Liu et al., 2006; Tao et al., 2006; Wen et al., 2002). The anticancer drug taxol is one of the most renowned terpene-based drugs (Zhang and Demain, 2005). Phenolic compounds are another characteristic group of components that are abundant in the plant kingdom. The anticancer property of many phenolic compounds has been well documented (Brisdelli et al., 2007; Losso et al., 2004; Ma et al., 2005; Son et al., 2006).

## 2.5. Conclusions

In conclusion, the present study positively demonstrated the antiproliferative activities of the six selected Chinese medicinal herbs. Terpenes and phenolic compounds, were found to exist in most of the active fractions (*n*-hexane and ethyl acetate fractions). These results suggest that the active constituents of the herbs are generally water-insoluble compounds. This study reiterates the notion that Chinese medicinal herbs traditionally applied to cancer treatment may be a good source of anticancer drug discovery. Besides, *C. minima*, the most effective herb in this study, is worth to further investigation to find out the responsible principals.

# Chapter 3: Bioactivity-guided isolation of the *n*-hexane fraction of *Centipeda minima* and the mechanism study of the isolated compound, 2β-(isobutyryloxy)florilenalin on the human nasopharyngeal cancer CNE cells

## 3.1. Introduction

Nasopharyngeal carcinoma (NPC), originated from the epithelial lining of the nasopharynx, is the most common cancer in the head and neck regions (Yu and Yuan, 2002). Although its occurrence is very low in other parts of the world (<1/100,000 person per year), its incidence is unusually high in southern China (>20/100,000 persons per year) (Parkin, 2006). Three factors including of Epstein-Barr virus (EBV) infection, carcinogen exposure and genetic susceptibility, have been suggested to play significant roles in the NPC development (Tiwawech, 2006). The combination of radiotherapy and adjuvant chemotherapy has become the prevalent treatment of NPC (Wang et al., 2002). Recent progress in chemotherapy of NPC has shed light on the cytotoxic agent cisplatin. However, toxicity and resistance make cisplatin far from satisfactory, which result in its limit applications in NPC chemotherapy (Wang et al., 2008; Xie et al., 2008). In this regard, there is a great demand for novel agents that selectively induce NPC cell death without producing cytotoxic effects on normal cells.

*Centipeda minima* (L.) A. Br. (Compositae) is an annual plant distributed throughout high humidity geographic locations throughout China, Korea, Japan, India, Malaysia and Oceania (Shi and Fu, 1983). Six *Centipeda* species are known, but only *C. minima* grows in China (Shi and Fu, 1983). The whole plant, which is harvested during its anthesis in both summer and autumn, has pharmaceutical applications (Lin and Shi, 2005). Based on the record in the Pharmacopoeia of China (Lin and Shi, 2005), the dried herb is used to treat nasal allergies, rhinitis and sinusitis, coughs and headaches. In addition, it is used in the Chinese folk medicine to treat nasopharyngeal carcinoma (Cheng and Li, 1998; Zhang, 2000). Recent pharmacological interest has focused on its anti-allergy and anti-bacterial effects (Wu et al., 1985, 1991; Taylor and Towers, 1998;

Liang et al., 2007b and 2007d). However, there is a paucity of information (Li et al., 2008) on the anticancer activities of *C. minima*. Besides, both the anti-NPC potential and the potent constituents of *C. minima* remain elusive.

In the previous study, we have showed the potency of the *n*-hexane fraction of *C. minima* displaying antiproliferative effects in a broad spectrum of cancer cell lines. Therefore, the objectives of this study were to isolate and identify the active principal(s) in the *n*-hexane fraction of *C. minima* based on the bioactivity-guided isolation approach using the human nasopharyngeal cancer epithelial cells (CNE) as the target and elucidate the underlying mechanism leading to the cell death.

## 3.2. Materials and methods

### 3.2.1. Generals

MTT dye [3-(4,5-dimethylthiazol-2-yl)-2,5-diphenyl tetrazolium bromide)], RPMI-1640 medium, propidium iodide (PI), 4',6-diamidino-2-phenylindole (DAPI) and 5,5',6,6'-tetrachloro-1,1',3,3'-tetraethylbenzimidazolcarbocyanine iodide (JC-1) were purchased from Sigma (St. Louis, MO, USA); DMEM medium and fetal bovine serum (FBS) were obtained from Gibco (Rockville, MD, USA); ELISA-BrdU chemiluminescence assay kit, cytotoxicity detection kit and complete™ protease inhibitor cocktail were purchased from Roche (Germany); Bradford reagent were purchased from Bio-Rad (Hercules, CA, USA); Caspase-3 substrate (Ac-Asp-Glu-Val-Asp-*p*NA) was purchased from Calbiochem (Germany); Anticaspase-3, anticaspase-7, anticaspse-8, anticaspase-9, anti-PARP [poly(ADP-ribose) polymerase], anti-Bax, anti-Bad, anti-Bim, anti-Bik, anti-Bmf, anti-Bcl-xL, anti-Mcl-1, anti-rabbit secondary horseradish peroxidase antibody, and chemiluminescent substrate were purchased from Cell Signal Technology (Beverly, MA); Anti-Bcl-2, anti-β-actin and anti-mouse secondary horseradish peroxidase antibody were obtained from Santa Cruz Biotech (Santa Cruz, CA, USA); Anti-cytochrome *c* was obtained from BD Biosciences (San Jose, CA, USA). All other chemicals were reagent grade.

Mass spectroscopy was measured by a gas chromatography-mass spectrometry

(GC-MS) equipment (Agilent Technologies 6890/5973N, Palo Alto, CA, USA). An HP-5 ms capillary column (30 m × 0.25 mm, i.d 25 μm film thickness) was used. Helium was used as the carrier gas at a constant flow rate of 1.5 mL/min. The injected sample volume was 1 μL. The oven temperature was kept at 60 °C and programmed to 150 °C at the rate of 3 °C/min and kept constant for 5 min. Then the temperature was programmed to 240 °C at the rate of 1.5 °C/min and kept constant for 10 min. The final temperature was increased to 300 °C at the rate of 2 °C /min, and kept constant for 10 min. MS were recorded at 70 eV. The $^{1}$H- (400 MHz) and $^{13}$C-NMR (100 MHz) spectra were recorded in $CDCl_3$ on a Bruker AVANCE 400 spectrometer (Bruker, Germany).

### 3.2.2. Extraction, fractionation and isolation guided by MTT assay

The aerial part of *C. minima* was collected in Baiyun mountain (Guangzhou, People's Republic of China). A voucher specimen (06115202) has been deposited in the Department of Biology, the Chinese University of Hong Kong. The herb (2.2 kg) was macerated 4 times successively in 95% ethanol (5 L) at 20 °C for 4 days. The supernatants were filtered, concentrated *in vacuo*, and lyophilized into the dried ethanolic extract (397 g). Then, 300 g of the ethanolic extract was suspended in distilled water (2 L) and partitioned sequentially with *n*-hexane (2 L × 5). After concentrated *in vacuo*, the *n*-hexane fraction was subjected to further isolation. Briefly, the *n*-hexane fraction (50 g) was chromatographed on a silica gel column (70-230 mesh, 1.2 kg, Merck; diameter: 7 cm, length: 100 cm) by eluting it with a *n*-hexane-EtOAc gradient system (100:0, 99:1, 98:2, 96:4, 94:6, 92:8, 88:12, 80:20 and 0:100, [v/v]; each step used 1 L of solvent). Eleven fractions were produced on the basis of the TLC profiles. Fraction 11 (*n*-hexane-EtOAc, 0:100, 15 g) was rechromatographed on a silica gel column (70-230 mesh, 750 g, Merck; diameter: 5 cm, length: 60 cm) with a gradient of *n*-hexane-EtOAc (92:8, 90:10, 0:100, [v/v]; each step used 2.5 L of solvent) to yield nine sub-fractions. Sub-fraction 9 (*n*-hexane-EtOAc, 0:100, 8 g) was further purified by repeated column chromatographies on a sephadex LH-20 column (25-100 μm, Fluka, Switzerland; diameter: 1.5 cm, length: 30 cm) using a mixture of chloroform-methanol (5:5, v/v) to yield 2β-(isobutyryloxy)-florilenalin (IF), which chemical structure was identified by spectroscopic methods and comparison with the published data in literature

(Bohlmann and Chen, 1984). The flowchart of isolation of 2β-(isobutyryloxy)-florilenalin (IF) was shown in Figure 3.1.

### 3.2.3. Cell lines and cell culture

Human nasopharyngeal cancer epithelial cells (CNE) and human normal skin cells (Hs68) were purchased from the Cell Bank of Type Culture Collection of Chinese Academy of Sciences (Shanghai, People's Republic of China) and the American Type Culture Collection (Rockville, MD, USA), respectively. CNE cells were maintained in RPMI-1640 medium, while Hs68 cells were maintained in DMEM medium. Both media were supplemented with 10% fetal bovine serum and 1% penicillin-streptomycin at 37 °C in a humidified incubator with 5% $CO_2$ atmosphere.

### 3.2.4. MTT assay

Cell viability was determined by a MTT assay. Briefly, different concentrations of samples were added to the cells after 24-h incubation in a 96-well microtiter plate. Following incubation for specific times, MTT solution [20 μL, 5 mg/mL in phosphate buffered saline (PBS)] was added to each well, and the cells were further incubated for 4 h. Excess medium was removed and replaced by DMSO (150 μL) to dissolve the formazan crystals. The optical densities were determined by a microplate spectrophotometer (SPECTRAmax 250, Molecular Devices, MN, USA) at the wavelength of 570 nm.

### 3.2.5. Cell proliferation analysis by BrdU assay

Cell proliferation was determined by the BrdU (5-bromo-2'-deoxyuridine) chemiluminescence assay which was based on the measurement of BrdU incorporation during DNA synthesis in proliferating cells. The ELISA-BrdU chemiluminescence assay kit (Roche, Germany) was employed. Briefly, after incubating the cells with various concentrations of IF for 24 h in a 96-well microtiter plate, BrdU labeling solution (100 μM, final concentration) was added, and the plate was incubated for 2 h. The labeling solution was removed and the cells were fixed with FixDenat solution for 30 min. After

removal of the FixDenat solution, anti-BrdU-POD solution was added and further incubated for 1.5 h. The chemiluminescence intensity was determined according to the manufacturer's instruction. Cell proliferation was expressed as the percentage relative to the control which contained no IF.

### 3.2.6. Lactate dehydrogenase (LDH) assay

Cytotoxicity as reflected by the LDH activity was determined by the Cytotoxicity Detection Kit (Roche, Germany). Briefly, both treated and untreated cells were centrifuged at 500 *g* for 10 min at 20 °C. Supernatants (100 μL) were collected and transferred to a new 96-well microtiter plate. LDH activity was determined according to the manufacturer's instruction. Cytotoxicity was evaluated by measuring the percentage of LDH released into the medium. Cells treated with 1% triton X-100 were used as positive control (i.e. 100% lysis of the cells).

### 3.2.7. DNA contents analysis by flow cytometry

The effect of IF on the cell cycle distribution of CNE cells were determined by flow cytometric analysis. Briefly, treated or untreated CNE cells were harvested and washed with PBS twice. Cells were stained with freshly prepared DNA staining solution containing propidium iodide (PI, 20 μg/mL), RNase A (200 μg/mL) and 0.1% triton X-100 after fixed in 70% ethanol at -20 °C overnight. Stained cells were then subjected to analyze by a flow cytometer (EPICS XL Flow cytometry, Beckman Coulter, Miami, FL, USA). Cells displaying hypodiploid DNA content were quantified and regarded as the apoptotic population. In each experiment, 10,000 events per sample were recorded.

### 3.2.8. Nuclear staining with DAPI

Morphological changes in the nuclear chromatin of cells undergoing apoptosis were revealed by a nuclear fluorescent dye, DAPI. Briefly, cells after treatment for 72 h were harvested, washed with PBS twice. After fixed with 4% paraformaldehyde and permeated with 0.1% triton X-100, the cells were stained with 2 μg/mL of DAPI for 15 min. The cells were then observed under a fluorescence microscope (Nikon Eclipse 80i,

Japan).

### 3.2.9. Mitochondrial membrane potential ($\Delta\Psi m$) assay

A cationic dye JC-1 was used to measure the depletion of mitochondrial membrane potential. JC-1 exhibits potential-dependent accumulation in mitochondria, indicated by a fluorescence emission shift from green to red. Briefly, after treatment with IF for 72 h, cells were washed with PBS twice and stained with 10 μM of JC-1. After incubation in dark at 37 °C for 15 min, cells were analyzed by the flow cytometer. Data are expressed in percentage of cells with changed $\Delta\Psi m$.

### 3.2.10. Caspase activity assay

Caspase activity was determined by using the colorimetric peptite caspase-3 substrate Ac-Asp-Glu-Val-Asp-*p*NA. Briefly, cell lysates were placed in 96-well plate, and 100 μM of the substrate was added. The plate was incubated at 37 °C for 1 h and caspase activity was determined by the microplate spectrophotometer at the wavelength of 405 nm.

### 3.2.11. Western blotting

To obtain cytosolic proteins, cells were harvested and lysed in hypotonic lysis buffer (250 mM sucrose, 20 mM Hepes, 1.5 mM $MgCl_2$, 10 mM KCl, 1 mM EGTA, 1 mM DTT, complete™ protease inhibitor cocktail) for 30 min on ice. Then the cells were homogenized in a Dounce homogenizer with optimal gentle strokes. After centrifugation at 1,000 *g* for 10 min at 4 °C to remove the unlysed cells and nuclei, the supernatants were further centrifuged at 14,000 *g* for 15 min at 4 °C. The supernatant was collected as the cytosolic proteins. The total cellular proteins were extracted by lysing cells in a lysis buffer [1% IGEPAL CA 630 (Fluka, Switzerland), 150 mM NaCl, 50 mM Tris-HCl (pH 7.5), complete™ protease inhibitor cocktail] for 30 min on ice. Lysates were clarified by centrifugation for 15 min at 14,000 *g*. The supernatant was collected as the total cellular proteins. Protein concentrations were determined with Bradford reagent. Equal amounts of proteins (20-40 μg protein) were resolved on 7.5-12% SDS-polyacrylamide gels,

followed by electrophoretic transfer to PVDF (Polyvinylidene fluoride, Millipore, Bedford, MA, USA) membranes. The membranes were blocked with 5% non-fat dry milk in TBST (Tris-Buffered Saline Tween-20) for 1 h, followed by incubation sequentially with primary antibodies at 4 °C and the horseradish peroxidase-conjugated secondary antibodies at 20 °C. Protein bands were detected on X-ray film (Fuji, Japan) using the chemiluminescent substrate.

### 3.2.12. Statistical analysis

All results were expressed as mean ± SD from three independent experiments. Statistical analysis was performed using a two-tailed Student's *t*-test. Difference with $p < 0.05$ (*) was considered statistically significant.

## 3.3. Results and discussion

### 3.3.1. Chemical structure elucidation

Based on the previous study, the *n*-hexane fraction was the most effective, so it was subjected to further fractionation to search for the active principal(s). This led to the purification of 2β-(isobutyryloxy)-florilenalin (IF) (Figure 3.2). The spectral data of IF (colorless gum) was shown as follows (The spectra are showed in Appendix 1).

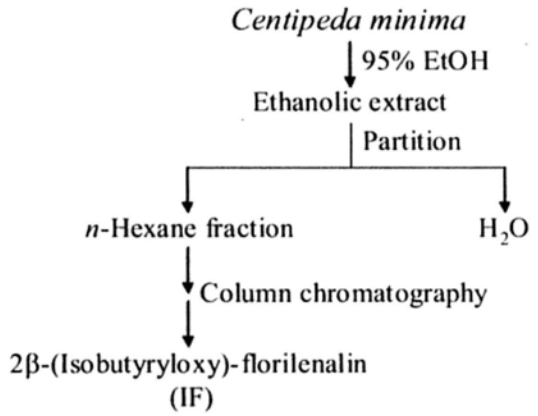


**Figure 3.1.** Flowchart of isolation of 2β-(isobutyryloxy)-florilenalin (IF) from *Centipeda minima*

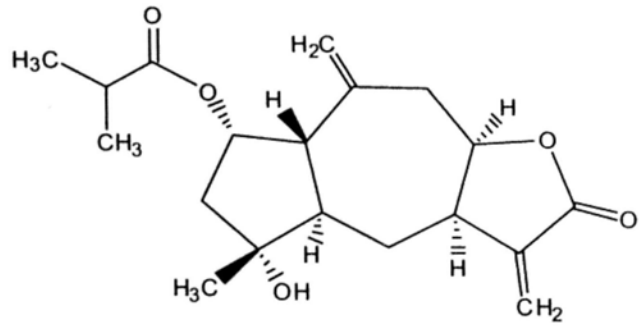


**Figure 3.2.** Chemical structure of 2β-(isobutyryloxy)-florilenalin (IF) isolated from *Centipeda minima*

EI-MS *m/z*: 334 $[M]^+$;

$^1$H-NMR (in $CDCl_3$): $\delta$ 1.13 (3H, d, $J$ = 0.8 Hz, H-18), 1.14 (3H, d, $J$ = 0.7 Hz, H-19), 1.23 (3H, s, H-15), 1.60 (1H, m, H-6β), 1.86 (1H, br d, $J$ = 15.7 Hz, H-3β), 2.10 (1H, dd, $J$ = 4.7, 14.2 Hz, H-6α), 2.17 (1H, s, H-5), 2.17 (1H, s, H-1), 2.20 (1H, dd, $J$ = 5.8, 15.7 Hz, H-3α), 2.30 (1H, dd, $J$ = 11.7, 12.4 Hz, H-9β), 2.52 (1H, m, H-17), 2.70 (1H, dd, $J$ = 3.6, 12.4 Hz, H-9α), 3.23 (1H, m, H-7), 4.59 (1H, m, H-8), 4.85 (1H, s, H-14'), 5.04 (1H, s, H-14), 5.27 (1H, dd, $J$ = 2.4, 5.2 Hz, H-2), 5.65 (1H, d, $J$ = 2.4 Hz, H-13'), 6.27 (1H, d, $J$ = 2.8 Hz, H-13);

$^{13}$C-NMR (in $CDCl_3$): $\delta$ 18.7 ($-CH_3$), 18.8 ($-CH_3$), 25.3 (C-15), 29.7 (C-6), 34.2 (C-17), 39.6 (C-9), 42.2 (C-7), 49.1 (C-3), 51.6 (C-5), 53.4 (C-1), 73.5 (C-2), 78.4 (C-4), 80.4 (C-8), 115.6 (C-14), 122.6 (C-13), 139.2 (C-11), 139.8 (C-10), 169.7 (C-12) and 176.4 (C-16).

### 3.3.2. IF inhibited the growth of CNE cells

In the present study, MTT results showed that IF exhibited significant dose- and time- dependent effects on the growth of CNE cells, with $IC_{50}$ values of 25.6 (24 h), 8.1 (48 h) and 3.1 μg/mL (72 h), respectively (Figure 3.3A). Despite its potency in CNE cells, IF exerted lower inhibitory effect on the normal Hs68 cells with an $IC_{50}$ value larger than 50 μg/mL at 72-h treatment (Figure 3.3B). Similar dose-dependent inhibitory effect was observed in the ELISA-BrdU assay for 24-h incubation, which

is based on the incorporation of the pyrimidine analogue BrdU instead of thymidine into the DNA of proliferating cells (Figure 3.3C. Lactate dehydrogenase (LDH) is a stable cytoplasmic enzyme present in cells and rapidly released into the cell culture supernatant upon damage of the plasma membrane. Hence, the activity of LDH correlates to the number of lysed cells. In this study, no significant cytotoxic effects on both CNE and Hs68 cells were found when the leakage of LDH into the cell medium was evaluated (Figure 3.3D).

Sesquiterpene lactones, most widely distributed within the *Compositae*, have received considerable attention for their anticancer properties (Zhang et al., 2005). The highly electrophilic α,β-unsaturated carbonyl structures, such as the α-methylene-γ-lactone ring and the α,β-unsaturated cyclopentenone, are considered as the general bioactive functional groups in sesquiterpene lactones (Zhang et al., 2005), as they allow the structures to interact rapidly with the nucleophilic sites of biological molecules in a Michael-type addition. Covalent binding of sesquiterpene lactones to free sulfhydryl groups in proteins is possible and may interfere with the normal protein function. Besides, alkylation with the DNA molecules presents a potential molecular cytotoxicity for cells (Beekman et al., 1997). Previous phytochemical studies of *C. minima* have identified more than ten sesquiterpene lactones which are all pseudo-guanianolide or guaianolide types (Wu et al., 1985, 1991; Taylor and Towers, 1998; Bohlmann and Chen, 1985; Yu et al., 1994). Among them, 6-*O*-angeloylenolin, a sesquiterpene lactone containing an α, β-unsaturated cyclopentenone, isolated from *C. minima* was reported to induce apoptosis in HL-60 cells *in vitro* and inhibit the solid cancer growth in Lewis lung cancer xenograft model (Li et al., 2008). IF, isolated in this study, contains a bioactive functional group of sesquiterpene lactone, the α-methylene-γ-lactone ring. This led to our deduction that IF might possess similar apoptotic activity. However, other than a report on the sensitivity Gram-positive bacteria (Liang et al., 2007a), no other information has reported such activity in IF.

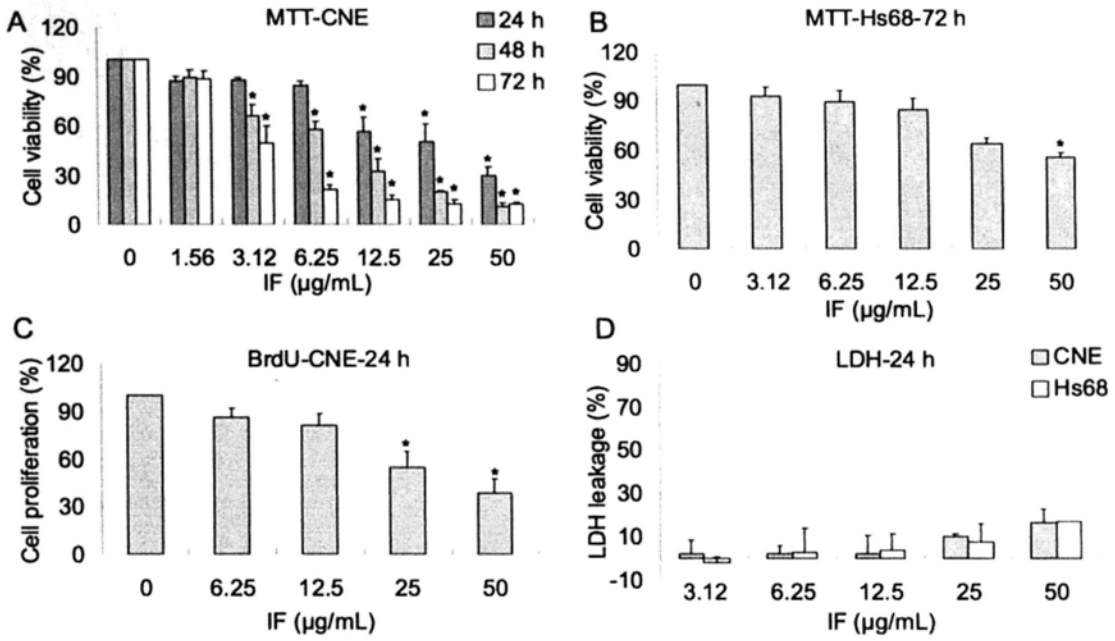


**Figure 3.3.** Effects of IF on the growth of CNE and Hs68 cells. (A) Effect of IF on the viability of CNE cells at 24-, 48-, 72-h treatments evaluated by MTT assay. (B) Effect of IF on the viability of Hs68 normal cells at 72-h treatment evaluated by MTT assay. (C) Effect of IF on the proliferation of CNE cells at 24-h treatment evaluated by BrdU assay. (D) Cytotoxic effects of IF on CNE and Hs68 cells at 24-h treatment evaluated by LDH assay. Each value represents the mean of three independent experiments. Difference between treatments and control with $p < 0.05$ (*) was considered statistically significant.

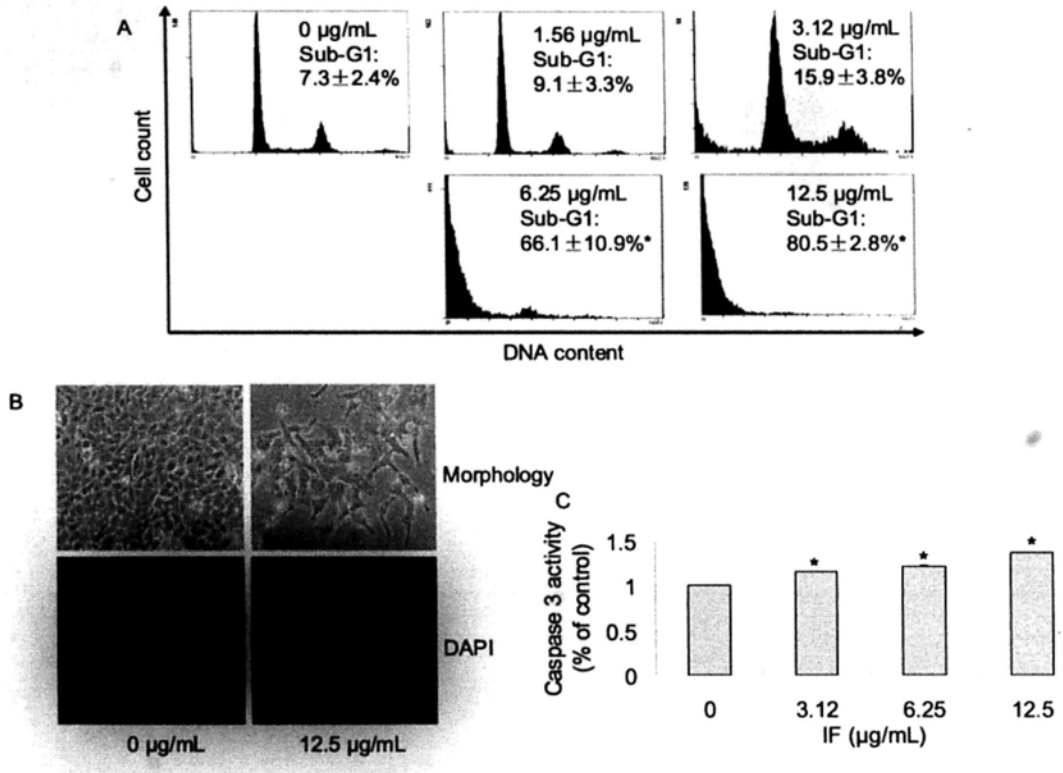


**Figure 3.4.** Apoptosis induction of IF in CNE cells. (A) Effect of IF on cell cycle distribution analyzed by flow cytometry. (B) Effect of IF on the morphology of CNE cells. Morphology (upper): phase-contrast microscopy. DAPI (lower): fluorescence microscopy. (C) Activation of caspase by IF. Difference between treatments and control with $p < 0.05$ (*) was considered statistically significant.

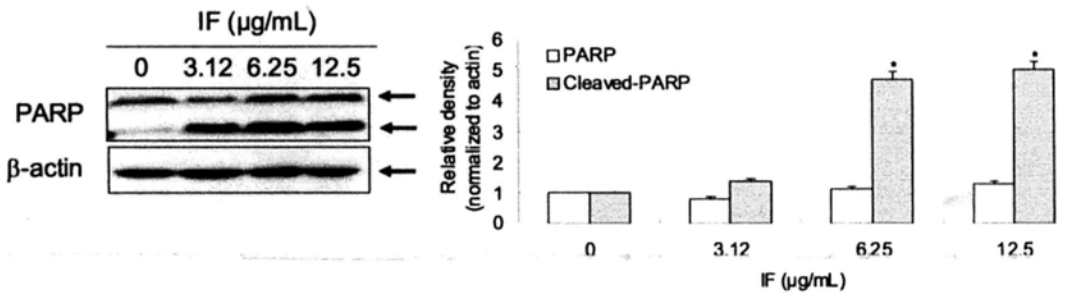


**Figure 3.5.** Effect of IF on cleavage of PARP. β-Actin was used as the loading control. Results were representatives of three independent experiments. The values on the right figure represent relative density of the bands normalized to β-actin. Difference between treatments and control with $p < 0.05$ (*) was considered statistically significant.

### 3.3.3. IF induced apoptosis in CNE cells

As IF demonstrated strong inhibition on the growth of CNE cells, its underlying mode of action was investigated. Apoptotic cells, which have a decreased content of DNA when compared to living cells, will have a hypodiploid DNA content (sub-G1 phase) when analyzed in a flow cytometer after staining with PI. Therefore, DNA cell cycle analysis of CNE cells treated with IF was carried out. Results showed that the accumulation of cells in the sub-G1 phase significantly increased in a dose-dependent way (Figure 3.4A), suggesting apoptosis was induced by IF. The sub-G1 cell populations were 7.3 ± 2.4, 9.1 ± 3.3, 15.9 ± 3.8, 66.1 ± 10.9 and 80.5 ± 2.8% with IF concentrations of 0, 1.56, 3.12, 6.25 and 12.5 μg/mL, respectively. Additional confirmations of apoptosis in the presence of IF were from the measurements of three other apoptotic markers including DNA fragmentation, caspase-3 activation, and PARP cleavage (Figures 3.4B, 3.4C, 3.5). Irregularity in shape and cellular detachment in the treated CNE cells (12.5 μg/mL of IF) were observed under a phase-contrast microscopy (Figure 3.4B). Similarly, DNA fragmentation and nuclear condensation were observed in the treated CNE cells (12.5 μg/mL of IF) after DAPI staining. Our data also revealed that IF induced significant dose-dependent increase in caspase-3 activity in CNE cells after 72-h treatment (Figure 3.4C). Additionally, cleavage of PARP with treated cells undergoing apoptosis resulted in the presence of an 89 kDa fragment (Figure 3.5). These results proved strongly that IF induced apoptosis in CNE cells.

### 3.3.4. IF activated caspases in CNE cells

Caspases are a family of cystein-dependent asparate-directed proteases that act as important regulators in apoptosis cascade. They are important components in the two apoptotic pathways, namely, the extrinsic and the intrinsic pathways (Riedl and Shi, 2004). Similar to the proteolytic cleavage of PARP, the two downstream effectors, namely caspase-3 and caspase-7, were cleaved to become the active forms (Figure 3.6). Caspase-8 is regarded as the key initiator in the extrinsic pathway. Figure 4

shows that the level of procaspase-8 was significantly reduced at the concentration of 12.5 μg/mL, whereas the cleaved product, caspase-8, was also found. Caspase-9 is the central initiator in the intrinsic pathway. Dose-dependent cleavage of procaspase-9 was observed. These results indicated that both the extrinsic and intrinsic apoptotic pathways were activated in the presence of IF.

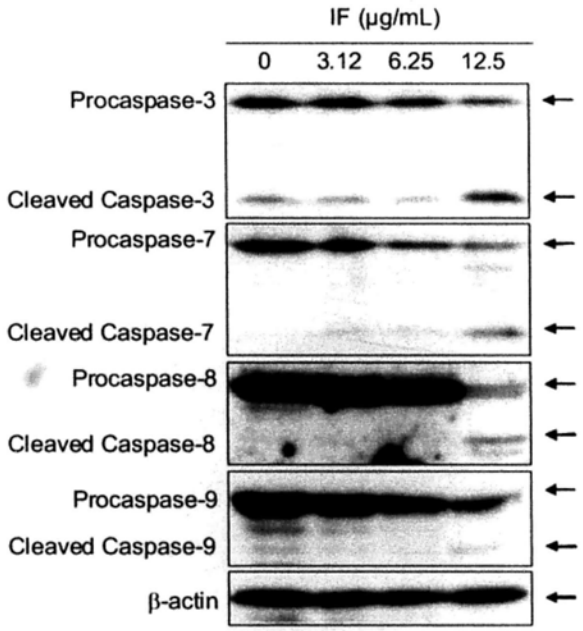


**Figure 3.6.** Effect of IF on the expressions of caspases in CNE cells. β-Actin was used as the loading control. Results were representatives of three independent experiments.

### 3.3.5. IF induced mitochondrial dysfunction in CNE cells by regulating the Bcl-2 family proteins

Mitochondria play a crucial role in the apoptotic cascade by serving as a convergent center of apoptotic signals originated from both the extrinsic and intrinsic pathways (Kim et al., 2006). Depletion of $\Delta\Psi m$ causes the opening of the mitochondria permeability transition pore, which leads to the release of apoptogenic factors, such as cytochrome *c* in the apoptotic cascade, and activation of caspases (Mattson and Kroemer, 2003). Figure 3.7A showed that IF induced dose-dependent depletion of $\Delta\Psi m$ in CNE cells while Figure 3.7B showed a dose-dependent increase of cytochrome *c* in the cytosol in the presence of IF.

Tightly mediating the mitochondrial apoptotic pathway are three groups of Bcl-2 family proteins, namely, (i) Bcl-2-like survival factors which act as anti-apoptotic proteins including Bcl-2 and Bcl-xL; (ii) Bax-like death factors which serve as pro-apoptotic proteins including Bax and finally (iii) BH3-only death factors which are pro-apoptotic protein, such as Bad and Bim (Burlacu, 2003). In response to an apoptotic stress, the BH3-only proteins were activated and interacted with Bcl-2-like survival factors on the outer mitochondrial membrane. Such interaction triggered the release of Bax-like pro-apoptotic factors which underwent a conformational change and inserted themselves into the outer mitochondrial membrane. Such insertion induced membrane permeabilization and the release of caspase-activating and other pro-apoptotic factors (Borner 2003). From the net ratio between the pro- and anti-apoptotic proteins, cells undergone apoptosis can be deduced. Our results showed that IF increased the expression of pro-apoptotic proteins, including Bax, Bad, Bim, Bik and Bmf (Figure 3.8A), but decreased the expression of anti-apoptotic proteins such as Bcl-2 and Bcl-xL when its concentration levels increased (Figure 3.8B). These observations implied that the net ratio of the two types of proteins shifted in favor of apoptosis. It was reported that Bcl-2 was detected in most samples (80%) of undifferentiated nasopharyngeal carcinoma NPC (Lu et al., 1993). Also, the

expression of Bcl-2 protein was significantly higher in NPC tissues than in both the normal noncancerous nasopharyngeal epithelial (NPE) and hyperplasic NPE (Fan et al., 2003). However, significant down-regulation of Bcl-2 in CNE cells in the presence of IF was observed in our investigation which suggested that IF was effective in controlling the NPC.

### 3.4. Conclusions

In conclusion, the phytochemical in *C. minima* that possessed strong antiproliferative effect on the CNE cells is 2β-(isobutyryloxy)florilenalin (IF), a sesquiterpene lactone. Both extrinsic and intrinsic apoptotic pathways were involved in its action. In the extrinsic pathway, IF activated caspase-8, which further induced the activation of caspase-3 and caspase-7. In the intrinsic pathway, IF regulated the levels of Bcl-2 family proteins, followed by depletion of mitochondrial membrane potential ($\Delta\Psi m$), the release of cytochrome *c* to cytosol, the activation of caspase-9 and other downstream caspases, and finally the induction of apoptosis. Such activities as a result of the presence of IF may imply that *C. minima* deserves more extensive investigation for its potential medicinal application in the treatment of NPC and other cancers.

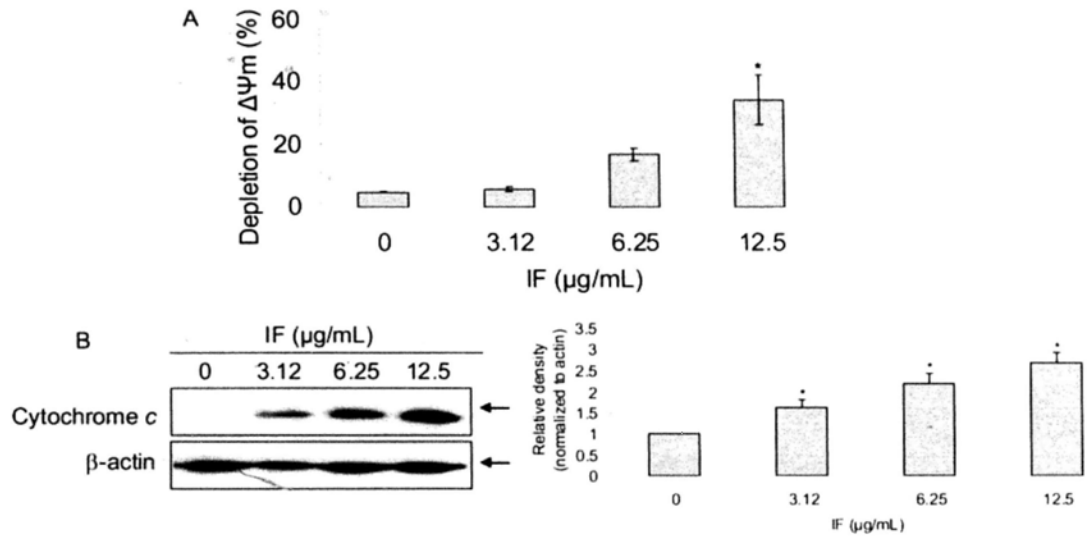


**Figure 3.7.** Effect of IF on mitochondria dysfunction. (A) Effect of IF on mitochondrial membrane potential ($\Delta\Psi m$). (B) The level of cytochrome *c* in the cytosol. β-Actin was used as the loading control. Results were representatives of three independent experiments. The values on the right figure represent relative density of the bands normalized to β-actin. Difference between treatments and control with $p < 0.05$ (*) was considered statistically significant.

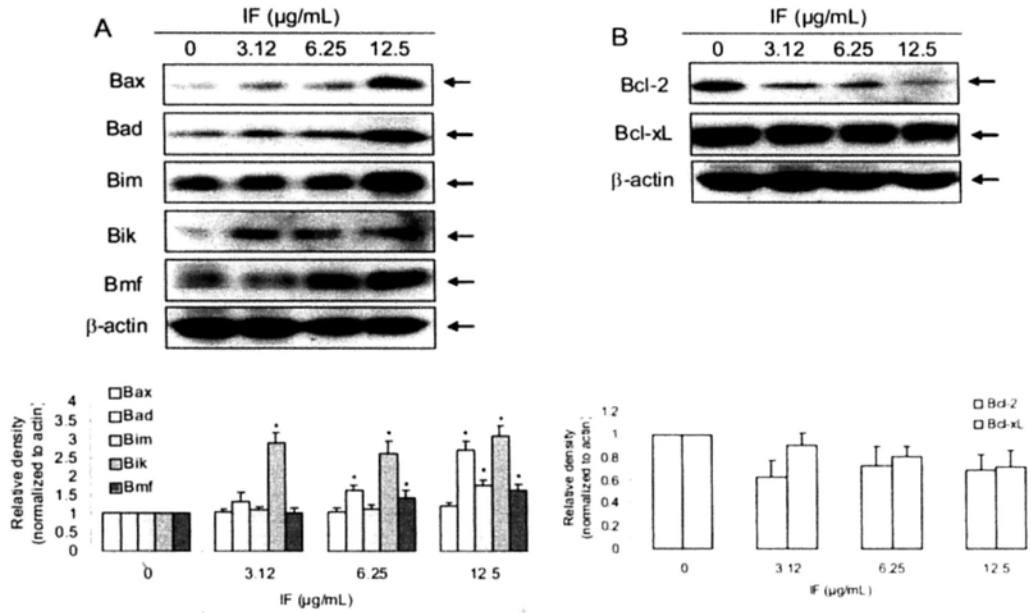


**Figure 3.8.** Effect of IF on the expressions of Bcl-2 family proteins. (A) IF up-regulated the expressions of pro-apoptotic Bcl-2 family proteins. (B) IF suppressed the expressions of anti-apoptotic Bcl-2 family proteins. β-Actin was used as the loading control. Results were representatives of three independent experiments. The values on the lower-panel figures represent relative density of the bands normalized to β-actin.

# Chapter 4: Antiproliferative effects of volatile oils from *Centipda minima* on human nasopharyngeal cancer CNE cells

## 4.1. Introduction

Nasopharyngeal carcinoma (NPC), a cancer in which malignant cells form in the tissues of the nasopharynx, is one of the most common cancers among the southern Chinese or those with Asian ancestry (Cho, 2007). It remains one of the most serious health problems in southern China with an annual incidence of more than 20 cases per 100,000 (Cho, 2007). The interaction among the Epstein-Barr virus chronic infection, the environment and the host genes contributes to the development of NPC (Chien et al., 2001). Recent progress in the treatment of NPC has focused on high-dose radiotherapy with adjunctive chemotherapy (Baujat et al., 2006). However, side effects such as resistance were observed in some patients after chemotherapy, making the current chemotherapeutic agents far from satisfactory (Wang et al., 2008; Xie et al., 2008). Thus, there is a demand to develop alternatives for the NPC treatment.

*Centipeda minima* (L.) A. Br. (Compositae) which distributes widely in China and some southeast Asian countries (Shi and Fu, 1983), has been recorded in the Chinese Pharmacopoeia to treat nasal allergies, rhinitis and sinusitis, cough and headache (Lin and Shi, 2005). Several complex Chinese herbal preparations containing *C. minima* as a principal ingredient are clinically used to treat rhinitis and sinusitis in China. In addition, *C. minima* is used in the Chinese folk medicine to treat nasopharyngeal carcinoma (Cheng and Li, 1998; Zhang, 2000). Previous pharmacological studies of *C. minima* reported that the herb possessed anti-tumor (Li et al., 2008; Su et al., 2009a), anti-mutagenic (Lee and Lin, 1988), anti-allergic (Wu et al., 1985, 1991; Yu et al., 2001; Liu et al., 2005), anti-protozol (Yu et al, 1994), anti-bacterial (Taylor and Towers, 1998; Liang et al., 2007b, c, d), anti-inflammatory (Qin et al., 2005a, b) and liver protective (Qian et al., 2004) properties. Our

preliminary study of the *n*-hexane soluble fraction from the ethanolic extract of *C. minima* showed strong anti-NPC effect (Su et al., 2009a). Gas chromatography-Mass spectrometry (GC-MS) analysis showed that the *n*-hexane fraction contained quite a few volatile constituents. As the volatile oil from *C. minima* was reported to be effective to treat allergic rhinitis (Yu et al., 2001; Liu et al., 2005), we hypothesized that it might also possess active volatile principals capable of controlling NPC. In this study, the volatile oils of *C. minima* extracted by steam distillation (SD) and supercritical fluid extraction (SFE) were investigated for their antiproliferative effects on the human nasopharyngeal cancer CNE cells to find out the active principals of the herb. The underlying mechanism of the active one (SFE oil), which showed a stronger effect on the induction of CNE cell death was further investigated.

## 4.2. Materials and methods

### 4.2.1. Generals

3-(4,5-dimethylthiazol-2-yl)-2,5-diphenyl tetrazolium bromide (MTT), RPMI-1640 medium, propidium iodide (PI), 4',6-diamidino-2-phenylindole (DAPI) and 5,5',6,6'-tetrachloro-1,1',3,3'-tetraethylbenzimidazolcarbocyanine iodide (JC-1) were purchased from Sigma (St. Louis, MO). ELISA-BrdU chemiluminescence assay kit, Cytotoxicity detection kit and complete™ protease inhibitor cocktail were purchased from Roche (Germany); Bradford reagent was obtained from Bio-Rad (Hercules, CA); Caspase-3 substrate (Ac-Asp-Glu-Val-Asp-*p*NA) was purchased from Calbiochem (Germany). Antibodies for caspase-3, caspase-7, caspse-8, caspase-9, poly(ADP-ribose) polymerase (PARP), Bax, Bad, Bok, Bmf, PUMA, Bcl-xL, anti-rabbit secondary horseradish peroxidase antibody, and chemiluminescent substrate were purchased from Cell Signaling Technology (Beverly, MA). Antibodies for Bcl-2, β-actin and anti-mouse secondary horseradish peroxidase antibody were obtained from Santa Cruz Biotech (Santa Cruz, CA). Antibody for cytochrome *c* was obtained from BD Biosciences (San Jose, CA). *n*-Alkanes ($C_{10}$-$C_{30}$), palmitic acid and stearic acid were brought from Aldrich

Chemical Inc. (Milwaukee, Wisconsin). Lupeol and lupeol acetate were isolated from another herb (*Elephantopus scaber*), and their structures were identified by spectroscopic methods and comparison with the published data (Su et al., 2009b). All other chemicals were analytical grade.

### 4.2.2. Plant material

The aerial parts of *C. minima* was collected in Baiyun mountain, Guangzhou, China, and were authenticated by Mr. Zhenqiu Mai, a senior herbalist at the Chinese Medicinal Material Company, Guangzhou, China. A voucher specimen (06115202) has been deposited in the Department of Biology, the Chinese University of Hong Kong.

### 4.2.3. Volatile oil extraction

Volatile oils of *C. minima* were extracted by two different methods, namely, steam distillation and supercritical fluid extraction. Briefly, in steam distillation, the dried and cut herbs (308 g) were distilled for 5 h using a Clevenger-type apparatus (800-7-B, Kimble Bomex, Beijing, China). The steam distilled oil (SD oil) was dried over anhydrous sodium sulphate and stored at -20 °C until used (yield 0.13%). In supercritical fluid extraction, a supercritical extraction equipment (HA121-50-02, Jiangsu Nantong SFE Inc., Jiangsu, China) containing a 2 L stainless steel vessel was employed to extract the herbs (309 g). Supercritical fluid extraction was conducted at a pressure of 20 MPa and at a temperature of 40 °C for a duration of 2 h. The flow rate of $CO_2$ was 20 L/h. The yield of the supercritical extracted oil (SFE oil) was 5.05%.

### 4.2.4. Cell line and cell culture

CNE (human nasopharyngeal cancer epithelial cell) cells were purchased from the Cell Bank of Type Culture Collection of the Chinese Academy of Sciences (Shanghai, China). CNE cells were maintained in the RPMI-1640 medium

supplemented with 10% fetal bovine serum (Gibco, Rockville, MD) and 1% penicillin-streptomycin. They were incubated at 37 °C, 95% relative humidity and with 5% $CO_2$ atmosphere.

### 4.2.5. MTT assay

Cell viability was determined by MTT assay. Briefly, different concentrations of samples were added to the cells after 24-h incubation in a 96-well microtiter plate. Following incubation for specific times (24, 48, and 72 h), 20 μL of the MTT solution [5 mg/mL in phosphate buffered saline (PBS)] was added to each well, and the cells were further incubated for 4 h. Medium was removed and replaced by 150 μL of DMSO in each well to dissolve the formazan crystals. The optical densities were determined by a microplate spectrophotometer (SPECTRAmax 250, Molecular Devices, Minnesota) at the wavelength of 570 nm.

### 4.2.6. 5-Bromo-2'-deoxyuridine (BrdU) chemiluminescence assay

Cell proliferation was determined by the BrdU chemiluminescence assay kit which was based on the measurement of BrdU incorporation during DNA synthesis in proliferating cells. Briefly, after incubating the cells with various concentrations of the more active oil (SFE oil) based on MTT assay for 24 h in a 96-well microtiter plate, BrdU labeling solution (100 μM, final concentration) was added, and the plate was incubated for 2 h. The labeling solution was removed and the cells were fixed with FixDenat solution for 30 min. After removal of the FixDenat solution, anti-BrdU-POD solution was added and further incubated for 1.5 h. The chemiluminescence intensity was determined according to the manufacturer's instruction.

### 4.2.7. Lactate dehydrogenase (LDH) assay

Cytotoxicity as reflected by the LDH activity was determined by the Cytotoxicity Detection Kit. Briefly, both treated and untreated cells were centrifuged at 500 *g* for

10 min at 20 °C. Supernatants (100 μL) were collected and transferred to a new 96-well microtiter plate. LDH activity was determined according to the manufacturer's instructions. Cytotoxicity was evaluated by measuring the percentage of LDH released into the medium. Cells treated with 1% triton X-100 were used as positive control (i.e. 100% lysis of the cells).

### 4.2.8. DNA contents analysis by flow cytometry

The effect of SFE oil on the cell cycle of CNE cells were determined by flow cytometry as previously described (Su et al., 2009a). Briefly, treated or untreated CNE cells were harvested and washed twice with PBS. Cells were stained with freshly prepared DNA staining solution containing PI (20 μg/mL), RNase A (200 μg/mL) and 0.1% triton X-100 after fixed in 70% ethanol at -20 °C overnight. Stained cells were then subjected to analyze by a flow cytometer (EPICS XL Flow cytometry, Beckman Coulter, Miami, FL). Cells displaying hypodiploid DNA content were quantified and regarded as the apoptotic population. In each experiment, 10000 events per sample were recorded.

### 4.2.9. Nuclear staining with 4',6-diamidino-2-phenylindole (DAPI)

Morphological changes in the nuclear chromatin of cells undergoing apoptosis were revealed by a nuclear fluorescent dye, DAPI, as previously described (Su et al., 2009a). Briefly, cells after treatment for 48 h were harvested, washed with PBS twice. After fixed with 4% paraformaldehyde and permeated with 0.1% triton X-100, the cells were stained with 2 μg/mL of DAPI for 15 min. The cells were then observed under a fluorescence microscope (Nikon Eclipse 80i, Japan).

### 4.2.10. Mitochondrial membrane potential ($\Delta\Psi m$) assay

A cationic dye, JC-1, was used to measure the depletion of mitochondrial membrane potential as previously described (Su et al., 2009a). JC-1 exhibits potential-dependent accumulation in mitochondria, indicated by a fluorescence

emission shift from green to red. Briefly, after washed with PBS twice, cells were stained with 10 μM of JC-1, incubated in dark at 37 °C for 15 min and analyzed by the flow cytometer. Data are expressed in percentage of cells with changed $\Delta\Psi m$.

### 4.2.11. Caspase activity assay

Caspase activity was determined by using the colorimetric peptite caspase-3 substrate Ac-Asp-Glu-Val-Asp-*p*NA. Briefly, cell lysates were placed in a 96-well plate, and 100 μM of the substrate was added. The plate was incubated at 37 °C for 1 h and caspase activity was determined by the microplate spectrophotometer at the wavelength of 405 nm.

### 4.2.12. Western blotting

To obtain cytosolic proteins, cells were harvested and lysed in a lysis buffer containing 250 mM sucrose, 20 mM HEPES, 1.5 mM $MgCl_2$, 10 mM KCl, 1 mM EGTA, 1 mM DTT, complete™ protease inhibitor cocktail for 30 min on ice. Then the cells were homogenized on ice. The homogenates were centrifuged for 10 min at 1000 *g* and 4 °C to remove both unlysed cells and nuclei. Then the supernatants were further centrifuged for 15 min at 14000 *g* and 4 °C to separate the cytosolic and mitochondria fractions.

The total cellular proteins were extracted by lysing cells in a lysis buffer [1% IGEPAL CA 630 (Fluka, Switzerland), 150 mM NaCl, 50 mM Tris-HCl (pH 7.5), complete™ protease inhibitor cocktail] for 30 min on ice. Lysates were clarified by centrifugation for 15 min at 14000 *g*. The supernatant was collected as the total cellular proteins.

Protein concentrations were determined with Bradford reagent. Equal amounts of proteins were separated on SDS-polyacrylamide gels, followed by electrophoretic transfer to PVDF membranes (Immobilon-P, Millipore, Bedford, MA). The membranes were blocked with 5% non-fat dry milk in TBST (Tris-Buffered Saline

Tween-20) for 1 h, followed by incubation sequentially with primary antibodies at 4 °C and the horseradish peroxidase-conjugated secondary antibodies at 20 °C. Protein bands were detected on X-ray film (Fuji, Japan) using the chemiluminescent substrate.

### 4.2.13. Analysis of chemical components and identification of compounds

The chemical compositions of the two oils were analyzed by a gas chromatography system (6890N series, Agilent, Santa Clara, CA) equipped with a 5973 series mass spectrometer (Agilent). An HP-5 ms capillary column (30 m × 0.25 mm, i.d 25 μm film thickness) was used. Helium was used as the carrier gas at a constant flow rate of 1.5 mL/min. The detector temperature was 300 °C. The analytical conditions were as follows: the oven temperature was kept at 60 °C and programmed to 150 °C at the rate of 3 °C/min and kept constant for 5 min. Then the temperature was programmed to 240 °C at the rate of 1.5 °C/min and kept constant for 10 min. The final temperature was increased to 300 °C at the rate of 2 °C/min, and kept constant for 10 min. Mass spectrum data were recorded at 70 eV. Mass interface temperature was kept at 310 °C, while mass quadruple temperature and mass source temperature were 150 and 230 °C, respectively. For analysis, oils were dissolved in acetone to prepare concentrations at 2.4 and 2.3 mg/mL for the SD and SFE oils, respectively. A volume of 5 μL was injected into the GC. Tentative identification of compounds was performed by matching each mass spectrum of an unknown with that suggested by the Wiley Chemical database (7th ed., Wiley, New York, NY). Positive identification of each compound was done by comparing the linear retention index (RI) (van den Dool and Kratz, 1963) and mass spectrum of an unknown with those of the reference compounds under the same analytical conditions as previously described (Chung et al., 1999). *trans*-Chrysanthenyl acetate was tentatively identified by comparing RI, while palmitic acid, stearic acid, lupeol and lupeol acetate were positively identified by comparing RI and mass spectrum with the reference compounds.

### 4.2.14. Statistical analysis

Data are expressed as mean ± SD. Statistical analysis was performed using Student's *t*-test. Difference with $p < 0.05$ (*) was considered statistically significant.

## 4.3. Results

### 4.3.1. Effects of volatile oils on the growth of CNE cells

In this study, both steam distillation and supercritical fluid extraction were employed to extract the volatile oils of *C. minima*. Both oils induced dose- and time-dependent inhibitory effects on the growth of CNE cells to different extents as determined by MTT assay (Figure 4.1). The inhibitory effect of the volatile oil extracted by supercritical fluid extraction (i.e. SFE oil) was much stronger than that extracted by steam distillation (i.e. SD oil). The $IC_{50}$ values of the SFE oil were 56.6, 8.7 and 5.2 μg/mL at 24-, 48- and 72-h treatments, respectively, whereas those of the SD oil were found to be 123.5 μg/mL (24 h), 97.1 μg/mL (48 h) and 83.3 μg/mL (72 h), respectively.

### 4.3.2. Antiproliferative and cytotoxic effects of SFE oil on CNE cells

As the SFE oil exerted stronger effect than the SD one, it was chosen to further confirm its antiproliferative effect on CNE cells. Various concentrations of the SFE oil were applied to the CNE cells, and DNA synthesis was analyzed by the BrdU incorporation assay. As shown in Figure 2A, CNE cell proliferation was inhibited in a dose-dependent manner after 24-h incubation. On the other hand, the integrity of the cell membrane deteriorated in a dose-dependent manner as measured by the release of LDH into the cell medium (Figure 2B).

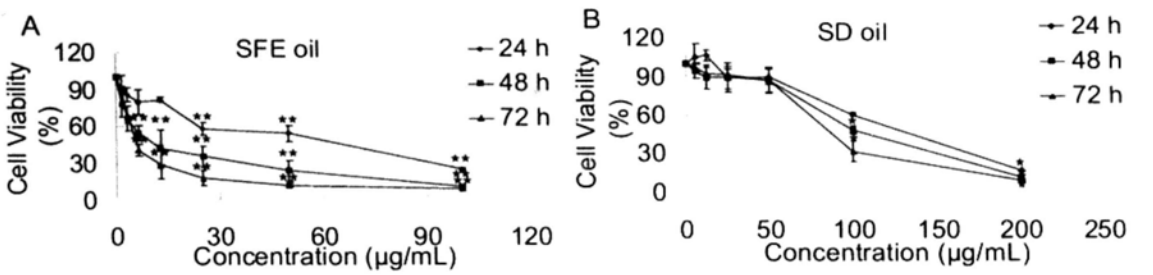


**Figure 4.1.** Effects of volatile oils prepared from *Centipeda minima* on the growth of CNE cells. CNE cells were treated with various concentrations of (A) SFE oil and (B) SD oil for different times (24, 48, and 72 h), and cell viability was determined by MTT assay. Each value represents the mean from three independent experiments. Difference between treatments and control with $p < 0.05$ (*) or $p < 0.01$ (**) was considered statistically significant.

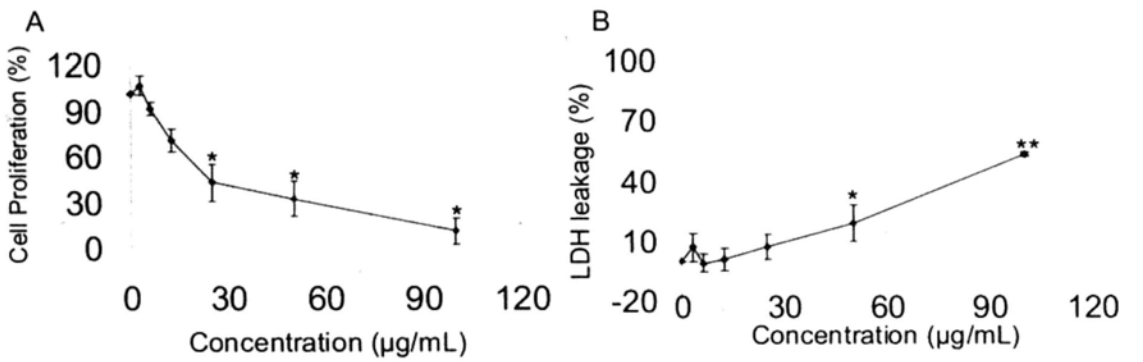


**Figure 4.2.** Antiproliferative and cytotoxic effects of SFE oil on CNE cells. (A) Effect of SFE oil on the proliferation of CNE cells. CNE cells were treated with various concentrations of the SFE oil for 24 h, and cell proliferation was determined by BrdU chemiluminescence assay. (B) Cytotoxic effect of SFE oil on CNE cells. Cells were treated with various concentrations of the SFE oil for 24 h, and cytotoxicity was determined by LDH assay. Each value represents the mean from three independent experiments. Difference between treatments and control with $p < 0.05$ (*) or $p < 0.01$ (**) was considered statistically significant.

### 4.3.3. SFE oil induced apoptosis in CNE cells

To determine whether apoptosis induction contribute to the inhibitory effect of the SFE oil on the growth of CNE cells, three apoptotic biomarkers were evaluated. Flow cytometric analysis revealed that the SFE oil (25 μg/mL) significantly increased the percentage of CNE cells at the sub-G1 phase in a time-dependent manner, ranging from 2.0 ± 0.3% at 0 h to 68.5± 6.6% at 72 h (Figure 4.3A). Dose-dependent increase in the population of sub-G1 cells was also observed in 48-h treatment (0-25 μg/mL) (Figure 4.3B). DAPI staining and caspase activity assay also confirmed induction of apoptosis in CNE cells. Indeed, irregularity in shape and cellular detachment in CNE cells treated with 25 μg/mL of SFE oil were observed under a phase-contrast microscopy. At the same time, apoptotic bodies with condensed chromatin and degraded nuclei were observed (Figure 4.4A). Caspase-3 activity was significantly augmented in the CNE cells after 48-h treatment with 12.5 and 25 μg/mL of SFE oil (Figure 4.4B), which was another hallmark of the apoptotic process.

### 4.3.4. SFE oil triggered mitochondria dysfunction in CNE cells

Mitochondria play a critical role in the apoptotic cascade (Jeong and Seo, 2008). To determine whether induction of apoptosis by SFE oil was associated with the dysfunction in mitochondria, changes in the mitochondria membrane potential ($\Delta\Psi m$) in CNE cells were evaluated by using the JC-1 dye. Figure 4.5A showed that the treatment of the SFE oil caused a significant dose-dependent change in $\Delta\Psi m$ in the CNE cells. Translocation of cytochrome *c* to cytosol was also detected after SFE oil treatment by the western analysis (Figure 4.5B).

As Bcl-2 family proteins were reported to be key regulators in the mitochondria-mediated apoptotic pathway (Wong and Puthalakath, 2008), our next study was to determine whether SFE oil could affect the expressions of these proteins. Figure 4.6 showed a remarkable increase in the level of the pro-apoptotic protein Bad,

while the expression of the pro-survival protein Bcl-xL was suppressed. However, the expressions of Bax, Bik, Bmf, PUMA and Bcl-2 were not affected by the SFE oil.

### 4.3.5. SFE oil caused caspases activation in CNE cells

The main effectors of apoptosis encompass proteases from the caspase family (Salvesen and Riedl, 2008). As shown in Figure 4.7, treatment with the SFE oil caused the cleavage of caspase-3, caspase-7, and caspase-9 in CNE cells. Such activation also led to the proteolysis of PARP, which was another biochemical hallmark of apoptosis (Figure 4.7).

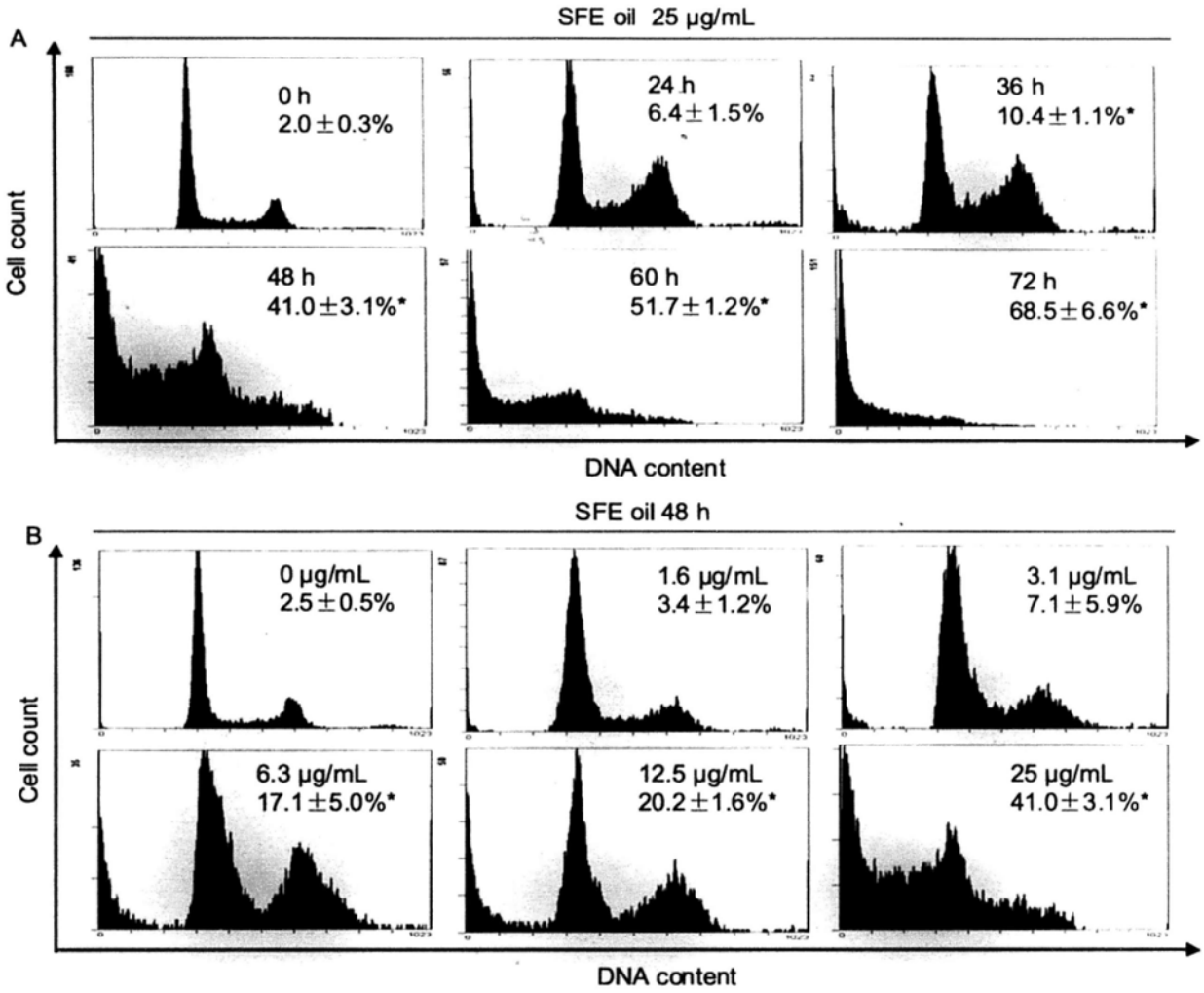


**Figure 4.3.** Effect of SFE oil on cell cycle distribution of CNE cells. (A) CNE cells were treated with 0 or 25 μg/mL of the SFE oil for 24, 36, 48, 60, and 72 h, respectively. (B) CNE cells were treated with various concentrations of SFE oil for 48 h. After treatment, the cells were stained with PI and analyzed by flow cytometry. Each value represents the mean of three independent experiments. Difference between treatments and control with $p < 0.05$ (*) was considered statistically significant.

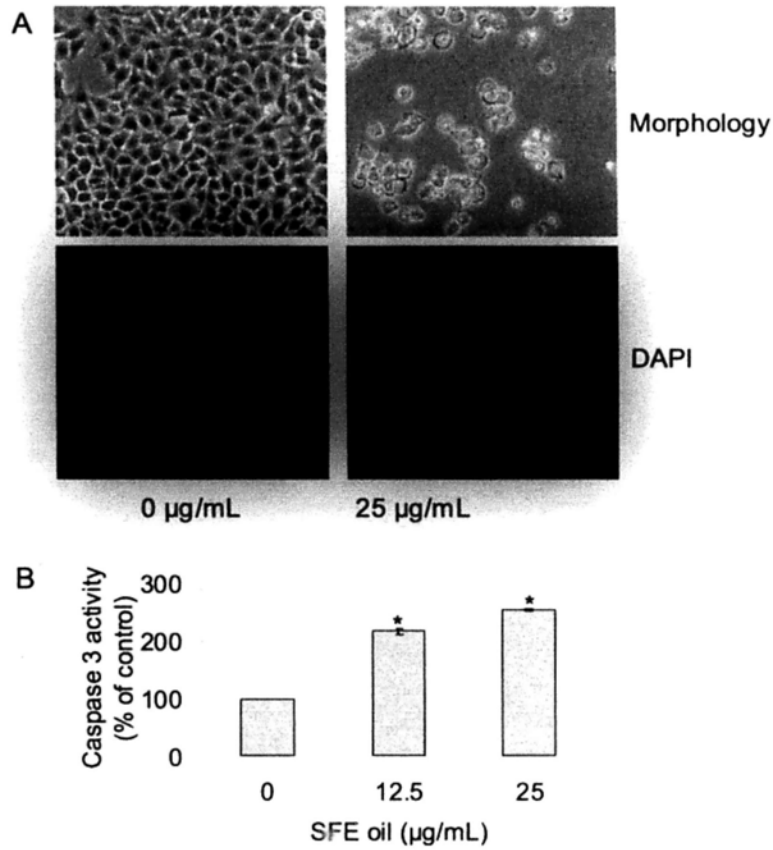


**Figure 4.4.** SFE oil induced apoptosis in CNE cells. (A) Effect of the SFE oil on the morphology of cells. Morphology: Cells were incubated with 0 or 25 μg/mL of the SFE oil for 48 h and observed under phase-contrast microscopy. DAPI: After exposure to the SFE oil for 48 h, cells were stained with DAPI and analyzed by fluorescence microscopy. (B) Activation of caspase by SFE oil. After treatment of the SFE oil for 48 h, cells were lysed, and caspase-3 activity was measured using a colorimetric caspase-3 specific substrate. Difference between treatments and control with $p < 0.05$ (*) was considered statistically significant.

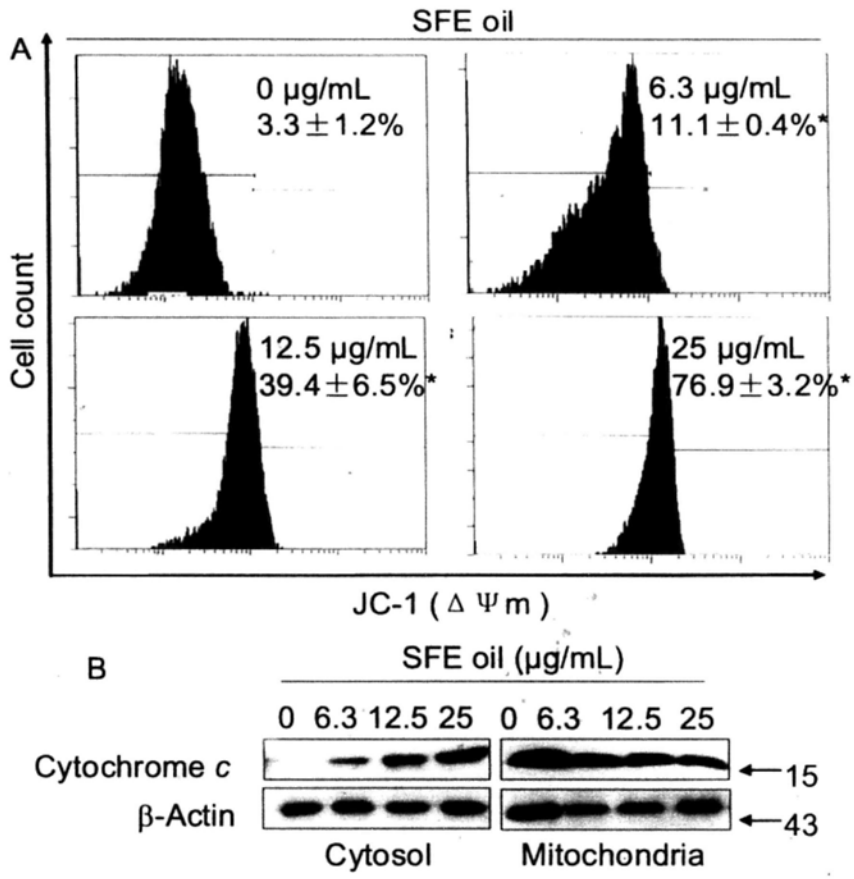


**Figure 4.5.** SFE oil induced mitochondria dysfunction in CNE cells. (A) Effect of the SFE oil on mitochondrial membrane potential ($\Delta\Psi m$). After treatment with different concentrations of the SFE oil for 48 h, cells were stained with JC-1 dye and analyzed by flow cytometry. Each value represents the mean of three independent experiments. Difference between treatments and control with $p < 0.05$ (*) was considered statistically significant. (B) The level of cytochrome *c* in the cytosol and mitochondria. β-Actin was used as the loading control. All experiments were repeated three times, and a representative blot is shown.

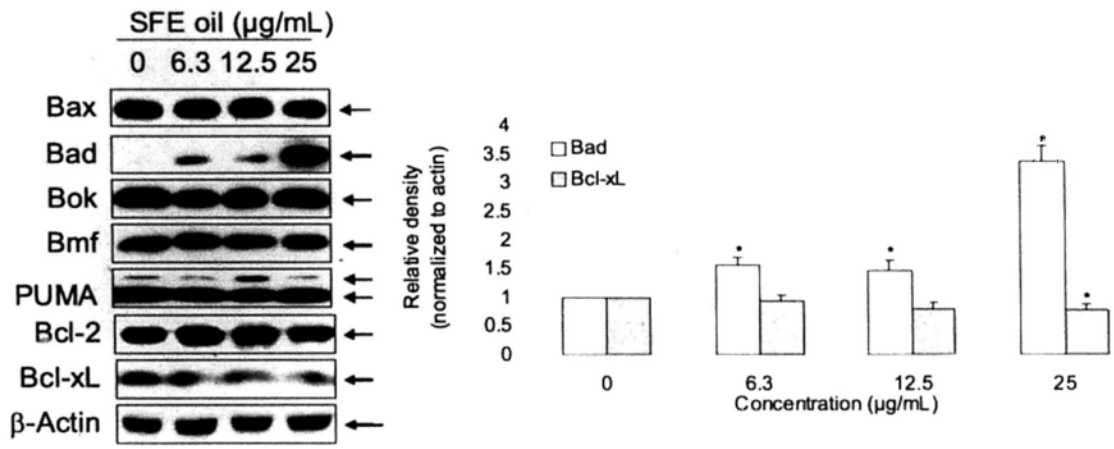


**Figure 4.6.** Effect of the SFE oil on the expressions of Bcl-2 family proteins. β-Actin was used as the loading control. Results were representatives of three independent experiments. The values on the right figure represent relative density of the bands of Bad and Bcl-xL normalized to β-actin.

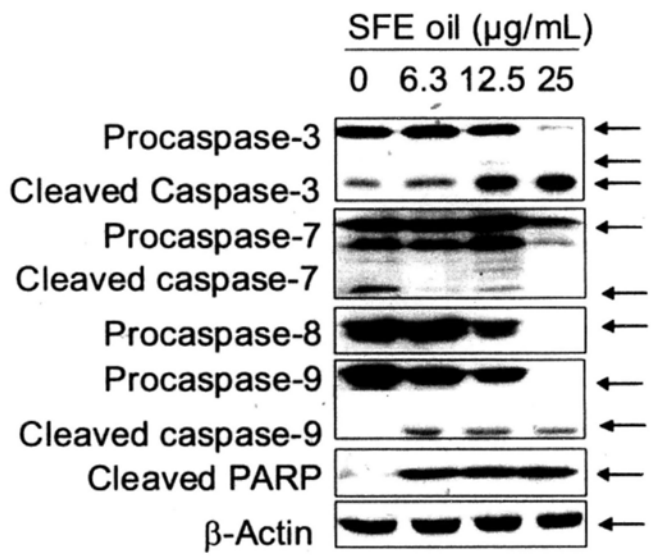


**Figure 4.7.** SFE oil triggered caspases activation in CNE cells. Cell lysates were separated by SDS-PAGE and immunoblotted with specific primary antibodies. β-Actin was used as the loading control. All experiments were repeated three times, and a representative blot is shown.

### 4.3.6. GC-MS analysis of the volatile oils

Since CNE cells showed different susceptibility to SFE oil and SD oil, GC-MS was utilized to compare the compositions of the two oils. Results showed that their compositions were markedly different (Figure 4.8, Table 4.1). In SFE oil, components were mostly found in retention times between 70 to 120 min with an area percentage of 42.25% (Table 4.2). Components located in this region have common mass/charge (*m/z*) fragments of 173, 231, 246 (or 247), 264 (Table 4.2), indicative of the presence of homologues of 11, 13-dihydrohelenalin (Figure 4.7B), the pseudoguaianolide-type sesquiterpene lactone (Willuhn et al., 1983). Additionally, another 37.67% of the components in the SFE oil eluted after 120 min. They were lupeol and its derivatives on the basis of their mass spectra (Table 4.2). Fatty acids and monoterpenes dominated the first 70 min and accounted for 19.75% of the total components in the SFE oil. On the contrary, components of the SD oil were mainly eluted in retention times before 70 min. Their identities were the same as those found in the first 70 min of the SFE oil.

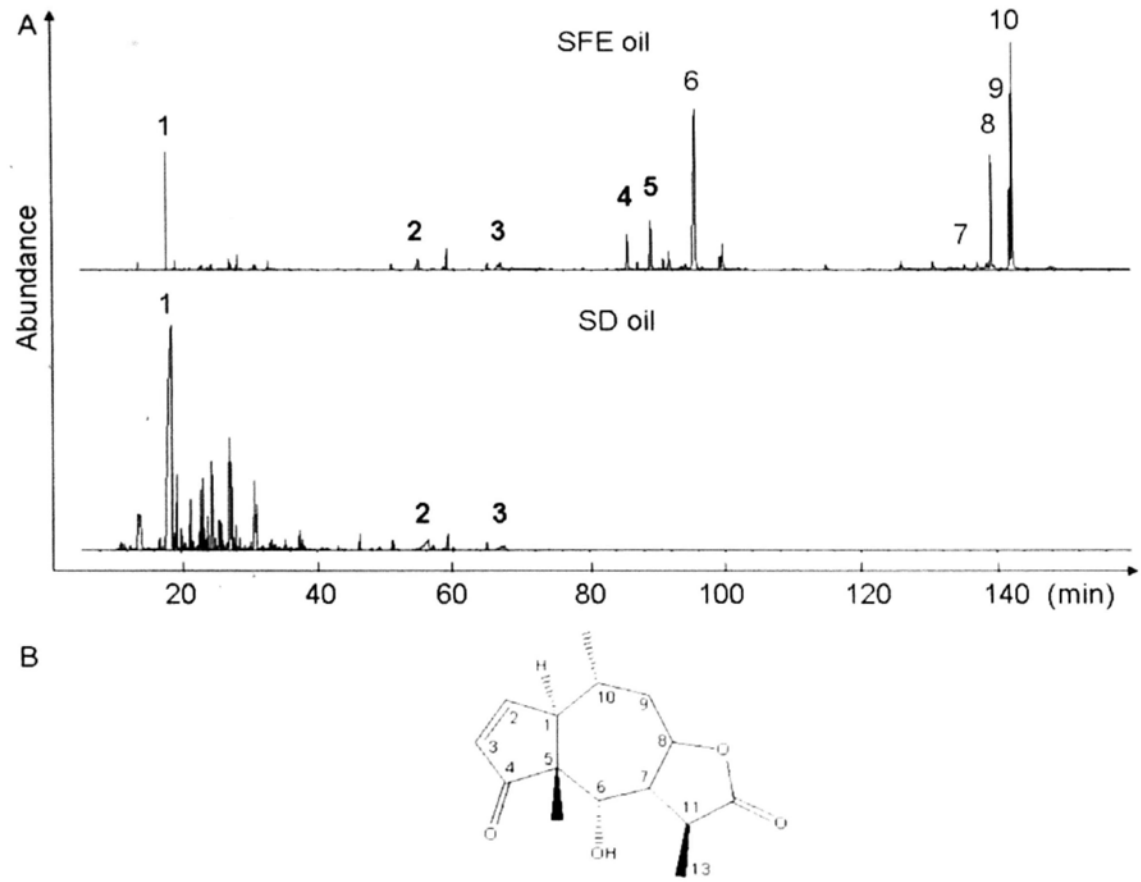


**Figure 4.8.** GC-MS analysis of volatile oils from *Centipeda minima* and chemical structure of 11, 13-dihydrohelenalin. (A) GC profiles of the two volatile oils, namely, supercritical fluid extracted oil (SFE oil) and steam distilled oil (SD oil); **1**. *trans*-Chrysanthenyl acetate (retention time: 17.683 min; RI=1242); **2**. palmitic acid (retention time: 54.598 min; RI=1970); **3**. stearic acid (retention time: 68.579 min; RI=2162); **4**. unknown (retention time: 85.306 min, RI=2414); **5**. unknown (retention time: 88.768 min, RI=2468); **6**. unknown (retention time: 95.275 min, RI=2575); **7**. lupeol (retention time: 134.904 min; RI>3000) ; **8**. lupeol acetate (retention time: 138.732 min; RI>3000). **9**. unknown (retention time: 141.444 min, RI>3000); **10**. unknown (retention time: 141.861 min, RI>3000). *trans*-Chrysanthenyl acetate (**1**) was tentatively identified by comparing RI, while palmitic acid (**2**), stearic acid (**3**), lupeol (**7**) and lupeol acetate (**8**) were positively identified by comparing RI and mass spectrum with the reference compounds. (B) Chemical structure of 11, 13-dihydrohelenalin.

**Table 4.1.** Area percentage of components of the two volatile oils

| Sample | Area percentage (%) | | |
|---|---|---|---|
| | 0-70 (min) | 71-120 (min) | 121-160 (min) |
| SFE oil | 19.75 | 42.25 | 37.67 |
| SD oil | 100 | 0 | 0 |

**Table 4.2.** Major mass/charge (*m/z*) fragments of the unknown components in the SFE oil eluted between 70 to 120 min, and 120 to 160 min from the GC-MS

| Compound (Retention time) | Major mass/charge (*m/z*) fragment |
|---|---|
| Unknown compound **4** (85.306 min) | 69, 145, 173, 231, 246, 264 |
| Unknown compound **5** (88.768 min) | 69, 145, 173, 231, 246, 264 |
| Unknown compound **6** (95.275 min) | 83, 173, 231, 246, 247, 264 |
| Unknown compound **9** (141.444 min) | 121, 189, 229, 365, 408, 468 |
| Unknown compound **10** (141.861 min) | 121, 189, 229, 365, 408, 468 |

## 4.4. Discussion

In this study, results of the MTT assay showed that CNE cells were sensitive to volatile oils prepared from *C. minima*. Particularly, the effect of the SFE oil on CNE cells was much stronger than that of the SD oil (Figure 4.1). Further investigation on the SFE oil using BrdU assay showed a significant dose-dependent antiproliferative effect on the CNE cells (Figure 4.2A). Interestingly, the SFE oil also induced cell membrane damaged as reflected by the LDH release to the medium (Figure 4.2B). LDH, a stable cytoplasmic enzyme present in cells, was released into the medium upon damage of the plasma membrane. Since under the *in vitro* cell culture conditions, the apoptotic cells cannot undergo rapid phagocytosis as *in vivo* conditions (Hu et al., 2007), LDH release in this investigation could be a feature of the late apoptotic cell death (Grub et al., 2000). Inhibition of apoptosis is reported to be critical to NPC tumorigenesis (Chou et al., 2008). To elucidate the mode of cell death induced by SFE oil, further experiments were carried out. Results revealed that apoptosis was induced by SFE oil as evidenced by the augmentations of sub-G1 population (Figure 4.3), fragmentation of DNA and condensation of nuclei (Figure 4.4A), elevation of caspase-3 activity (Figure 4.4B), and cleavage of PARP (Figure 4.6).

Recent studies have unraveled the critical function of mitochondria at the core of the apoptotic pathway (Adams, 2004; Jeong and Seo, 2008). Both the loss in the mitochondria membrane potential ($\Delta\Psi m$) and the release of apoptogenic factors such as cytochrome *c* from the mitochondria were related to the dysfunction in mitochondria, and led to apoptosis (Jeong and seol, 2008). In the present study, the SFE oil showed the same two observations, i.e. significant depletion of $\Delta\Psi m$ and the release of cytochrome *c* to cytosol in a dose-dependent manner (Figure 4.5A and 4.5B).

Members of the Bcl-2 family proteins, which are categorized into pro-survival

(anti-apoptotic) and pro-apoptotic family members, precisely regulate the mitochondria-mediated pathway by controlling the mitochondrial outer membrane permeability (Chipuk and Green, 2008). The pro-survival family proteins are localized on the cytoplasmic part of the nuclear envelope, the endoplasmic reticulum, and the outer mitochondrial membrane. But the pro-apoptotic family proteins are translocated to the outer mitochondrial membrane, then oligomerized and permeabilized the outer mitochondrial membrane to release pro-apoptogenic factors such as cytochrome *c*, and promote activation of caspases (Wong and Puthalakath, 2008). Figure 4.6 showed that the SFE oil up-regulated the expression of the pro-apoptotic protein Bad, whereas down-regulated the expression of the pro-survival protein Bcl-xL. These observations confirmed that the SFE oil triggered mitochondria dysfunction by regulating the expression of the Bcl-2 family proteins.

The release of cytochrome *c* into the cytosol causes the formation of the apoptosome by recruiting both Apaf-1 and caspase-9. The activation of caspase-9 sequentially activates caspase-3 and caspase-7 (MacKenzie and Clark, 2008). Our results showed that caspase-3, caspase-7, and caspase-9 were all activated (Figure 4.7), confirming that caspases activation were involved in apoptosis induced by SFE oil.

Different compositions between the two volatile oils accounted for their different activities (Figure 4.8), indicating that the active principals in *C. minima* could be recovered more effectively by the supercritical fluid extraction. Components in the SD oil were all found in the retention times between 0-70 min, suggesting components of fatty acids and monoterpenes in this region may be probably not the active principals. On the other hand, lupeol (**7**) and lupeol acetate (**8**) showed less effect on the CNE cells having $IC_{50}$ values larger than 20 μg/mL at 72-h treatment (Su et al., 2009b), suggesting components eluted between 120-160 min were also less likely to contain the active principals.

As described previously, most components in the SFE oil were eluted between 70-120 min, and contributed 42.25% of the total amount. From the mass spectra

(Figure 4.8B), most of the components in this period were the homologues of 11, 13-dihydrohelenalin (Figure 4.8A), the pseudoguaianolide-type sesquiterpene lactone (Willuhn et al., 1983). Several studies have documented that supercritical fluid extraction was both selective and highly efficient in the isolation of sesquiterpenes (Stashenko et al., 1996; Fadel et al., 1999; Stashenko et al., 2004). In fact, phytochemical studies of *C. minima* have identified more than ten sesquiterpene lactones which were either pseudoguanianolide or guaianolide types (Bohlmann and Chen, 1984; Wu et al., 1985, 1991; Yu et al., 1994; Taylor et al., 1998; Liang et al., 2007d). Their anti-allergic and anti-bacterial activities were reported and were due to the possessing of the bioactive functional group in the sesquiterpene lactone, such as the α-methylene-γ-lactone ring and the α,β-unsaturated cyclopentenone moiety. Recently, 6-*O*-angeloylenolin, an 11, 13-dihydrohelenalin-type sesquiterpene lactone isolated from the herb was shown to inhibit the growth of HL-60 cells with $IC_{50}$ value of 4 μg/mL by modulation of *Bcl-2* gene family expression and destruction of mitochondrial function (Li et al., 2008). Our SFE oil also induced mitochondria-mediated signaling pathway by regulating the expression of the Bcl-2 family proteins. Therefore, we deduced that sesquiterpene lactones eluted between 70 to 120 min were likely responsible for the potent anti-NPC property of SFE oil.

### 4.5. Conclusions

In conclusion, supercritical fluid extraction is more effective than the steam distillation to recover the active principals in *C. minima*, particularly, the sesquiterpene lactones. The SFE oil, as the active fraction of *C. minima*, significantly inhibited the growth of CNE cells by induction of apoptosis. This study provided important evidence on the anti-NPC potential of the volatile oil from *C. minima*, and sesquiterpene lactones could be a leading group of compounds displaying anti-NPC effects. However, the active compositions involved in its anti-NPC action have yet to be elucidated. Bioactivity-guided isolation of the active compositions in the SFE oil is needed.

# Chapter 5: 6-*O*-Angeloylenolin isolated from the volatile oil of *Centipeda minima* induced cell cycle arrest and apoptosis in human nasopharyngeal cancer CNE cells

## 5.1. Introduction

Nasopharyngeal carcinoma (NPC), originated from the epithelial lining of the nasopharynx, is the most common cancer in the head and neck regions (Yu and Yuan, 2002). Its occurrence is very low in most parts of the world, with annual incidence below 1 per 100,000 persons. However, unusually high incidence (>20/100,000 persons per year) is recorded among the Cantonese who inhabit in the Guangdong Province and Hong Kong SAR in southern China (Parkin, 2006). The combination of radiotherapy and adjuvant chemotherapy has become the prevalent treatment of NPC (Wang et al., 2002) due to its high sensitivity to radiotherapy and chemotherapy. Most chemotherapies of NPC currently are cisplatin-based agents. However, the best chemotherapy regimen has not been set up so far as a significant increase in acute and late toxicities, and resistance were observed in the concurrent chemotherapies (Wang et al., 2008; Xie et al., 2008). Therefore, there is a necessity of developing less toxic and more effective agents for NPC.

The cell cycle is a set of events responsible for cell duplication. Progression of the eukaryotic cell through the cell cycle is mediated by sequential activation and inactivation of cyclin-dependent kinases (CDKs). These activation are modulated by several activators (e.g. cyclins) and inhibitors (e.g. Ink4, and Cip and Kip inhibitors) (Malumbres and Barbacid, 2009). Cyclin D complexes with CDK4 and CDK6 during early G1 phase, which is crucial to the cell cycle by coupling extracellular signals to the cell cycle. Upon mitogenic stimulation, cyclin D/CDK complexes are activated and the cells progress from G0 into G1 phase. On the other hand, cyclin E activates CDK2 during the G1-to-S phase transition. Cyclin A binds to CDK2 during S-phase or to cdc2 in the G2-to-M phase transition (Pucci et al., 2000). The cdc2/cyclin B1

complex functions during the G2-to-M transition (de Souza et al., 2000). The CDK activity is also mediated by the CDK-inhibitory subunits (CKIs), which includes the Cip/Kip and the INK4 families. The Cip/Kip family, such as $p21^{Waf1/Cip1}$, predominantly inhibits the CDKs of the G1-to-S phase transition. In NPC, normal regulation of cell cycle progression is dysregulated (Chou et al., 2008). Inhibition of dysregulated cell cycle progression thus serves as an important strategy to halt the proliferation of NPC.

Apoptosis, an essential process for maintaining homeostasis in multi-cellular organisms, plays a crucial role in the control of various types of cancers (Shi, 2002). Two major apoptotic pathways, e.g. the extrinsic and the intrinsic pathways, have been identified in mammalian cells (Fulda, 2009). The extrinsic pathway is associated with the ligation of death receptors, such as Fas and TRAIL receptors (MacKenzie and Clark, 2008). The intrinsic pathway is regulated by Bcl-2 family proteins, which mediate the release of apoptogenic factors into the cytosol, such as cytochrome *c*, apoptosis-inducing factor (AIF), endonuclease G (Endo G), and SMAC/Diablo (Candé et al., 2002). Inhibition of apoptosis is also considered to be critical to NPC tumorigenesis. Researches have showed that up-regulation of antiapoptotic factors, such as Bcl-2, accounted for the dysregulation of apoptosis in NPC (Chou et al., 2008). A better understanding of the mechanisms by which NPC cells escape from apoptosis should contribute to the development of novel, targeted treatments for NPC.

*Centipeda minima* (L.) A. Br. (Compositae), a Chinese medicinal herb, is used to treat nasal allergies, rhinitis and sinusitis, cough and headache in China (Lin and Shi, 2005). In addition, it is used in the Chinese folk medicine to treat nasopharyngeal carcinoma (Wu et al., 1985; Zhang, 2000). Recently, we elucidated the potential of 2β-(isobutyryloxy)florilenalin (IF), a sesqutierpene lactone isolated from *C. minima* (Su et al., 2009a) and the volatile oil (SFE oil) extracted by supercritical fluid extraction from *C. minima* for the treatment of NPC. Both IF and SFE oil induced

apoptosis in CNE cells. The present study focused on another sesquiterpene lactone, 6-*O*-angeloylenolin, which was isolated as the major component in a bioactivity-guided approach from the SFE oil of *C. minima*. 6-*O*-Angeloylprenolin was reported to have anti-bacterial and anti-allergic effects (Taylor and Towers, 1998; Yu et al., 1994; Wu et al., 1985). It also showed inhibitory effects on platelet activating factor (PAF) (Iwakami et al., 1992) and FPTase (Oh et al., 2006). Besides, 6-*O*-angeloylenolin was reported to exert inhibitory effect on the human leukemia HL-60 cells and the solid cancer growth in Lewis lung cancer xenograft model (Li et al., 2008). Although the potential functions of 6-*O*-angeloylenolin were reported, its anti-NPC potential has yet to be elucidated.

In this study, the human nasopharyngeal cancer CNE cells were employed as a cell model to evaluate the *in vitro* anti-NPC potential of 6-*O*-angeloylenolin. We provided evidence that the effect of 6-*O*-angeloylenolin on CNE cell growth was associated with cell-cycle progression and induction of apoptosis. Their underlying mode of action leading to its profound effects was also investigated.

## 5.2. Materials and methods

### 5.2.1. Materials

6-*O*-Angeloylenolin, isolated from the volatile oil of *C. minima*, was provided by Prof. Yaolan Li, Jinan University, Guangzhou, China. 3-(4,5-dimethylthiazol-2-yl)-2,5-diphenyl tetrazolium bromide) (MTT), RPMI-1640 medium, propidium iodide (PI), 4',6-diamidino-2-phenylindole (DAPI), 5,5',6,6'-tetrachloro-1,1',3,3'-tetraethylbenzimidazolcarbocyanine iodide (JC-1) and cisplatin were purchased from Sigma (St. Louis, MO). DMEM medium and fetal bovine serum were obtained from Gibco (Rockville, MD). ELISA-BrdU chemiluminescence assay kit, Annexin-V-FLUOS staining kit, cytotoxicity detection kit and complete™ protease inhibitor cocktail were purchased from Roche (Germany). Bradford reagent was purchased from Bio-Rad (Hercules, CA).

Caspase-3 substrate (Ac-Asp-Glu-Val-Asp-*p*NA), the pan-caspase inhibitor (z-VAD-fmk), SP600125 and U0126 were purchased from Calbiochem (Germany). Anti-Bcl-2, anti-β-actin and anti-mouse secondary horseradish peroxidase antibody were obtained from Santa Cruz Biotech (Santa Cruz, CA). Anti-cytochrome *c*, anti-cyclin A and anti-cyclin E were obtained from BD Biosciences (San Jose, CA). All other primary antibodies used in this study, anti-rabbit secondary horseradish peroxidase antibody, chemiluminescent substrate, and LY294002 were purchased from Cell Signal Technology (Beverly, MA). All other chemicals were reagent grade.

### 5.2.2. Cell line and cell culture

Human nasopharyngeal cancer cells (CNE) and human normal skin cells (Hs68) were purchased from the Cell Bank of Type Culture Collection of Chinese Academy of Sciences (Shanghai, China) and the American Type Culture Collection (Rockville, MD), respectively. CNE cells were maintained in RPMI-1640 medium, while Hs68 cells were maintained in DMEM medium. Both media were supplemented with 10% fetal bovine serum and 1% penicillin-streptomycin at 37 °C in a humidified incubator with 5% $CO_2$ atmosphere.

### 5.2.3. MTT assay

Cell viability was determined by MTT assay (Mosmaan, 1983). Briefly, 6-*O*-angeloylenolin and cisplatin (0, 1, 2, 4, 8, 16 μg/mL) were added to the cells after 24-h incubation in a 96-well microtiter plate. Following incubation for specific times, 20 μL of the MTT solution [5 mg/mL in phosphate buffered saline (PBS)] was added to each well, and the cells were further incubated for 4 h. Excess medium was removed and replaced by 150 μL of DMSO in each well to dissolve the formazan crystals. The optical densities were determined by a microplate spectrophotometer (SPECTRAmax 250, Molecular Devices, Minnesota) at the wavelength of 570 nm.

### 5.2.4. ELISA-BrdU chemiluminescence assay

Cell proliferation was determined by the ELISA-BrdU (5-bromo-2'-deoxyuridine) chemiluminescence assay kit which was based on the measurement of BrdU incorporation during DNA synthesis in proliferating cells. Briefly, after incubating the cells with various concentrations of 6-*O*-angeloylenolin for 24 h in a 96-well microtiter plate, BrdU labeling solution (100 μM, final concentration) was added, and the plate was incubated for 2 h. The labeling solution was removed and the cells were fixed with FixDenat solution for 30 min. After removal of the FixDenat solution, anti-BrdU-POD solution was added and further incubated for 1.5 h. The chemiluminescence intensity was determined according to the manufacturer's instruction. Cell proliferation was expressed as the percentage relative to the control which contained no 6-*O*-angeloylenolin.

### 5.2.5. Lactate dehydrogenase (LDH) assay

Cytotoxicity as reflected by the LDH activity was determined by the Cytotoxicity Detection Kit. Briefly, both treated and untreated cells were centrifuged at 500 *g* for 10 min at 20 °C. Supernatants (100 μL) were collected and transferred to a new 96-well microtiter plate. LDH activity was determined according to the manufacturer's instruction. Cytotoxicity was evaluated by measuring the percentage of LDH released into the medium. Cells treated with 1% triton X-100 were used as positive control (i.e. 100% lysis of the cells).

### 5.2.6. Cell cycle analysis

The cell cycle distribution was determined by flow cytometry. Briefly, treated or untreated CNE cells were harvested and washed with PBS twice. Cells were stained with freshly prepared DNA staining solution containing PI (20 μg/mL), RNase A (200 μg/mL) and 0.1% triton X-100 after fixed in 70% ethanol at -20 °C overnight. Stained cells were then subjected to analyze by a flow cytometer (EPICS XL Flow cytometry, Beckman Coulter, Miami, FL). MultiCycle software (Phoenix Flow

Systems, San Diego, CA) was used to analyze cell cycle distribution. The proportion of cells in G1, S, G2/M phases was represented as DNA histograms. Cells displaying hypodiploid DNA content as reflected by the sub-G1 peak in the cell cycle distribution were quantified and regarded as the apoptotic population. In each experiment, 10000 events per sample were recorded.

### 5.2.7. Annexin-V-FLUOS staining assay

Translocation of phosphatidylserine (PS) in the inner part of the plasma membrane to the outer layer is an early marker of apoptosis. Annexin-V is a $Ca^{2+}$ -dependent phospholipid-binding protein with high affinity for PS. Hence, it is suitable to detect apoptotic cells. In this study, the Annexin-V-FLUOS staining kit was employed. Briefly, after treatment with 6-*O*-angeloylenolin for specific times, CNE cells were collected and washed with PBS. Then the cell pellet was resuspended in the Annexin-V-FLUOS labeling solution which contained Annexin-V-Fluorescein and PI. After incubated for 15 min, the samples were analyzed by a flow cytometer. In each experiment, 10000 events per sample were recorded.

### 5.2.8. Nuclear staining with DAPI

Morphological changes in the nuclear chromatin of cells undergoing apoptosis were revealed by a nuclear fluorescent dye, DAPI, as described previously (Su et al., 2009a). Briefly, cells after treatment for 24 h were harvested, washed with PBS twice. After fixed with 4% paraformaldehyde and permeated with 0.1% triton X-100, the cells were stained with 2 μg/mL of DAPI for 15 min. The cells were then observed under a fluorescence microscope (Nikon Eclipse 80i, Japan).

### 5.2.9. Caspase-3 activity assay

Caspase-3 activity was determined by using the colorimetric peptite caspase-3 substrate Ac-Asp-Glu-Val-Asp-*p*NA. Briefly, cell lysates were placed in 96-well plate, and 100 μM of the substrate was added. The plate was incubated at 37 °C for 1

h and caspase activity was determined by the microplate spectrophotometer at the wavelength of 405 nm.

### 5.2.10. Mitochondrial membrane potential ($\Delta\Psi m$) assay

JC-1, a cationic dye, which exhibits potential-dependent accumulation in mitochondria, indicated by a fluorescence emission shift from green to red, was employed to measure the depletion of mitochondrial membrane potential. Briefly, after washed with PBS twice, cells were stained with 10 μM of JC-1. After incubation in dark at 37 °C for 15 min, cells were analyzed by a flow cytometer. The percentage of the green fluorescence from JC-1 monomers was used to represent the cells that changed $\Delta\Psi m$.

### 5.2.11. Western blotting

To obtain cytosolic proteins, cells were harvested and lysed in hypotonic lysis buffer (250 mM sucrose, 20 mM Hepes, 1.5 mM $MgCl_2$, 10 mM KCl, 1 mM EGTA, 1 mM DTT, complete™ protease inhibitor cocktail) for 30 min on ice. Then the cells were homogenized in a Dounce homogenizer with optimal gentle strokes. After centrifugation at 1000 *g* for 10 min at 4 °C to remove the unlysed cells and nuclei, the supernatants were further centrifuged at 14 000 *g* for 15 min at 4 °C. The supernatant was collected as the cytosolic proteins.

The total cellular proteins were extracted by lysing cells in a lysis buffer [1% IGEPAL CA 630 (Fluka, Switzerland), 150 mM NaCl, 50 mM Tris-HCl (pH 7.5), complete™ protease inhibitor cocktail] for 30 min on ice. Lysates were clarified by centrifugation for 15 min at 14000 *g*. The supernatant was collected as the total cellular proteins.

Protein concentrations were determined with Bradford reagent. Equal amounts of proteins were resolved on 7.5-12% SDS-polyacrylamide gels, followed by electrophoretic transfer to PVDF (Polyvinylidene fluoride, Millipore, Bedford, MA)

membranes. The membranes were blocked with 5% non-fat dry milk in TBST (Tris-Buffered Saline Tween-20) for 1 h, followed by incubation sequentially with primary antibodies at 4 °C and the horseradish peroxidase-conjugated secondary antibodies at 20 °C. Protein bands were detected on X-ray film (Fuji, Japan) using the chemiluminescent substrate. Afterwards, membranes were re-blotted with anti-β-actin antibody for normalization and equal protein loading.

### 5.2.12. Statistical analysis

All results were expressed as mean ± SD. Statistical analysis was performed using SPSS statistical package (SPSS 16.0 for windows, SPSS, Inc., Chicago, IL). Difference between two groups was analyzed by two-tailed Student's *t*-test. With more than two groups, they were compared by one-way ANOVA. Multiple comparison using post hoc were carried out if ANOVA was shown to be significant. Statistical significance was set at $p < 0.05$ (*), $p < 0.01$ (**) or $p < 0.001$ (***).

## 5.3. Results

### 5.3.1. 6-*O*-Angeloylenolin inhibited the growth of CNE cells

The inhibitory effect of 6-*O*-angeloylenolin on the growth of CNE cells was determined by MTT assay. As shown in Figure 5.2A, 6-*O*-angeloylenolin caused a dose-dependent inhibition on the growth of CNE cells under 24-h treatment, accounting for 12-56% inhibition at various concentrations (1-16 μg/mL). On the contrary, its inhibitory effect on the normal Hs68 cells was much less than that on the CNE cells (Figure 5.2A). When the incubation time was increased to 48 h, the inhibitory effect of 6-*O*-angeloylenolin on CNE cells increased dramatically, accounting for 10-84% inhibition, which was comparable to that of the positive control (2-83%), namely, cisplatin, which was clinically used to treat NPC (Figure 5.2B). To further study the effect of 6-*O*-angeloylenolin on the proliferation of CNE cells, ELISA-BrdU assay was employed to analyze DNA synthesis of CNE cells exposed to 6-*O*-angeloylenolin. Results showed that treatment with increasing

concentrations of 6-*O*-angeloylenolin contributed to an increase in the inhibition of cell proliferation after 24 h (Figure 5.2C). Additionally, results on the cell membrane integrity as determined by LDH assay showed that 6-*O*-angeloylenolin induced LDH leakage in CNE cells in a dose-dependent manner (Figure 5.2D).

### 5.3.2. 6-*O*-Angeloylenolin induced cell cycle arrest in CNE cells

To delineate the mechanism responsible for the action of 6-*O*-angeloylenolin on the death of the CNE cells, cell cycle distribution was determined by the flow cytometry. Results showed that treatment with 6-*O*-angeloylenolin caused a significant inhibition of cell cycle progression in the CNE cells, resulting in a clear increase in the percentage of cells in both S and G2/M phases when compared with the control at 24-h treatment. The percentage of cells in the S phase increased by 12.5% from 23.9 to 36.4% while that of G2/M phase increased by 13.5% from 7.4 to 20.9%. Concomitant with these increases, 6-*O*-angeloylenolin induced a significant decrease in the percentage of cells in the G0/G1 phase by 25.9%, from 68.6 to 42.7% (Figure 5.3A).

To investigate the time course for the cell cycle arrest, CNE cells were treated with 16 μg/mL of 6-*O*-angeloylenolin and incubated for various times (0, 6, 12, 18 and 24 h). Cells were harvested and the cell cycle profiles were evaluated by the flow cytometry. Results (Figure 5.3B) showed that S and G2/M populations significantly increased as early as 12 h. Population in S phase continued to increase in the next 12 h, whereas G2/M population peaked at approximately 18 h, and decreased afterwards. However, the sub-G1 population which reflects the apoptotic cells was maintained at less than 10% at the aforementioned times (Figure 5.3B).

Due to the arrest in both S and G2/M phases in the CNE cells, the effects of 6-*O*-angeloylenolin on cell cycle-regulatory proteins were examined. The protein expressions of cyclin A, cyclin E, cyclin D1, cyclin D3, CDK4, CDK6, p-Rb and $p21^{Waf1/Cip1}$, which are known to regulate the G0/G1-S phases were firstly evaluated.

Results (Figure 5.4A) showed that 6-*O*-angeloylenolin decreased the expression of cyclin A at a concentration of 16 μg/mL after 24-h treatment. Besides, 6-*O*-angeloylenolin caused a pronounced decreased in the expressions of cyclin D1 and cyclin D3 which started early after 1-h treatment. It also led to the decrease in the expression of CDK4 after 12-h treatment, but showed no effect on the expression of CDK6. 6-*O*-Angeloylenolin down-regulated the expressions of both cyclin E and p-Rb (Ser780). Additionally, the expression of $p21^{Waf1/Cip1}$ in CNE cells was very weak, and after exposed to 6-*O*-angeloylenolin, its expression was further reduced in the 18-h treatment. We further confirmed the absence of p53 (no band was observed in the western blotting), the tumor suppressor protein, in CNE cells as reported in the literature data (Li et al., 2007).

We next evaluated the expression levels of key regulators in the G2/M phase. Cdc2/cyclin B1 acts as an M-phase kinase. No change in the cyclin B1 expression was observed in the CNE cells after exposed to 6-*O*-angeloylenolin at either the studied time points or the treated doses (Figure 5.4B). In contrast, the expressions of cdc2 and its phorsphorylated form p-cdc2 (Tyr15) were markedly down-regulated which started after 12-h treatment. Moreover, cdc25c and its phorsphorylated form p-cdc25c (Ser216) were pronouncedly reduced early after 1-h treatment. Besides, it decreased the expressions of cdc25c and p-cdc25c (Ser216) at a concentration as low as 4 μg/mL at 24-h treatment.

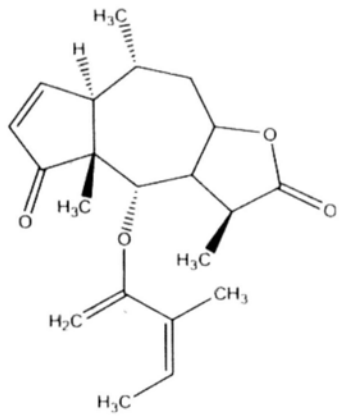

**Figure 5.1.** Chemical structure of 6-*O*-angeloylenolin

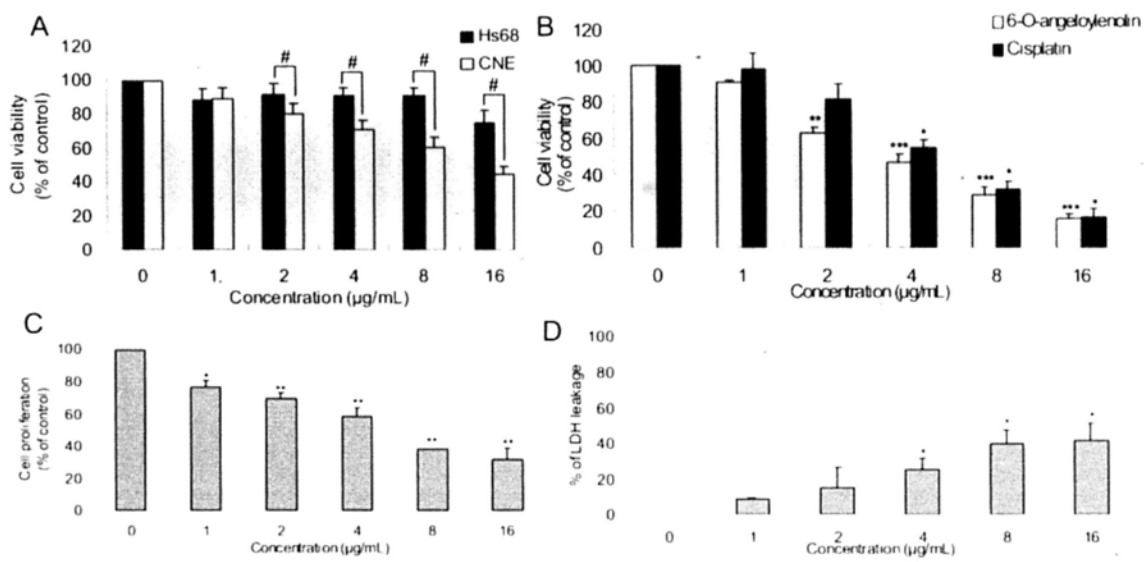


**Figure 5.2.** Effect of 6-*O*-angeloylenolin on cell growth. (A) Hs68 and CNE cells were treated with 6-*O*-angeloylenolin for 24 h and the viability was determined by MTT assay. (B) CNE cells were treated with 6-*O*-angeloylenolin and cisplatin (positive control) for 48 h, respectively, and the cell viability was determined by MTT assay. (C) CNE cells were exposed to 6-*O*-angeloylenolin for 24 h and cell proliferation was evaluated by ELISA-BrdU assay. (D) CNE cells were exposed to 6-*O*-angeloylenolin for 24 h and LDH leakage was measured by LDH assay. Each value is expressed as mean ± SD ($n$ = 3). Significant difference between CNE cells and Hs68 cells at the same concentration of 6-*O*-angeloylenolin is indicated at $p < 0.05$ (#) level; Significant difference between treatment and control groups is indicated at $p < 0.05$ (*), $p < 0.01$ (**) or $p < 0.001$ (***) level.

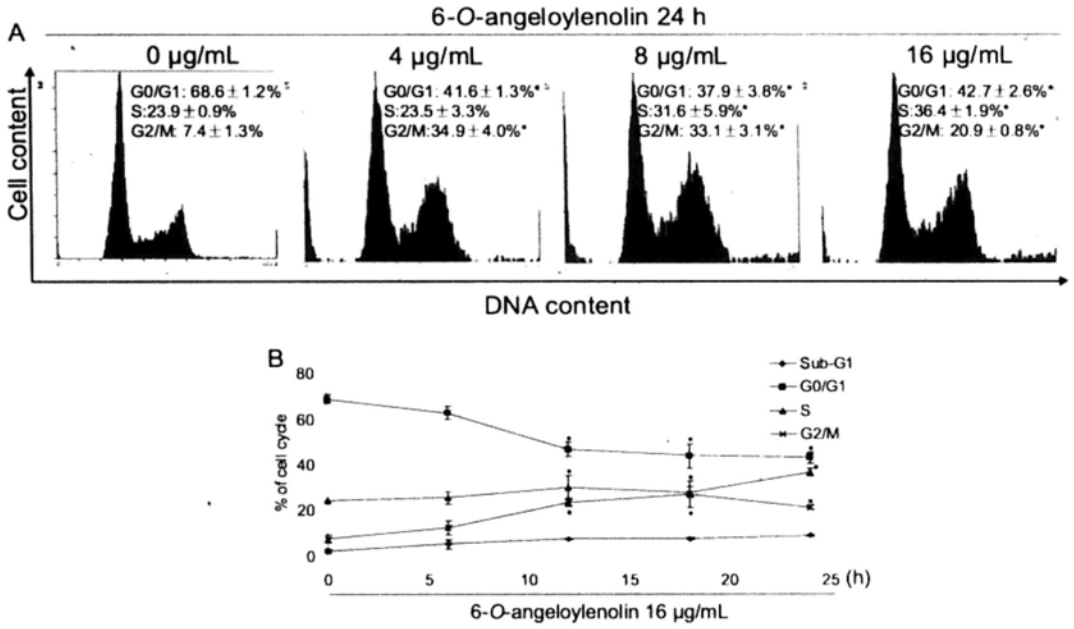


**Figure 5.3.** 6-*O*-Angeloylenolin caused S and G2/M phases arrest in CNE cells. (A) Effect of 6-*O*-angeloylenolin on cell cycle distribution in CNE cells after 24 h treatment. (B) Time course analysis of 6-*O*-angeloylenolin-induced S and G2/M phases arrests. Each value is expressed as mean ± SD ($n$ = 3). Significant difference between treatment and control groups is indicated at $p < 0.05$ (*) level.

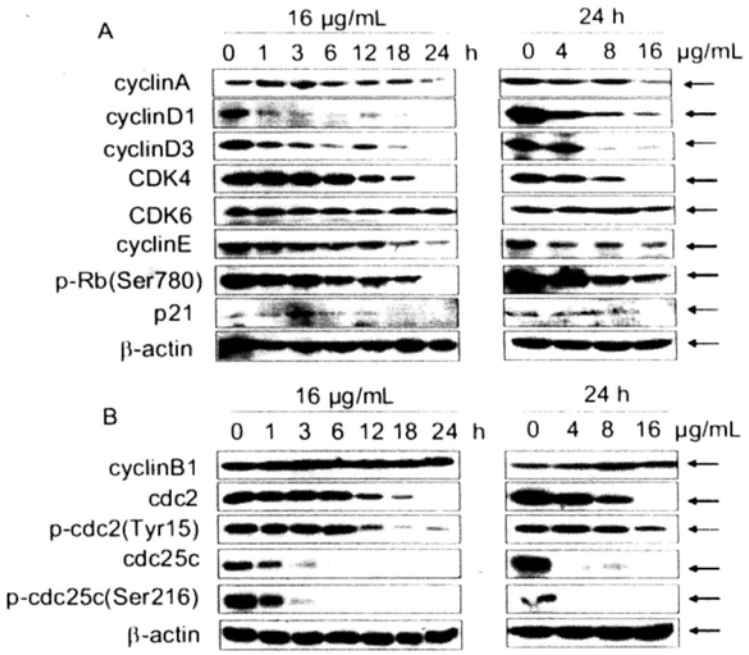


**Figure 5.4.** Effects of 6-*O*-angeloylenolin on protein expressions of S and G2/M phases related proteins in CNE cells. (A) Effects of 6-*O*-angeloylenolin on protein expressions of cyclin D1, cyclin D3, CDK4, CDK6, cyclin A, cyclin E, p-Rb (Ser780) and $p21^{Waf1/Cip1}$. (B) Effects of 6-*O*-angeloylenolin on protein expressions of G2/M phase related proteins [cyclin B1, cdc2, p-cdc2 (Tyr15), cdc25c, and p-cdc25c (Ser216)]. Equal loading of protein was confirmed by stripping the immunoblot and reprobing it for β-actin. The immunoblots shown here are representative of three independent experiments with similar results.

**5.3.3.** 6-*O*-Angeloylenolin induced apoptosis in CNE cells

To determine the outcomes of the arrest in S and G2/M phases, increasing incubation time from 24 to 72 h with the same concentration of 6-*O*-angeloylenolin were performed, and cell cycle distribution was analyzed. Results showed that exposed to 16 μg/mL of 6-*O*-angeloylenolin led to a significant time-dependent increment in sub-G1 population after 36-h treatment (Figure 5.5A). Furthermore, 6-*O*-angeloylenolin caused a significant dose-dependent increase in sub-G1 populations at 48-h treatment (Figure 5.5B).

Exposure of phosphatidylserine to the outer layer of the plasma membrane is an early marker of apoptosis due to the loss of plasma membrane polarity. Annexin-V, the phospholipid-binding protein binds to cells with externally exposed phosphatidylserine, whereas PI binds to cells with loss of membrane integrity (Vermes et al., 1995). Therefore, the double-staining method can distinguish between live cells (lower left), early apoptotic cells (lower right), late apoptotic cells (upper right) and necrotic cells (upper left). Results showed that exposed to 16 μg/mL of 6-*O*-angeloylenolin increased the percentage of apoptotic cells in a time-dependent manner, and the early apoptotic cells was 3.8 versus 17.8% at 0 and 12 h (Figure 5.6). These results suggested that 6-*O*-angeloylenolin induced externalization of phosphatidylserine early in the process of apoptosis. Sub-G1 cells were detected only after 36-h treatment of 6-*O*-angeloylenolin, even though Annexin-V positive cells were significantly observed as early as 12 h.

Depletion of mitochondria membrane potential ($\Delta\Psi m$) is another early marker in the apoptotic process. Therefore, $\Delta\Psi m$ was measured to find out whether this apoptotic feature was also apparent after 12-h treatment of 6-*O*-angeloylenolin. JC-1, a cationic dye exhibiting potential-dependent accumulation in mitochondria was employed to determine the loss of $\Delta\Psi m$. Results showed that significant depletion of $\Delta\Psi m$ was detected after 12-h treatment with 16 μg/mL of 6-*O*-angeloylenolin, from

0.2% at 0 h to 20.1% at 12 h (Figure 5.7A). Such depletion of $\Delta\Psi m$ was in time- and dose- dependent manners (Figure 5.7A, 5.7B).

To confirm the possibility that prolonged incubation with 6-*O*-angeloylenolin induced apoptosis in CNE cells, two more apoptotic markers, including DAPI nuclear staining and caspase activity were evaluated (Figure 5.8A-5.8B). As shown in Figure 5.8A, irregularity in shape and cellular detachment in CNE cells treated with 16 μg/mL of 6-*O*-angeloylenolin were observed under a phase-contrast microscopy. Apoptotic bodies with condensed chromatin and degraded nuclei were also observed after DAPI staining. Besides, caspase activity assay showed that caspase-3 activity was augmented in a dose-dependent way when the CNE cells were exposed to 16 μg/mL of 6-*O*-angeloylenolin (Figure 5.8B). Taken together, S and G2/M phases arrest by 6-*O*-angeloylenolin finally led to apoptosis in CNE cells.

**5.3.4.** 6-*O*-Angeloylenolin induced caspase-independent apoptosis in CNE cells

As notably significant augmentation in the sub-G1 population was starting at 48 h treatment with 6-*O*-angeloylenolin, the time was chosen for further investigation to delineate the detail mechanism of apoptosis. PARP cleavage, which acts as a marker in the apoptotic process, was observed in the 6-*O*-angeloylenolin-treated CNE cells (Figure 5.5A). Additionally, dose-dependent cleavage of caspase-3, -7, -8 and -9 were observed, though caspase-10 was slightly cleaved (Figure 5.9A-5.9B). These results suggested the activation of both the intrinsic and extrinsic apoptotic pathways. Moreover, truncation of Bid, a unique BH3-only pro-apoptotic protein serving as a bridge of the extrinsic and intrinsic pathways (Yi et al., 2003), was observed (Figure 5.5B).

To evaluate the role of caspases in the apoptosis, the pan-caspase inhibitor, z-VAD-fmk, was employed. As shown in Figure 5.10, pretreatment of CNE cells with z-VAD-fmk failed to attenuate 6-*O*-angeloylenolin-induced CNE cell death and apoptosis as measured by both MTT assay and flow cytometric analysis. z-VAD-fmk

did not prevent 6-*O*-angeloylenolin-induced CNE cell death even at the concentration of 100 μM (Figure 5.10A). Besides, pretreatment of z-VAD-fmk showed no protection on cell morphology and cell attachment in the treated CNE cells when observed under the microscopy (Figure 5.10B). These results suggested that 6-*O*-angeloylenolin induced apoptosis via a caspase-independent way.

**5.3.5.** 6-*O*-Angeloylenolin induced mitochondria dysfunction in CNE cells

Mitochondria play an important role in regulating apoptosis as they could release apoptogenic factors such as AIF and cytochrome *c*. As loss of $\Delta\Psi m$ was observed in 6-*O*-angeloylenolin-treated CNE cells (Figure 5.7), the release of apoptogenic factors was examined. Results showed that AIF, which is a key factor in the caspase-independent pathway, was released to the cytosol at 8 μg/mL of 6-*O*-angeloylenolin. This further confirmed that the caspase-independent pathway was activated. Moreover, cytochrome *c* was markedly released to the cytosol in a dose-dependent manner (Figure 5.11A).

Bcl-2 family proteins are key regulators of mitochondria permeability. 6-*O*-Angeloylenolin down-regulated the expression of the pro-survival protein Bcl-2, whereas up-regulated the expression of the pro-apoptotic proteins Bad (Figure 5.11B). At the same time, 6-*O*-angeloylenolin failed to affect the expressions of Bcl-xL, Mcl-1, Bax, Bik, PUMA, Bim, Bok and Bmf.

**5.3.6.** 6-*O*-Angeloylenolin induced the activation of JNK pathway in CNE cells

Akt (protein kinase B), a serine/threonine kinase, has emerged as a central regulator of various cellular processes including cell cycle progression and apoptosis (Eriko et al., 2008). MAPKs, another family of serine/theronine kinases, have been known to be important in regulating cell growth and cell death (Pearson et al., 2001). Therefore, both the total and the phosphorylated forms of these kinases were examined by western blotting to determine whether the Akt and MAPKs pathways were involved in the death of 6-*O*-angeloylenolin-induced CNE cells. Results

showed that the expressions of the two phosphorylated forms of Akt, namely, p-Akt (Thr308) and p-Akt (Ser473) decreased both in time- and dose- dependent manners (Figure 5.12A). On the contrary, the phosphorylated form of ERK increased in both time- and dose- dependent manners. Phosphorylation of JNK showed a rapid onset after 1-h treatment, which peaked at about 3 h and declined to the control level at 6 h. However, the activation of p38 was not observed in either studied time points or treated doses.

To confirm the roles of Akt, ERK and JNK in the death of 6-*O*-angeloylenolin-induced CNE cells, their specific inhibitors on the cell death were studied. MTT assay showed that pretreatment with U0126 (an ERK inhibitor) and LY294002 (an Akt inhibitor) offered no protection against the 6-*O*-angeloylenolin-induced CNE cell death (Figure 5.12B). However, pretreatment with SP600125 (a JNK inhibitor) significantly decreased the extent of cell death induced by the 6-*O*-angeloylenolin at both concentrations of 8 and 16 μg/mL (Figure 5.7B). Consistent with these results, flow cytometric analysis revealed that pretreatment with SP600125 led to significant decrease in the sub-G1 populations (Figure 5.12C). These results suggested that JNK, rather than Akt and ERK, played an important role in 6-*O*-angeloylenolin-induced apoptosis.

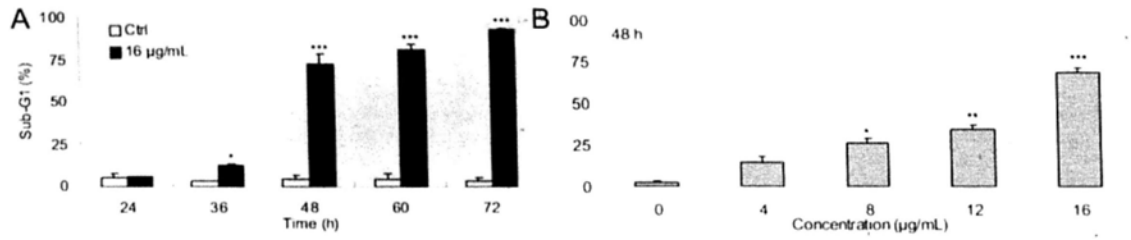


**Figure 5.5.** 6-*O*-Angeloylenolin induced both time- and dose- dependent CNE apoptosis by measuring the sub-G1 cell population. Harvested cells treated with 6-*O*-angeloylenolin were stained with propidium iodide (PI) and analyzed using flow cytometry. Each value is expressed as mean ± SD ($n$ = 3). Significant difference between treatment and control groups is indicated at $p < 0.05$ (*), $p < 0.01$ (**) or $p < 0.001$ (***) level.

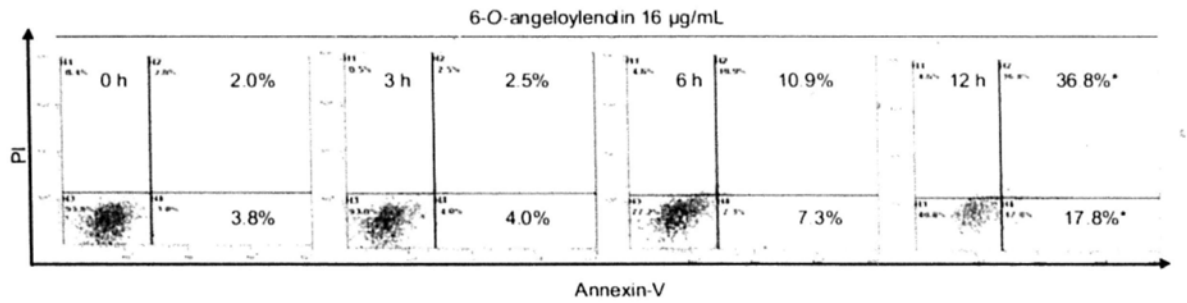


**Figure 5.6.** 6-O-Angeloylenolin induced apoptosis in CNE cells was determined by using double-staining system. Harvested cells were labeled with Annexin-V-Fluorescein and PI and then analyzed on a flow cytometer. Dual parameter dot plot of Annexin-V fluorescence (x-axis) versus PI fluorescence (y-axis) has been shown in logarithmic fluorescence intensity. Quadrants: lower left, live cells (−Annexin-V, −PI); lower right, early phase of apoptotic cells (+Annexin-V, −PI); upper right, late phase of apoptotic cells (+PI, +Annexin-V); upper left, necrotic cells (−Annexin-V, +PI). Significant difference between treatment and control groups is indicated at $p < 0.05$ (*), $p < 0.01$ (**) or $p < 0.001$ (***) level.

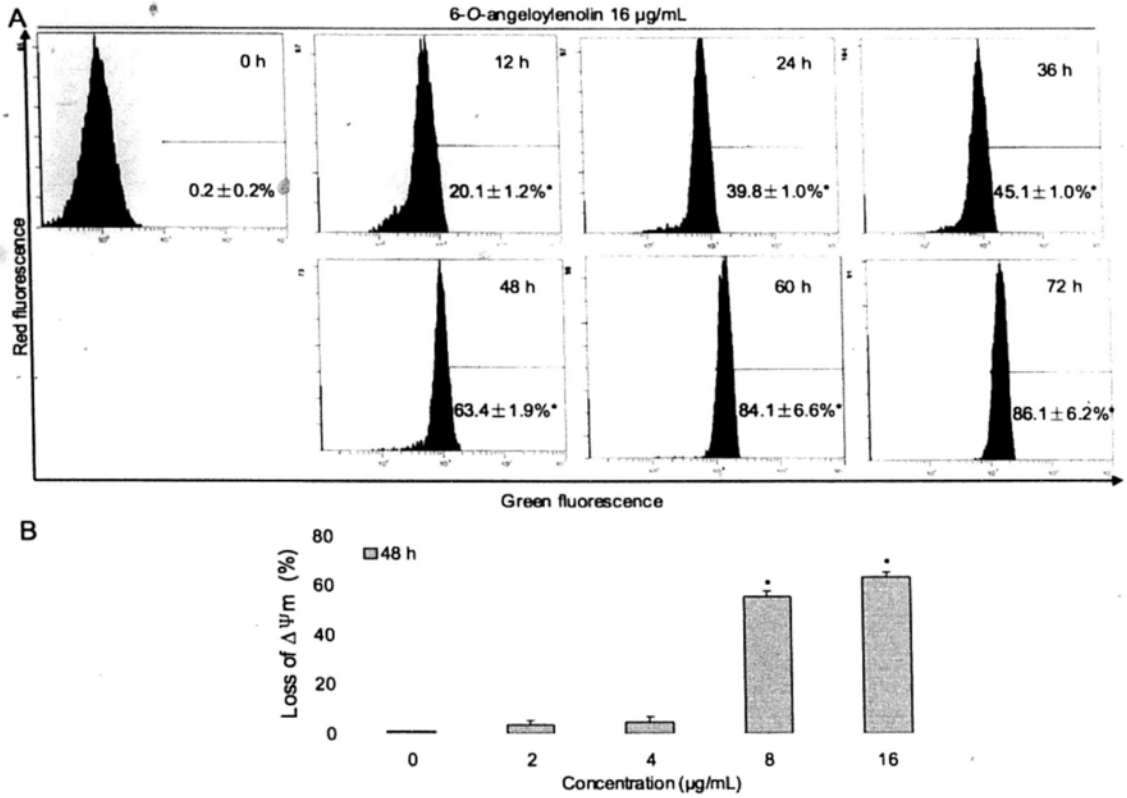


**Figure 5.7.** 6-*O*-Angeloylenolin caused the disruption of mitochondrial membrane potential ($\Delta\Psi m$) in CNE cells. CNE cells treated with different concentrations of 6-*O*-angeloylenolin for indicated time were stained with JC-1 and analyzed by flow cytometry. Each value is expressed as mean ± SD ($n$ = 3). Significant difference between treatment and control groups is indicated at $p < 0.05$ (*), $p < 0.01$ (**) or $p < 0.001$ (***) level.

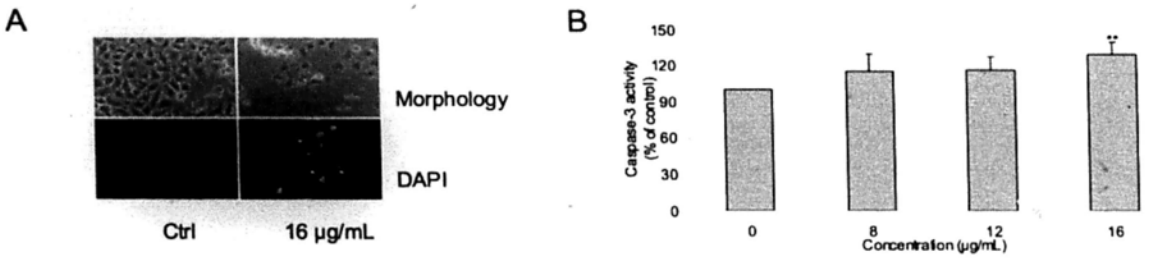


**Figure 5.8.** 6-*O*-Angeloylenolin induced CNE apoptosis by using DAPI staining and measuring caspase 3 activity. (A) Representative images of DNA fragmentation and nuclear condensation in CNE cells exposed to 6-*O*-angeloylenolin for 48 h. Morphology (upper): Cells were incubated with 0 or 16 μg/mL of 6-*O*-angeloylenolin for 48 h and observed under phase-contrast microscopy. DAPI (lower): After exposure to 6-*O*-angeloylenolin for 48 h, cells were stained with DAPI and analyzed by fluorescence microscopy. (B) Activation of caspase-3 activity by 6-*O*-angeloylenolin. After treatment of 6-*O*-angeloylenolin for 48 h, cells were lysed, and caspase-3 activity was measured using a colorimetric caspase-3 specific substrate. Significant difference between treatment and control groups is indicated at $p < 0.01$ (**) level.

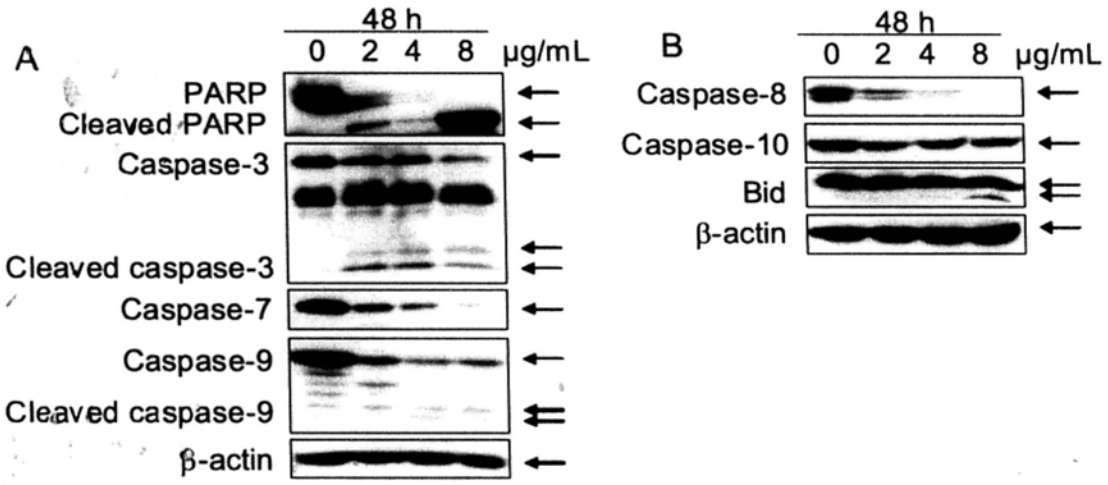


**Figure 5.9.** 6-*O*-Angeloylenolin induced both intrisinc and extrinsic apoptotic pathways in CNE cells. (A) Protein expressions of PARP, caspase-3, -7 and -9 in CNE cells after treated with indicated concentrations of 6-*O*-angeloylenolin for 48 h. (B) Protein expressions of caspase-8 and -10, and Bid in CNE cells after treated with indicated concentrations of 6-*O*-angeloylenolin for 48 h. Equal loading of protein was confirmed by stripping the immunoblot and reprobing it for β-actin. The immunoblots shown here are representative of three independent experiments with similar results.

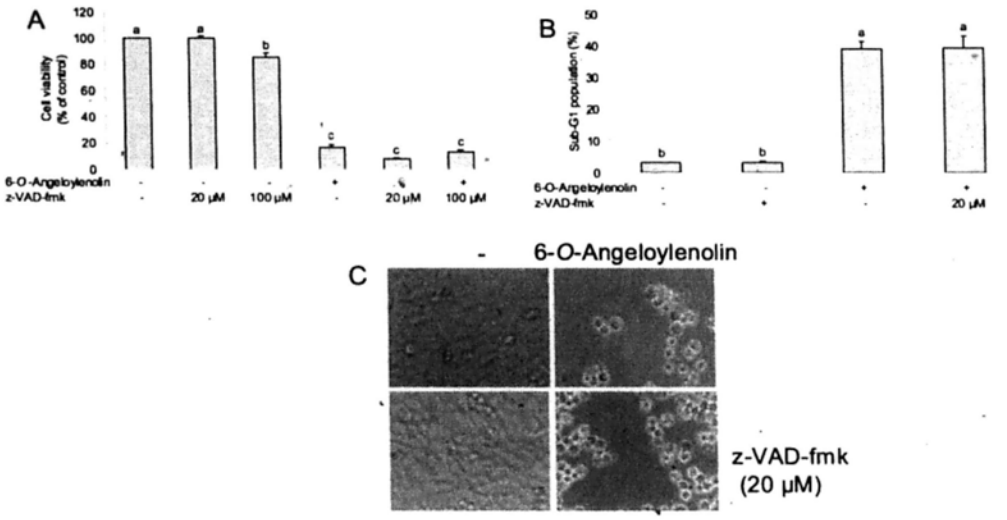


**Figure 5.10.** 6-*O*-Angeloylenolin induced caspase-independent apoptosis in CNE cells. (A) Effect of pan-caspase inhibitor (z-VAD-fmk) on CNE cell growth induced by 6-*O*-angeloylenolin. Cells were pretreated with 20 or 100 μM of z-VAD-fmk for 2 h followed by co-incubation with 16 μg/mL of 6-*O*-angeloylenolin for 48 h. Cell viability was determined by MTT assay. (B) Effect of z-VAD-fmk on CNE cell apoptosis induced by 6-*O*-angeloylenolin.Cells were pretreated with 20 μM of z-VAD-fmk for 2 h followed by co-incubation with 16 μg/mL of 6-*O*-angeloylenolin for 48 h. Apoptosis was quantified by flow cytometry. Equal loading of protein was confirmed by stripping the immunoblot and reprobing it for β-actin. The immunoblots shown here are representative of three independent experiments with similar results. (C) Morphology of CNE cells under different treatments. z-VAD-fmk: pretreatment with 20 μM z-VAD-fmk for 2 h; 6-*O*-angeloylenolin: treatment with 16 μg/mL of 6-*O*-angeloylenolin for 48 h. Each value is expressed as mean ± SD ($n = 3$). Bars with different characters are statistically different at $p < 0.05$ level.

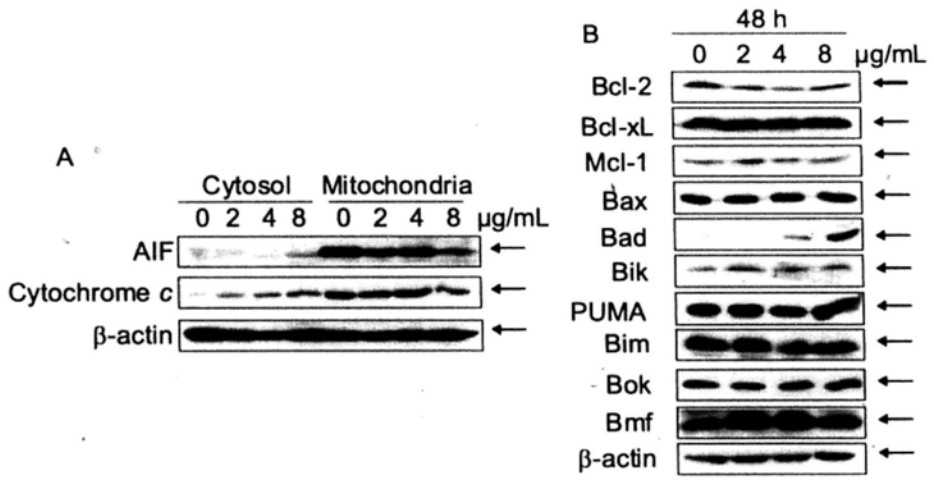


**Figure 5.11.** 6-*O*-Angeloylenolin regulated the release of apoptogenic factors and the expressions of the Bcl-2 family proteins in CNE cells. (A) Protein expressions of apoptosis-inducing factor (AIF) and cytochrome *c* in the cytosol and mitochondria of CNE cells after exposed of indicated concentrations 6-*O*-angeloylenolin for 48 h. (B) Protein expressions of Bcl-2 family proteins (Bcl-2, Bcl-xL, Mcl-1, Bax, Bad, Bik, PUMA, Bim, Bok, Bmf and Bid) in CNE cells treated with indicated concentrations of 6-*O*-angeloylenolin for 48 h. Equal loading of protein was confirmed by stripping the immunoblot and reprobing it for β-actin. The immunoblots shown here are representative of three independent experiments with similar results.

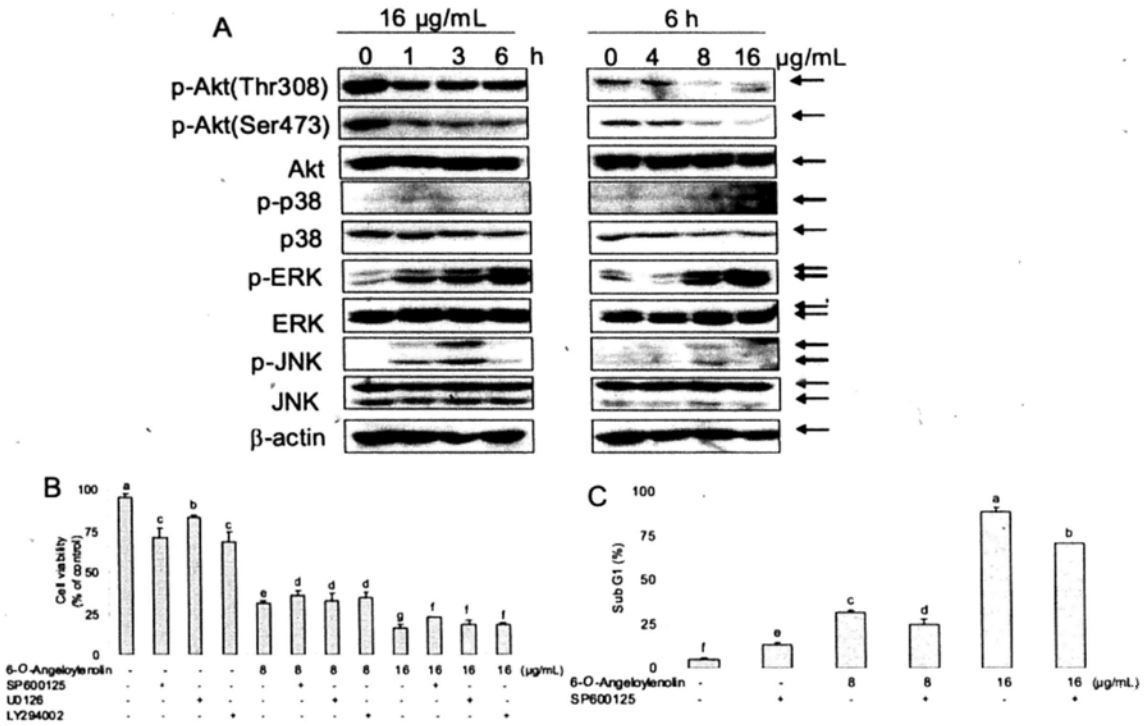


**Figure 5.12.** Roles of Akt and MAPKs in 6-*O*-angeloylenolin-induced growth inhibition in CNE cells. (A) Effect of 6-*O*-angeloylenolin on the protein expressions of Akt and MAPKs. Cells were treated with indicated concentration of 6-*O*-angeloylenolin for specific times. Equal loading of protein was confirmed by stripping the immunoblot and reprobing it for β-actin. The immunoblots shown here are representative of three independent experiments with similar results. (B) Effects of SP600125 (JNK inhibitor), U0126 (ERK inhibitor) and LY294002 (Akt inhibitor) on 6-*O*-angeloylenolin-induced growth inhibition. Cells were pretreated with 20 μM concentrations of different inhibitors 1 h prior to the treatment with 8 or 16 μg/mL of 6-*O*-angeloylenolin for 48 h (total inhibitor exposure time was 49 h). Cell viability was determined by MTT assay. (C) Effect of SP600125 (JNK inhibitor) on 6-*O*-angeloylenolin-induced apoptosis. Cells were pretreated with 20 μM concentrations of SP600125 1 h prior to the treatment with 8 or 16 μg/mL of 6-*O*-angeloylenolin for 48 h (total inhibitor exposure time was 49 h). Sub-G1 cell population was determined by flow cytometry. Bars with different characters are statistically different at $p < 0.05$ level.

## 5.4. Discussion

The high incidence of lymph node spread and distant metastasis make prognosis in NPC poor (Sham et al., 1990). Although NPC is a chemosensitive tumor compared with other head and neck cancers, significant toxicities were the critical challenging problem faced by the concurrent chemotherapy (Ma and Chan, 2005). Therefore, better treatment for NPC is needed.

Recently, great deals of attentions have been drawn towards the anticancer actions of sesquiterpene lactones (Zhang et al., 2005). However, there is only a paucity of information about their effects on NPC. We have previously elucidated the effect of 2β-(isobutyryloxy)florilenalin (IF), a sesquiterpene lactone isolated from the *n*-hexane soluble fraction of *C. minima* on the growth of CNE cells (Su et al., 2009a). In this study, 6-*O*-angeloylenolin (Figure 5.1), another sesquiterpene lactone isolated from the volatile oil of *C. minima*, showed strong inhibitory effect on the growth of CNE cells. Its effect was slightly stronger than that of cisplatin (Figure 5.2B), the positive control, albeit statistical insignificance. Besides, data also showed that its effect on the normal Hs68 cells was much weaker, suggesting that 6-*O*-angeloylenolin induced selectivity between cancer and normal cells (Figure 5.2A).

Cell cycle analysis revealed that inhibition of cell growth by 6-*O*-angeloylenolin ascribed to cell cycle arrest in both S and G2/M phases, followed by an increase in sub-G1 population (5.3A and 5.3B, 5.5A and 5.5B). Although S phase arrest has been observed in several cell-type systems exposed to various compounds, the mechanism of S phase arrest is poorly understood when compared to that of G0/G1 and G2/M arrest (Kuo et al., 2009). Recently, some studies have showed that the alterations in the expressions of cyclins and CDK inhibitors contribute to the S phase arrest (Kubista et al., 2006; Ding et al., 2008; Kuo et al., 2009; Tian et al., 2009). Similarly, this study showed that the expressions of both cyclin D1 and cyclin D3 were sharply decreased in CNE cells after 1-h treatment. Besides, CDK4, cyclin A, cyclin E,

p-Rb(Ser780) and $p21^{Waf1/Cip1}$ were all down-regulated as well (Figure 5.4A). Rb, which is a phosphoprotein, is an important player in the G1-S checkpoint. It is phorsphorylated progressively as quiescent cells progress though G1, reaching a hyperphosphorylated form at the G1/S border (Hughes and Mehmet, 2003). 6-*O*-Angeloylenolin stimulated S phase arrest and caused Rb phosphorylation in CNE cells, suggesting Rb played an important role in G1/S checkpoint in response to 6-*O*-angeloylenolin. $p21^{Waf1/Cip1}$ binds to and inhibits the S-phase-promoting CDK2/cyclin E complex, resulting to the enhancement of G1/S progression (Ory et al., 2007). Attenuation of $p21^{Waf1/Cip1}$ was also found in two NPC cells, e.g. HK-1 and CNE-2, after treated with the alkylating agent, SarCNU (Nguyen et al., 2005). The repression of $p21^{Waf1/Cip1}$ thus implied its important role in destroying the normal repair process induced by 6-*O*-angeloylenolin.

The cdc2/cyclin B1 is a critical complex regulating the G2/M phase. The activation of cdc2 is responsible for the cell entry into mitosis. The crucial regulatory step in the activation of cdc2 appears to be dephosphorylation at Thr14 and Tyr15, which is controlled by phosphorylation of cdc25c at Ser216 (Hunter, 1995; Peng et al., 1997). After phosphorylation, cdc25c binds to members of the 14-3-3 family of proteins, sequestering cdc25c in the cytoplasm and preventing premature mitosis. The western blotting results showed that cdc25c was down-regulated as early as 1 h after treatment, and cdc2 was sequentially down-regulated as a later event after 12-h treatment (Figure 5.4B). Repressions in the phosphorylated from of cdc25c and cdc2 (p-cdc25c and p-cdc2) were also observed at the same time points corresponding to the down-regulation of cdc25c and cdc2, respectively. However, the expression of cyclin B1 was not affected. Taken together, 6-*O*-angeloylenolin induced cell cycle arrest through the regulation of multiple regulators important in S and G2/M phases progression.

Prolonged the incubation time with 6-*O*-angeloylenolin in CNE cells resulted in an increase in the sub-G1 population, indicating apoptotic cell death. The sub-G1 population was significantly detected after 36-h treatment (Figure 5.5A). Besides,

6-*O*-angeloylenolin caused the externalization of phosphatidylserine and the depletion of $\Delta\Psi m$ as early as 12 h after treatment (5.6, 5.7A and 5.7B), which both served as the early markers of apoptosis. Apoptosis induction was further confirmed by other apoptotic features including the observation of apoptotic bodies (Figure 5.8A), the activation of caspase-3 activity (Figure 5.8B) and the cleavage of PARP (Figure 5.9A), at 48-h treatment. These results reiterate the notion that the emphasized that treatment of 6-*O*-angeloylenolin could lead to unavoidable apoptosis in CNE cells.

Caspases, a family of cysteine-*asp*artic acid proteases, are key regulators of apoptosis. Cleavage of caspase-8/-10 and caspase-9 in this study suggested that both extrinsic and intrinsic apoptotic pathways were activated (Figure 5.9). The two pathways were further found to crosstalk through the truncation of Bid (Figure 5.9B) which transduced the apoptotic signals from the cell surface to mitochondria. Although caspases were activated in CNE cells exposed to 6-*O*-angeloylenolin, the pan-caspase inhibitor, z-VAD-fmk, failed to attenuate the apoptosis induction effect of 6-*O*-angeloylenolin (Figure 5.10). Furthermore, z-VAD-fmk did not inhibit the effect of 6-*O*-angeloylenolin-induced morphological changes in CNE cells (Figure 5.10). These results suggested that caspase-independent apoptotic pathway was activated. In contrast to cytochrome *c*, the translocation of AIF from the mitochondria to the cytosol and nucleus is regarded as a key factor in the caspase-independent pathway (Candé et al., 2002). Overexpression of AIF induces peripheral chromatin condensation and DNA fragmentation (Lorenzo and Susin, 2007). 6-*O*-Angeloylenolin treatment resulted in an increase of AIF expression in cytosol (Figure 5.11A). Overall, these results suggested that caspases activation played an important, but not critical, role in the triggering of apoptotic machinery by 6-*O*-angeloylenolin in CNE cells. Consistent with our results, pretreatment of the pan-caspase inhibitor or caspse-3 inhibitor failed to inhibit the apoptotic induction effect of parthenolide, an analogue to 6-*O*-angeloylenolin, in the human nasopharyngeal carcinoma CNE1 cells (Lin et al., 2003).

Mitochondria have been unraveled the critical function at the core of the apoptotic pathway (Jeong and Seo, 2008). The loss of $\Delta\Psi m$ is crucial for both caspase-dependent and caspase-independent apoptotic pathways (Kim et al., 2006). In the present study, 6-*O*-angeloylenolin caused the depletion of $\Delta\Psi m$ in CNE cells in time- and dose- dependent manners (Figure 5.7). Upon the $\Delta\Psi m$ collapse, a large conductance channel known as the mitochondrial permeability transition pore opens and leads to the release of the apoptogenic factors, such as cytochrome *c*, AIF, Endo G, and SMAC/Diablo (Green and Reed, 1998). In fact, both cytochrome *c* and AIF were detected in the cytosol in this investigation (Figure 5.11A). Cytosolic cytochrome *c* then formed an apoptosome with caspases-9, which further activated caspase-3 and -7 and resulted in PARP cleavage, while AIF in the cytosol would translocate to the nucleus and lead to large-scale DNA fragmentation (Cregan et al., 2004). These results indicated that mitochondria played a pivotal role in the triggering of apoptotic machinery by 6-*O*-angeloylenolin in CNE cells.

Members of the Bcl-2 family proteins, which are categorized into pro-survival (anti-apoptotic) and pro-apoptotic family members, act as gatekeepers of mitochondria function by controlling the permeabilization of the mitochondrial outer membrane (Chipuk and Green, 2008). The pro-survival family proteins (Bcl-2 subfamily), which are localized on the cytoplasmic part of the nuclear envelope, the endoplasmic reticulum, and the outer mitochondrial membrane, function to keep the mitochondria membranes intact and thereby prevent the release of the apoptogenic factors. But when activated, the pro-apoptotic family proteins (Bax subfamily and BH3-only subfamily) oligomerize and permeabilize the outer mitochondrial membrane to release the apoptogenic factors, and promote activation of caspase -dependent or -independent pathways (Wong and Puthalakath, 2008). In HL-60 cells, 6-*O*-angeloylenolin induced apoptosis by modulation of *Bcl-2* gene family expression (Li et al., 2008). In CNE cells, we documented previously that 2β-(isobutyryloxy)florilenalin (IF) induced apoptosis by regulating the expression of Bcl-2 family proteins (Su et al., 2009a). In this study, the level of Bcl-2 was

down-regulated in CNE cells (Figure 5.11B). Bcl-2 is reported to be overexpressed in a higher percentage of NPC tumors (Yang et al., 2001). Moreover, Bcl-2 and wild-type p53 could act synergistically to increase the growth of NPC tumor cell through the up-regulation of the proliferating cell nuclear antigen, a protein required for DNA synthesis and cell proliferation, suggesting that Bcl-2 played important role in NPC tumorigenesis (Niemhom et al., 2000; Chou et al., 2008). p53 was reported to be absent in CNE cells (Li et al., 2007). The ability of 6-*O*-angeloylenolin to down-regulate the expression of Bcl-2 in CNE cells infers its important role in interfering the tumorigenesis of NPC. Besides, the increase in the expression of Bad (Figure 6B), the pro-apoptotic protein, might enhance its interacting with Bcl-2-like survival factors (Borner, 2003). Truncation of Bid was also detected in CNE cells treated with 6-*O*-angeloylenolin (Figure 5.9B), which not only served as the caspase-8 substrate, but also could increase mitochondrial permeability (Bossy-Wetzel and Green, 1999).

The PI3K/Akt constitutes an important pathway regulating the signaling of a variety of biological processes including apoptosis, cell proliferation and cell growth. Akt, an important downstream target of P13K, helps regulate cell proliferation and prevent apoptosis by directly phosphorylating proteins involving in cell cycle regulation, such as glycogen synthase kinase 3$\beta$ (GSK3$\beta$), the forkhead transcription factors, CDK inhibitors $p21^{Waf1/Cip1}$, and key proteins of the apoptotic machinery, such as Bad and procaspase-9 (Datta et al., 1999; Liang et al., 2003). The abnormalities in Akt occur early in NPC tumorigenesis and contribute to disease advancement and metastasis (Chou et al., 2008). In addition to Akt, the MAPK family is able to regulate diverse cellular programs including proliferation, differentiation and apoptosis by phosphorylating various transcription factors that are already bound to DNA (Raman et al., 2007). In mammals, the best known kinases in this MAPK family are the extracellular signal-regulated kinases 1 and 2 (ERK1/2), c-Jun N-terminal kinase/stress-activated protein kinases (JNK/SAPKs) and p38 MAPKs. Generally, activation of ERK1/2 is considered to be a survival signal

responding to many cellular responses such as proliferation, differentiation and survival (Yoon and Seger, 2006). On the other hand, JNK/SAPKs and p38 MAPKs are generally activated in response to a wide range of extracellular stimuli including inflammatory cytokines, environmental stresses such as UV radiation, osmotic shock, hypoxia and growth factors (Johnson and Lapadat, 2002). However, these three MAPK pathways can be differentially activated, and their involvement in apoptosis depends on kinds of stimuli and types of cells. The most studied MAPKs in NPC are the JNK and ERK. Constitutive activation of JNK has been well demonstrated in NPC (Li et al., 2007). ERK was reported to contribute to NPC development as tumors exhibiting high ERK levels have poorer prognoses, with shorter overall survival rates and faster disease progression for patients (Wang et al., 2006). Therefore, the P13K/Akt and MAPK pathways could play significant potential targets for NPC treatment. In this study, 6-*O*-angeloylenolin was showed to trigger the activation of Akt, ERK and JNK pathways to different extents (Figure 5.12A). Further investigation employing specific inhibitors suggested that Akt and ERK did not play important roles in regulating cell death induced by 6-*O*-angeloylenolin in the CNE cells (Figure 5.12B). In contrast, pretreatment with the JNK inhibitor significantly decreased the extents of cell death and apoptosis in CNE cells induced by 6-*O*-angeloylenolin (Figure 5.12B-5.7C). Therefore, JNK appears to be the major pathway activated by 6-*O*-angeloylenolin in CNE cells.

## 5.5. Conclusions

In conclusion, this study showed for the first time that 6-*O*-angeloylenolin, a plant derived sesquiterpene lactone, caused proliferation inhibition in nasopharyngeal cancer CNE cells through both cell cycle arrest and apoptosis. The results in this study thus imply the potential of 6-*O*-angeloylenolin as a candidate for NPC treatment.

# Chapter 6: Conclusions

Nasopharyngeal carcinoma (NPC), originated from the epithelial lining of the nasopharynx, is the most common cancer in the head and neck regions (Yu and Yuan, 2002). Its occurrence is very low in most parts of the world, with annual incidence below 1 per 100,000 persons. However, unusually high incidence (>20/100,000 persons per year) is recorded among the Cantonese who inhabit in the Guangdong Province and Hong Kong SAR in southern China (Parkin, 2006). In NPC, normal function of cell cycle progression and apoptosis are dysregulated (Chou et al., 2008). Currently, the combination of radiotherapy and adjuvant chemotherapy has become the prevalent treatment of NPC (Wang et al., 2002) due to its high sensitivity to radiotherapy and chemotherapy. Most chemotherapies of NPC are currently cisplatin-based agents. However, a significant increase in both acute and late toxicities, and resistance were observed in the concurrent chemotherapies (Wang et al., 2008; Xie et al., 2008). The best chemotherapy regimen has yet to be explored. Therefore, there is a necessity of developing less toxic and more effective agents for NPC.

*Centipeda minima* (L.) A. Br. (Compositae), a Chinese medicinal herb, is used to treat nasal allergies, rhinitis and sinusitis, cough and headache in China (Lin and Shi, 2005). In addition, it is used in the Chinese folk medicine to treat nasopharyngeal carcinoma (Wu et al., 1985; Zhang, 2000). The preliminary screening results of MTT assay showed that the ethanolic extract of *C. minima* exhibited a broad spectrum of inhibitory effect on five human cancer cell lines, including the breast carcinoma MCF7 cells, the prostate carcinoma PC-3 cells, the hepatocellular carcinoma Hep G2 cells, the nasopharyngeal carcinoma epithelial CNE cells and the acute promyelocytic leukemia HL-60 cells. The ethanolic extract was subjected to further fractionation and the effects of the obtained fractions were again evaluated by the assay. Results showed that the *n*-hexane fraction exerted the most potent effect. All the tested cancer cell lines were sensitive to the *n*-hexane fraction with $IC_{50}$ values

ranging from 6.1 to 47.3 μg/mL. Bioactivity-guided separation of the *n*-hexane fraction using CNE cells as the cellular system led to the isolation of a sesquiterpene lactone, 2β-(isobutyryloxy)florilenalin (IF).

Sesquiterpene lactones, most widely distributed in the *Compositae*, have received considerable attention for their anticancer properties (Zhang et al., 2005). The highly electrophilic α,β-unsaturated carbonyl structures, such as the α-methylene-γ-lactone ring and the α,β-unsaturated cyclopentenone, are considered as the general bioactive functional groups in sesquiterpene lactones (Zhang et al., 2005), as they allow the structures to interact rapidly with the nucleophilic sites of biological molecules in a Michael-type addition. Covalent binding of sesquiterpene lactones to free sulfhydryl groups in proteins is possible and may interfere with the normal protein function. Besides, alkylation with the DNA molecules presents a potential molecular cytotoxicity for cells (Beekman et al., 1997). However, there is a paucity of information about the effects of sesquiterpene lactones on NPC.

In this study, IF exhibited significant dose- and time- dependent effects on the growth of CNE cells, with $IC_{50}$ values of 25.6 (24 h), 8.1 (48 h) and 3.1 μg/mL (72 h), respectively. Despite its potency in CNE cells, it showed a weaker effect on the normal Hs68 cells with an $IC_{50}$ value of larger than 50 μg/mL at 72-h treatment. These results suggested that IF induced selectivity between normal and cancer cells.

Apoptosis, an essential process for maintaining homeostasis in multi-cellular organisms, plays a crucial role in the development of various types of cancers (Shi, 2002). Two major apoptotic pathways, including the extrinsic and the intrinsic pathways, have been identified in mammalian cells (Fulda, 2009). The extrinsic pathway is associated with the ligation of death receptors, such as Fas and TRAIL receptors (MacKenzie and Clark, 2008). The intrinsic pathway is regulated by the Bcl-2 family members, which mediate the release of apoptogenic factors to the cytosol, such as cytochrome *c*, AIF, Endo G, and SMAC/Diablo, which are responsible for caspase-dependent and caspase-independent apoptosis (Candé et al.,

2002). Induction of apoptosis has been regarded as a principal method of the current chemotherapeutic practices.

Apoptosis induction was found to contribute to the inhibitory effect of cell growth by IF as evidenced by the accumulation of sub-G1 cell population, DNA fragmentation and nuclear condensation, caspase-3 activation and PARP cleavage. Mechanistic study showed that both extrinsic and intrinsic apoptotic pathways were involved in the apoptosis induction action of IF. In the extrinsic pathway, IF activated caspase-8, which further induced the activation of both caspase-3 and caspase-7. In the intrinsic pathway, IF regulated the expressions of Bcl-2 family proteins, followed by depletion of mitochondrial membrane potential ($\Delta\Psi m$), the release of cytochrome *c* to the cytosol, the activation of caspase-9 and other downstream caspases, and finally the induction of apoptosis.

The *n*-hexane fraction, which exerted strong anti-NPC effect, was found to contain quite a few volatile constituents based on the GC-MS analysis. As the volatile oil from *C. minima* was reported to be effective to treat allergic rhinitis (Yu et al., 2001; Liu et al., 2005), we hypothesized that the volatile oil should also possess active volatile principals capable of controlling NPC. Therefore, both volatile oils extracted by supercritical fluid extraction (SFE) and steam distillation (SD) were investigated for their anti-NPC potential. Our results showed that the SFE oil was much stronger than that of the SD oil, suggesting that the SFE is more effective than SD to recover the active principals in *C. minima*. Further investigation of the underlying mechanism revealed that the SFE oil significantly inhibited the growth of CNE cells through dysfunction of mitochondria and activation of caspases. GC-MS analysis revealed that the responsible principals of the SFE oil were likely homologues of the sesquiterpene lactones with the mother structure of 11, 13-dihydrohelenalin.

Bioactivity-guided separation of the SFE oil led to the isolation of another sesquiterpene lactone, 6-*O*-angeloylprenolin, which also contained a bioactive functional group of sesquiterpene lactone, the α, β-unsaturated cyclopentenone. MTT

results showed that the CNE cells were more susceptible to 6-*O*-angeloylenolin than the normal Hs68 cells. Besides, inhibitory effect of 6-*O*-angeloylenolin on the CNE cells was slightly stronger than that of cisplatin, the positive control, albeit stastical insignificance. These results suggested the potency of 6-*O*-angeloylenolin on the treatment of NPC.

Further mechanistic investigation showed that 6-*O*-angeloylenolin caused CNE cell cycle arrest at both S and G2/M phases followed by the induction of apoptosis. In S phase, 6-*O*-angeloylenolin sharply down-regulated the expressions of cyclin D1 and cyclin D3 shortly in 1 h. CDK4, cyclin A, cyclin E, p-Rb(Ser780) and $p21^{Waf1/Cip1}$ were also down-regulated. In G2/M phases, cdc25c and cdc2 were down-regulated in 1 h and 12 h, respectively. Simultaneously, repressions in both p-cdc25c and p-cdc2 were also observed. The expression of cyclin B1 was not affected. Phosphorylated cdc2 was unable to interact with cyclin B1, resulting in the blockage of the cell cycle at the G2/M phase and the entry into mitosis. Taken together, 6-*O*-angeloylenolin inhibited cell proliferation and caused arrest in S and G2/M phases via the control of the S and G2/M related proteins.

6-*O*-Angeloylenolin induced apoptosis in CNE cells after cell cycle arrest. The sub-G1 peak was significantly detected after 36-h treatment. Externalization of phosphatidylserine and the depletion of $\Delta\Psi m$ were detected as early as 12 h after treatment. Besides, other apoptotic features were observed including the presence of apoptotic bodies, the activation of caspase-3 activity and the cleavage of PARP. Activation of caspase-8 and caspase-10 were detected. Cleaved caspase-8 further truncated Bid and relayed the apoptotic signals from the cell surface to mitochondria. Besides, 6-*O*-angeloylenolin depleted $\Delta\Psi m$ by down-regulating the expression of Bcl-2 and up-regulating that of Bad. These led to the release of cytochrome *c* and AIF to cytosol. Cytochrome *c* formed apoptosome with caspase-9, which further activated both caspase-3 and caspase-7 and cleaved PARP. AIF in the cytosol may translocat to the nucleus and cause large-scale DNA fragmentation. These results

suggested that both the extrinsic and intrinsic apoptotic pathways were activated. However, the pan-caspase inhibitor z-VAD-fmk failed to attenuate the apoptosis induction effect of 6-*O*-angeloylenolin and to inhibit 6-*O*-angeloylenolin-induced morphological changes in CNE cells. Taken together, these results suggested that the activation of caspases played a role in triggering the apoptotic machinery, but other mechanism(s) may also involve enabling the completion of apoptosis even at the presence of pan-caspase inhibitor.

Families of serine/theronine kinase, including Akt and MAPKs (e.g. ERK, JNK and p38) were evaluated for their regulatory role in cell apoptosis. Results showed that Akt, ERK and JNK were activated differentially. 6-*O*-Angeloylenolin treatment down-regulated the phosphorylation of Akt while up-regulated the phosphorylation of ERK. As for JNK, its phosphorylation form showed a rapid onset after 1-h treatment, which peaked at about 3 h and declined to the control level at 6 h. Inhibitor of JNK (SP600125), but not those of Akt (LY294002) and ERK (U0126), significantly suppressed the 6-*O*-angeloylenolin-induced cell growth and protected apoptosis in CNE cells. This study provided a mechanistic relation between the JNK pathway and 6-*O*-angeloylenolin-induced apoptosis in CNE cells.

All in all, two sesquiterpene lactones, including IF and 6-*O*-angeloylenolin were found to be responsible for the potent anti-NPC activity of *C. minima*. Both lactones exerted strong inhibitory effects on the proliferation of CNE cells. The $IC_{50}$ value of IF was 3.1 μg/mL, while that of 6-*O*-angeloylenolin was 1.7 μg/mL. IF induced CNE cell death via the induction of apoptosis through activating both the extrinsic and intrinsic pathways. Such pathways were also found to be activated in 6-*O*-angeloylenolin-induced CNE cell death. Besides, caspase-independent pathway was also found to be involved in 6-*O*-angeloylenolin-induced CNE cell death as the pan-caspase inhibitor can not inhibit the apoptosis induction effect of 6-*O*-angeloylenolin. Additionally, cell cycle arrest in both S and G2/M phases were observed to occur prior to apoptosis induction when exposed to 6-*O*-angeloylenolin,

implying that cell cycle arrest also played an important role in 6-*O*-angeloylenolin-induced CNE cell death. Both lactones belong to the pseudoguanianolide-type and contain a bioactive functional group of sesquiterpene lactone, the α, β-unsaturated carbonyl structure. IF contains a α-methylene-γ-lactone ring, while 6-*O*-angeloylenolin possesses a α, β-unsaturated cyclopentenone. The observation that both lactones initiated both extrinsic and intrisinc pathways is probably ascribed to their similar mother skeleton in their chemical structures. However, the differences in the bioactive functional group of the two lactones may contribute to their mechanistic differences.

This study reiterates the notion that Chinese medicinal herbs traditionally applied to cancer treatment may be good sources of anticancer drug discovery, and sesquiterpene lactones may be a group of noteworthy lead compounds displaying anti-NPC potential. However, there are still two main issues needed to be resolved by other researchers:

Issue 1. Nuclear factor-κB (NF-κB) is well known as an inducible transcription factor that plays pivotal roles in regulating cell growth and modulating inflammation (Chou et al., 2008). NF-κB dysregulation is one of the most important components of NPC tumorigenesis, as supported by the fact that almost all NPC tumors exhibit NF-κB overexpression (Shi et al., 2006). In NPC, up-regulation of NF-κB leads to the activation of a number of proliferative signals, including Bcl-2, cyclooxygenase 2 (COX-2), and vascular endothelial growth factor (Chou et al., 2008). Besides, activation of NF-κB results in telomerase activation and cell immortalization (Ding et al., 2005). With these evidences, the NF-κB signaling pathway could be a possible molecular target to induce apoptosis to the NPC cells. Besides, increasing number of evidences showed that NF-κB is a major molecular target for many sesquiterpene lactones (Koo et al., 2001; Song et al., 2005; Oka et al., 2007; Li et al., 2008; Rozenblat et al., 2008). Sesquiterpene lactones influence NF-κB by directly alkylating specific cysteine residues (especially $Cys^{38}$) in the p65/RelA subunit of

NF-κB, thus preventing DNA binding of the active NF-κB (Garcia-Pineres et al., 2001). Sesquitepene lactones are found to be responsible for the potent anti-NPC effect of *C. minima*. In view of these, the NF-κB pathway should be studied to completely delineate the underlying mode of action by the two sesquiterpene lactones.

Issue 2. Although the two sesquiterpene lactones exerted potent effects on the CNE cells *in vitro*, their *in vivo* effects have yet to be elucidated for predicting their clinical activity.

# References


Adams J.M. 2004. Ways of dying: multiple pathways to apoptosis. *Genes Dev.* 17: 2481-2495.

Anonymous. Edited by Jiangsu New Medicine College. 1986. *Dictionary of traditional Chinese medicine*. Shanghai Science and Technology Press, Shanghai, China, p. 168, 780, 1086 and 1231.

Atkinson J.M., Siller C.S., Gill J.H. 2008. Tumour endoproteases: the cutting edge of cancer drug delivery? *Brit. J. Pharmacol.* 153: 1344-1352.

Balunas M.J. and Kinghorn A.D. 2005. Drug discovery from medicinal plants. *Life Sci.* 78: 431-441.

Baujat B., Audry H., Bourhis J., Chan A.T., Onat H., Chua D.T., Kwong D.L., Al-Sarraf M., Chi K.H., Hareyama M., Leung S.F., Thephamongkhol K., Pignon J.P. 2006. Chemotherapy in locally advanced nasopharyngeal carcinoma: an individual patient data meta-analysis of eight randomized trials and 1753 patients. *Int. J. Radiat. Oncol. Biol. Phys.* 64: 47-56.

Beekman A.C., Woerdenbag H.J., van Uden W., Pras N., Konings A.W., Wikstrom H.V., Schmidt T.J. 1997. Structure-cytotoxicity relationships of some helenanolide-type sesquiterpene lactones. *J. Nat. Prod.* 60: 252-257.

Bo Q.M., Wu Z.Y., Shun Q.S., Bao X.S., Mao Z.S., Ha S.Q., Lu S.Y., Huang J.M. 2002. *A selection of the illustrated Chinese anti-cancer herbal medicine*. Shanghai Science and Technology Literature Press, Shanghai, China, p. 10.

Bohlmann F. and Chen Z.L. 1984. *Chinese Science Bulletin (科學通報)* 29: 900-903.

Borner C. 2003. The Bcl-2 protein family: sensors and checkpoints for life-or-death decisions. *Mol. Immunol.* 39: 615-647.

Bossy-Wetzel E. and Green D.R., Apoptosis: checkpoint at the mitochondrial frontier. *Mutation Research* 434: 243-251.

Brisdelli F., Coccia C., Cinque B., Cifone M.G., Bozzi A. 2007. Induction of apoptosis by quercetin: different response of human chronic myeloid (K562)

and acute lymphoblastic (HSB-2) leukemia cells. *Mol. Cell. Biochem.* 296: 137-149.

Burlacu A. 2003. Regulation of apoptosis by Bcl-2 family proteins. *J. Cell. Mol. Med.* 7: 249-257.

Campbell M.J., Hamilton B., Shoemaker M., Tagliaferri M., Cohen I., Tripathy D. 2002. Antiproliferative activity of Chinese medicinal herbs on breast cancer cells *in vitro*. *Anticancer-Res.* 22: 3843-3852.

Candé C., Cecconi F., Dessen P., Kroemer G. 2002. Apoptosis-inducing factor (AIF): key to the conserved caspase-independent pathways of cell death? *J.Cell Sci.* 115, 4727-4734.

Cheng J.H. and Li Y.B. 1998. *Anti-tumor herbal medicines and their proved recipes.* Jiangxi Science and Technology Press: Jiangxi, China, p. 732.

Chien Y.C., Chen J.Y., Liu M.Y., Yang H.I., Hsu M.M., Chen C.J., Yang C.S. 2001. Serologic markers of Epstein-Barr virus infection and nasopharyngeal carcinoma in Taiwanese men. *N. Engl. J. Med.* 345: 1877-1882.

Chipuk J.E. and Green D.R. 2008. How do BCL-2 proteins induce mitochondrial outer membrane permeabilization? *Trends Cell Bio.*18: 157-164.

Cho W.C. 2007. Nasopharyngeal carcinoma: molecular biomarker discovery and progress. *Mol. Cancer* 6: 1-9.

Chou J., Lin Y., Kim J., You L., Xu Z., He B., Jablons D.M. 2008. Nasopharyngeal carcinoma--review of the molecular mechanisms of tumorigenesis. *Head Neck-J. Sci. Spec.* 30: 946-963.

Chung H.Y. 1999. Volatile components in fermented soybean (*Glycine max*) curds. *J. Agric. Food Chem.* 47: 2690-2696.

Cregan S.P, Dawson V.L., Slack R.S. 2004. Role of AIF in caspase-dependent and caspase-independent cell death. *Oncogene* 23: 2785-2796.

Datta S.R., Brunet A., Greenberg M.E. 1999. Cellular survival: a play in three Akts. *Genes Dev.* 13: 2905-2927.

de Souza, C.P.C., Ellem K.A.O., Gabrielli, Brian G. 2000. Centrosomal and cytoplasmic Cdc2/cyclin B1 activation precedes nuclear mitotic events. *Exp. Cell Res.* 257:11-21.

Ding H.M., Han C.H., Guo D.M., Wang D.S., Chen C.S., D'Ambrosio S.M. 2008. OSU03012 activates Erk1/2 and Cdks leading to the accumulation of cells in the S-phase and apoptosis. *J. Cancer* 123: 2923-2930.

Ding L., Li L., Yang J., Tao G., Ye M., Shi Y., Tang M., Yi W., Li X., Gong J., Cao Y. 2005. Epstein-Barr virus encoded latent membrane protein 1 modulates nuclear translocation of telomerase reverse transcriptase protein by activating nuclear factor-κB p65 in human nasopharyngeal carcinoma cells. *Int. J. Biochem. Cell Biol.* 37: 1881-1889.

Eriko T., Eiji O., Akinori E., Noriaki S., Masaru M., Yoshihiro K., Yoshihiko M. 2008. Deregulation of the Akt pathway in Human Cancer. *Curr. Cancer Drug Tar.* 8: 27-36.

Fan S.Q., Ma J., Zhou J., Xiong W., Xiao B.Y., Zhang W.L., Tan C., Li X.L., Shen S.R., Zhou M., Zhang Q.H., Ou Y.J., Zhuo H.D., Fan S., Zhou Y.H., Li G.Y. 2006. Differential expression of Epstein-Barr virus-encoded RNA and several tumor-related genes in various types of nasopharyngeal epithelial lesions and nasopharyngeal carcinoma using tissue microarray analysis. *Hum. Pathol.* 37: 593-60.

Fadel H., Marx F., El-Sawy A., El-Ghorab A. 1999. Effect of extraction techniques on the chemical composition and antioxidant activity of *Eucalyptus camaldulensis* var. brevirostris leaf oils. *Zeitschrift fuer Lebensmittel-Untersuchung und -Forschung A: Food Research and Technology* 208: 212-216.

Fulda S. 2009. Tumor resistance to apoptosis. *Int. J. Cancer* 124: 511-515.

Garcia-Pineres A.J., Castro V., Mora G., Schmidt T.J., Strunck E., Pahl H.L., Merfort I. 2001. Cysteine 38 in p65/NF-κB plays a crucial role in DNA binding inhibition by sesquiterpene lactones. *J. Biol. Chem.* 276: 39713-39720.

Green D.R. and Reed J.C. 1998. Mitochondria and apoptosis. *Science* 281:

1309-1312.

Grub S., Persohn E., Trommer W.E., Wolf A. 2000. Mechanisms of cyclosporine A-induced apoptosis in rat hepatocyte primary cultures. *Toxicol. Appl. Pharm.* 163: 209-220.

Hanahan D. and Weinberg R.A. 2000. The Hallmarks of Cancer. *Cell* 100: 57-70.

http://www.nature.sdu.edu.cn/artemisia/pics/000870.jpg

Hu X., Xu Y., Hu D., Hui Y., Yang F. 2007. Apoptosis induction on human hepatoma cells Hep G2 of decabrominated diphenyl ether (PBDE-209). *Toxicol. Lett.* 171:19-28.

Hughes D. and Mehmet H. 2003. Cell proliferation and apoptosis. BIOS Scientific: Oxford; p78.

Hunter T. 1995. Protein kinases and phosphatases: The yin and yang of protein phosphorylation and signaling. *Cell* 80: 225-236.

Ikezoe T., Chen S.S., Tong X.J., Heber D., Taguchi H., Koeffler H.P. 2003. Oridonin induces growth inhibition and apoptosis of a variety of human cancer cells. *Int. J. Oncol.* 23: 1187-1189.

Iwakami S., Wu J.B., Ebizuka Y., Sankawa U. 1992. Platelet activating factor (PAF) antagonists contained in medicinal plants: lignans and sesquiterpenes. *Chem. Pharm.Bull.*40: 1196-1198.

Jeong S.Y. and Seo D.W. 2008. The role of mitochondria in apoptosis. *BMB Rep.* 41: 11-22.

Johnson G.L. and Lapadat R. 2002. Mitogen-activated protein kinase pathways mediated by ERK, JNK, and p38 protein kinases. *Science* 298: 1911-1912.

Kim R., Emi M., Tanabe K. 2006. Role of mitochondria as the gardens of cell death. *Cancer Chemother. Pharmacol.* 57: 545-553.

Kintzios S.E. 2004. *What do we know about cancer and its therapy?* In: Kintzios S.E. and Barberaki M.G. (Eds.), *Plants that fight cancer*. CRC Press, Boca Raton, Florida, pp.1.

Koo T.H., Lee J.H., Park Y.J., Hong Y.S., Kim H.S., Kim K.W., Lee J. J. 2001. A

sesquiterpene lactone, costunolide, from *Magnolia grandiflora* inhibits NF-κB by targeting Iκ B phosphorylation. *Planta Med* 7: 103-107.

Kubista B., Trieb K., Sevelda F., Toma, C., Arrich F., Heffeter P., Elbling L., Sutterluty H., Scotlandi K., Kotz R., Micksche M., Berger W. 2006. Anticancer effects of zoledronic acid against human osteosarcoma cells. *J. Orthop. Res.* 24: 1145-1152.

Kuo P.L., Ni W.C., Tsai E.M., Hsu Y.L. 2009. Dehydrocostuslactone disrupts signal transducers and activators of transcription 3 through up-regulation of suppressor of cytokine signaling in breast cancer cells. *Mol. Cancer Ther.* 8: 1328-1339.

Lee H. and Lin J. Y. 1988. Antimutagenic activity of extracts from anticancer drugs in Chinese medicine. *Mutation research* 204: 229-234.

Lee K. 2004 Current developments in the discovery and design of new drug candidates from plant natural product leads. *J. Nat. Prod.*, *67*, 273-283

Li C., Shu D., Zhou Q., Ling B. 2003. Elimination of plasmids from *Pseudomonas aeruginosa* by herba Centipeda *in vitro*. *Journal of North Sichuan Medical College (川北醫學院學報)* 18: 1-2.

Li C., Wu H., Huang Y., Yang Y., Liu Y., Liu J. 2008. 6-*O*-Angeloylenolin induces apoptosis through a mitochondrial/caspase and NF-κB pathway in human leukemia HL60 cells. *Biomed. Pharmacother.* 62: 401-409.

Li L., Guo L., Tao Y., Zhou S., Wang Z., Luo W., Hu D., Li Z., Xiao L., Tang M., Yi W., Tsao S.W., Cao Y. 2007. Latent membrane protein 1 of Epstein-Barr virus regulates p53 phosphorylation through MAP kinases. *Cancer Lett.* 255: 219-231.

Li Y.Y., Wang R., Zhang G.L., Zheng Y.J., Zhu P., Zhang Z.M., Fang X.X., Feng Y. 2007. An archaeal histone-like protein mediates efficient p53 gene transfer and facilitates its anti-cancer effect *in vitro* and *in vivo*. *Cancer Gene Ther.* 14: 968-975.

Liang H., Bao F., Dong X. Zhu H., Lu X., Shi M., Lu Q., Cheng Y. 2007a. Two new antibacterial sesquiterpenoids from *Centipeda minima*. *Chem.Biodivers.*4:

2810-2816.

Liang H., Bao F., Dong X., Lu Q., Cheng Y. 2007b. Antibacterial triterpenes from *Centipeda minima* (Compositae). *Yunnan Zhiwu Yanjiu (Acta Botanica Yunnanica, 雲南植物研究)* 29: 479-482.

Liang H., Bao F., Dong X., Tan R., Zhang C., Qing L., Cheng Y. 2007c. Antibacterial thymol derivatives isolated from *Centipeda minima*. *Molecules* 12: 1606-1613.

Liang H., Bao F., Dong X., Zhu H., Lu X., Shi M., Lu Q., Cheng Y. 2007d. Two new antibacterial sesquiterpenoids from *Centipeda minima*. *Chem. Biodivers.* 4: 2810-2816.

Liang H. and Zhong Z. 2006. Advances in studies on the mechanisms of anticancer traditional Chinese medicines. *Chinese Archives of Traditional Chinese Medicine (中醫藥學刊)* 24: 2086-2088.

Liang J. and Slingerland J.M. 2003. Multiple roles of the PI3K/PKB (Akt) pathway in cell cycle progression. *Cell Cycle* 2: 339-345.

Lin R. and Shi Z. 2005. *Pharmacopoeia of China*. Science Publishing House: Beijing, China, p. 132.

Lin Z., Lin Y., Yang X., Zhu W., Yu G., Cai C., Wei Q. 2003. Parthenolide induces apoptosis in human nasopharyngeal carcinoma CNE1 cell line via non-caspase-activation pathway. *Carcinogenesis, Teratogenesis and Mutagenesis (癌變，畸變，突變)* 15: 195-198.

Liu J.J., Huang R.W., Lin D.J., Wu X.Y., Peng J., Pan X.L., Hou M., Zhang M. H., Chen F. 2006. Antiproliferation effects of oridonin on HPB-ALL cells and its mechanisms of action. *Am. J. Hematol.* 81: 86-94.

Liu Z., Yu H., Wen S., Liu Y. 2005. Histopathological study on allergic rhinitis treated with *Centipeda minima*. *China Journal of Chinese Materia Medica (中國中藥雜誌)* 30: 292-294.

Lorenzo H.K. and Susin S.A. 2007. Therapeutic potential of AIF-mediated caspase-independent programmed cell death. *Drug Resis. Updat.* 10: 235-255.

Losso J.N., Bansode R.R., Trappey A., Bawadi H.A., Truax R., 2004. *In vitro* anti-proliferative activities of ellagic acid. *J. Nutr. Biochem.* 15: 672-678.

Lu Q.L., Elia G., Lucas S., Thomas J.A. 1993. Bcl-2 proto-oncogene expression in Epstein-Barr-virus-associated nasopharyngeal carcinoma. *Int. J Cancer* 53: 29-35.

Ma B.B.Y. and Chan A.T.C. 2005. Recent perspectives in the role of chemotherapy in the management of advanced nasopharyngeal carcinoma .*Cancer* 103: 22-31.

Ma Z., Otsuyama K., Liu, S., Abroun, S., Ishikawa, H., Tsuyama, N., Obata, M., Li, F.J., Zheng, X., Maki, Y., Miyamoto, K., Kawano, M.M., 2005. Baicalein, a component of Scutellaria radix from Huang-Lian-Jie-Du-Tang (HLJDT), leads to suppression of proliferation and induction of apoptosis in human myeloma cells. *Blood* 105: 3312-3318.

MacKenzie S.H. and Clark A.C. 2008. Targeting cell death in tumors by activating caspases. *Curr. Cancer Drug Tar.* 8: 98-109.

Malumbres M., and Barbacid M. 2009. Cell cycle, CDKs and cancer: a changing paradigm. *Nat. Rev. Cancer* 9: 153-166.

Mattson M.P., Kroemer Guido. 2003. Mitochondria in cell death: novel targets for neuroprotection and cardioprotection. *Trends Mol. Med.* 9: 196-205.

Mosmann T. 1983. Rapid colorimetric assay for cellular growth and survival: application to proliferation and cytotoxicity assays. *J. Immuno. Methods*, 65: 55-63.

Mukherjee A.K., Basu S., Sarkar N., Ghosh A.C. 2001. Advances in cancer therapy

with plant based natural products. *Curr. Med. Chem.* 8: 1467-1486.

Nguyen T.H., Ong C.K., Wong E., Leong C.T., Panasci L., Huynh H. 2005. 2-Chloroethyl-3-sarcosinamide-1-nitrosourea (SarCNU) exhibits p53-dependent and -independent antiproliferative activity in human nasopharyngeal carcinoma cells *in vitro* and *in vivo*. *Int. J. Oncol.* 27: 1131-1140.

Niemhom S., Kitazawa S., Murao S., Kunachak S., Maeda S. 2000. Co-expression of p53 and bcl-2 may correlate to the presence of Epstein-Barr virus genome and the expression of proliferating cell nuclear antigen in nasopharyngeal carcinoma. *Cancer Lett.* 160: 199-208.

Oh H.M., Kwon B.M., Baek N.I., Kim S.H., Lee J.H., Eun J.S., Yang J.H., Kim D.K. 2006. Inhibitory activity of 6-*O*-angeloylprenolin from *Centipeda minima* on farnesyl protein transferase. *Arch. Pharm. Res.* 29: 64-66.

Oka D., Nishimura K., Shiba M., Nakai Y., Arai Y., Nakayama M., Takayama H., Inoue H., Okuyama A., Nonomura N. 2007. Sesquiterpene lactone parthenolide suppresses tumor growth in a xenograft model of renal cell carcinoma by inhibiting the activation of NF-κB. *Int. J. Cancer* 120: 2576-2581.

Ory B., Blanchard F., Battaglia S., Gouin F., Redini F., Heymann D. 2007. Zoledronic acid activates the DNA S-Phase checkpoint and induces osteosarcoma cell death characterized by apoptosis-inducing factor and endonuclease-G translocation independently of p53 and retinoblastoma status. *Mol. Pharmacol.* 71:333-343.

Paoletta S., Steventon G.B., Wildeboer D., Ehrman T.M., Hylands P.J., Barlow D.J. 2008. Screening of herbal constituents for aromatase inhibitory activity. *Bioorgan. Med. Chem.* 16: 8466-8470.

Parkin, D.M. 2006. The global health burden of infection-associated cancers in the year 2002. *Int. J. Cancer* 118: 3030-3044.

Pearson G., Robinson F., Beers G.T., Xu B.E., Karandikar M., Berman K., Cobb M.H. 2001. Mitogen-activated protein (MAP) kinase pathways: regulation and physiological functions. *Endocr. Rev.* 22: 153-183.

Peng C.Y., Graves P.R., Thoma R.S., Wu Z., Shaw A.S., Piwnica-Worms H. 1997.

Mitotic and G2 checkpoint control: Regulation of 14-3-3 protein binding by phosphorylation of Cdc25C on serine-216. *Science* 277: 1501-505.

Pucci B., Kasten M., Giordano A. 2000. Cell cycle and apoptosis. *Neoplasia* 2 : 291-299.

Qian Y., Zhao C.J., Yan Y. 2004. The liver-protective effect of the Ebushicao on hepatic injury in mice. *China Pharmaceuticals (中國藥業)* 13: 25-26.

Qin R.A., Chen M., Shi J.L., Yin H. 2001. Preliminary report on the anti-inflammatory effect of the volatile oil from *Centipeda minima* (鵝不食草揮發油抗炎作用的初步實驗報告). *Guizhou Medical Journal (贵州医药)* 25: 909-910.

Qin R., Mei X., Wan L., Shi J., Shen Y. 2005a. Effects of the volatile oil of *Centipeda minima* on acute pleural effusion in rats induced by an intrapleural injection of Car. *China Journal of Chinese Materia Medica (中國中藥雜誌)* 30: 1192-1194.

Qin R., Mei X., Wan L., Shi J.L., Shen Y.J. 2005b. Effects of the volatile oil of sandwort on expression of CD54 in the bronchial epithelium tissue of acute lung injury rat. *China Journal of Traditional Chinese Medicine and Pharmacy (中華中醫藥雜誌)* 20: 466-468.

Raman M., Chen W., Cobb M.H. 2007. Differential regulation and properties of MAPKs. *Oncogene* 26: 3100-3112.

Reed J.C. 2002. Apoptosis-based therapies. *Nat. Rev. Drug Discov.* 1: 111-121.

Reed J.C. 2003. Apoptosis-targeted therapies for cancer. *Cancer Cell* 3: 17-22.

Riedl S.J. and Shi Y. 2004. Molecular mechanisms of caspase regulation during apoptosis. *Nat. Rev. Mol. Cell Biol.* 5: 897-907.

Rozenblat S., Grossman S., Bergman M., Gottlieb H., Cohen Y., Dovrat S. 2008. Induction of G2/M arrest and apoptosis by sesquiterpene lactones in human melanoma cell lines. *Biochem. Pharmacol.* 75: 369-382.

Ruddon R.W. 2007. *Cancer biology*. Oxford University Press, Oxford, London, p. 7.

Satyajit D.S., Zahid L., Alexander I.G. 2006. *Natural products isolation*. Humana

Press, Totowa, New Jersey, p. 88-89.

Salvesen G.S. and Riedl S.J. 2008. *Caspase mechanism*. In: Khosravi-Far R. and White E. (Eds.), *Programmed cell death in cancer progression and therapy*, Springer Netherlands, pp. 13-23.

Schwartsmann G., Ratain M.J., Cragg G.M., Wong J.E., Saijo N., Parkinson D.R., Fujiwara Y., Pazdur R., Newman D.J., Dagher R., Di L.L. 2002. Anticancer drug discovery and development throughout the world. *J. Clin. Oncol.* 20: 47s-59s.

Sham J.S., Choy D., Choi P.H. 1990. Nasopharyngeal carcinoma: the significance of neck node involvement in relation to the pattern of distant failure. *Br. J. Radiol.* 63: 108-113.

Shi W., Bastianutto C., Li A., Perez-Ordonez B., Ng R., Chow K.Y., Zhang W., Jurisica I., Lo K.W., Bayley A., Kim J., O'Sullivan B., Siu L., Chen E., Liu F.F. 2006. Multiple dysregulated pathways in nasopharyngeal carcinoma revealed by gene expression profiling. *Int. J. Cancer* 119: 2467-2475.

Shi Y. 2002. Mechanisms of caspase activation and inhibition during apoptosis. *Mol. Cell* 9: 459-470.

Shi Z. and Fu G.X. 1983. *Flora of China*. Science Publishing House: Beijing, China, p. 132-133.

Shoemaker M., Hamilton B., Dairkee S.H., Cohen I., Campbell M.J. 2005. *In vitro* anticancer activity of twelve Chinese medicinal herbs. *Phytother. Res.* 19: 649-651.

Son Y.O., Kook S.H., Choi K.C., Jang Y.S., Jeon Y.M., Kim J.G., Lee K.Y., Kim J., Chung M.S., Chung G.H., Lee J.C., 2006. Quercetin, a bioflavonoid, accelerates TNF-α induced growth inhibition and apoptosis in MC3T3-E1 osteoblastic cells. *Eur. J. Pharmacol.* 529: 24-32.

Song Y.J., Lee D.Y., Kim S.N., Lee K.R., Lee H.W., Han J.W., Kang D.W., Lee H.Y., Kim Y.K. 2005. Apoptotic potential of sesquiterpene lactone ergolide

through the inhibition of NF-κB signaling pathway. *J. Pharm. Pharmacol.* 57: 1591-1597.

Stashenko E.E., Puertas M.A., Combariza M.Y. 1996. Volatile secondary metabolites from *Spilanthes americana* obtained by simultaneous steam distillation-solvent extraction and supercritical fluid extraction. *J. Chromatogr. A* 752(1+2): 223-232.

Stashenko E.E., Jaramillo B.E., Martinez J.R. 2004. Comparison of different extraction methods for the analysis of volatile secondary metabolites of *Lippia alba* (Mill.) N.E. Brown, grown in Colombia, and evaluation of its *in vitro* antioxidant activity. *J Chromatogr A* 1025: 93-103.

Su M., Li Y., Chung H.Y., Ye W. 2009a. 2β-(Isobutyryloxy)florilenalin, a sesquiterpene lactone isolated from the medicinal plant *Centipeda minima*, induces apoptosis in human nasopharyngeal carcinoma CNE cells. *Molecules* 14: 2135-2146.

Su M., Wu X., Chung H.Y., Li Y., Ye W. 2009b. Antiproliferative activities of five Chinese medicinal herbs and active compounds in *Elephantopus scaber*. *Nat. Prod. Commun.* 4: 1025-1030.

Tan L., Zeng Z., Meng S.J., Shen M.T., Zhang H. 2006. Study on the volatile constituents and fingerprints of *Centipeda minima*. *Journal of Instrumental Analysis (分析測試學報)* 25: 91-94.

Tao L., Zhou L., Zheng L.Y., Yao M., 2006. Elemene displays anti-cancer ability on laryngeal cancer cells *in vitro* and *in vivo*. *Cancer Chemoth. Pharm.* 58: 24-34.

Taylor R.S. and Towers G.H. 1998. Antibacterial constituents of the Nepalese

medicinal herb, *Centipeda minima*. *Phytochemistry* 47: 631-634.

Tian Z., An N., Zhou B., Xiao P., Kohane I.S., Wu E. 2009. Cytotoxic diarylheptanoid induces cell cycle arrest and apoptosis via increasing ATF3 and stabilizing p53 in SH-SY5Y cells. *Cancer Chemother. Pharmacol.* 63: 1131-1139.

Tiwawech D., Srivatanakul P., Karalak A., Ishida T. 2006. Cytochrome P450 2A6 polymorphism in nasopharyngeal carcinoma. *Cancer Lett.* 241: 135-141.

van den Dool H. and Kratz P.D. 1963. A generalization of the retention index system including linear temperature programmed gas-liquid partition chromatography. *J. Chromatogr.* 11: 463-471.

Varmus H. 2006. The new era in cancer research. *Science* 312: 1162-1165.

Vermes I., Haanen C., Steffens-Nakken H., Reutelingsperger C. 1995. A novel assay for apoptosis flow cytometric detection of phosphatidylserine early apoptotic cells using fluorescein labeled expression on Annexin V. *J. Immunol. Methods* 184: 39-51.

Verweij J. and de Jonge M.J. 2000. Achievements and future of chemotherapy. *Eur. J. Cancer* 36: 1479-1487.

Wang S., Zheng Z., Weng Y., Yu Y., Zhang D., Fan W., Dai R., Hu Z. 2004. Angiogenesis and anti-angiogenesis activity of Chinese medicinal herbal extracts. *Life Sci.* 74: 2467-2478.

Wang S., Guan Z., Xiang Y. Wang B., Lin T., Jiang W., Zhang L., Zhang H., Hou J. 2006. Significance of EGFR and p-ERK expression in nasopharyngeal carcinoma. *Chinese Journal of Oncology (中華腫瘤雜志)* 28: 28-31.

Wang X. 2001. The expanding role of mitochondria in apoptosis. *Gene. Dev.*15: 2922-2933.

Wang X., Chow L.S.N., Nicholls J.M., Kwong D.L.W., Sham J.S.T., Wong Y.C., Tsao S.W. 2002. Significance of scheduling on the cytotoxicity of radiation and cisplatin combination treatment in nasopharyngeal carcinoma cells. *Anti-cancer drug.* 13: 957-964.

Wang Y., He Q.Y., Tsao S.W., Cheung Y.H., Wong A., Chiu J.F. 2008. Cytokeratin 8 silencing in human nasopharyngeal carcinoma cells leads to cisplatin sensitization. *Cancer Lett.* 265: 188-196.

Wen J., You K.R., Lee S.Y., Song C.H., Kim D.G. 2002. Oxidative stress-mediated apoptosis. The anticancer effect of the sesquiterpene lactone parthenolide. *J. Biol. Chem.* 277: 38954-38963.

Willuhn G., Rottger P.M., Matthiesen U. 1983. Helenalin and 11,13-dihydrohelenalinester from flowers of *Arnica montana*. *Planta Med.* 49: 226-231.

Wong W.W.L. and Puthalakath H. 2008. Bcl-2 family proteins: The sentinels of the mitochondrial apoptosis pathway. *IUBMB Life* 60: 390-397.

Wu J.B., Chun Y.T., Ebizuka Y., Sankawa U. 1985. Biologically active constituents of *Centipeda minima*: isolation of a new plenolin ester and the antiallergy activity of sesquiterpene lactones. *Chem. Pharm. Bull.* 33: 4091-4094.

Wu J.B., Chun Y.T., Ebizuka Y., Sankawa U. 1991. Biologically active constituents of *Centipeda minima*: Sesquiterpenes of potential anti-allergy activity. *Chem. Pharm. Bull.* 39: 3272-3275.

Xie S.M., Fang W.Y., Liu Z., Wang S. X., Li X., Liu T.F., Xie W.B., Yao K.T. 2008. Lentivirus-mediated RNAi silencing targeting ABCC2 increasing the sensitivity of a human nasopharyngeal carcinoma cell line against cisplatin. *J. Transl. Med.* *6*: 55.

Yang H.J., Cho Y.J., Kim H.S., Chang M.S., Sung M.W., Kim W.H. 2001. Association of p53 and BCL-2 expression with Epstein-Barr virus infection in the cancers of head and neck. *Head Neck-J. Sci. Spec.* 23: 629-636.

Yi X., Yin X., Dong Z. 2003. Inhibition of Bid-induced apoptosis by Bcl-2. tBid insertion, Bax translocation, and Bax/Bak oligomerization suppressed. *J. Biol. Chem.* 278: 16992-16999.

Yoon S. and Seger R. 2006. The extracellular signal-regulated kinase: Multiple substrates regulate diverse cellular functions. *Growth Factors* 24: 21-44.

Yu H., Wen S., Liu Z., Fang Y., Wang H. 2001. An experimental study on the therapeutic effects of herba centipede on allergic rhinitis. *Chinese Otorhinolaryngologyical Journal of Integrative Medicine (中國中西醫結合耳鼻咽喉科雜誌)* 9: 220.

Yu H.W., Wright C.W., Cai Y., Yang S.L., Phillipson J.D., Kirby G.C., Warhurst D.C. 1994. Antiprotozoal activities of *Centipeda minima*. *Phytother. Res.* 8: 436-438.

Yu M.C. and Yuan J.M. 2002. Epidemiology of nasopharyngeal carcinoma. *Semin. Cancer Biol.* 12: 421-429.

Zhang L.X. and Demain A.L. 2005. *Natural products: drug discovery and therapeutic medicine*. In: Wang G., Tang W., Bidigare R.R. (Eds.), *Terpenoids as therapeutic drugs and pharmaceutical agents*. Humana Press, Totowa, New Jersey, pp. 198.

Zhang S., Won Y.K., Ong C.N., Shen H.M. 2005. Anti-cancer potential of sesquiterpene lactones: bioactivity and molecular mechanisms. *Curr. Med. Chem. - Anti-Cancer Agents* 5: 239-249.

Zhang Y.H. 2000. *A collection of anticancer Chinese medicines*. Jiangsu Science Technology Press, Nanjing, China, p. 17, 44, 184, and 435.

# Appendix 1: Spectra of 2β-(isobutyryloxy)florilenalin (IF)

**Appendix 1.1**. $^{1}$H-NMR of 2β-(isobutyryloxy)florilenalin (IF)

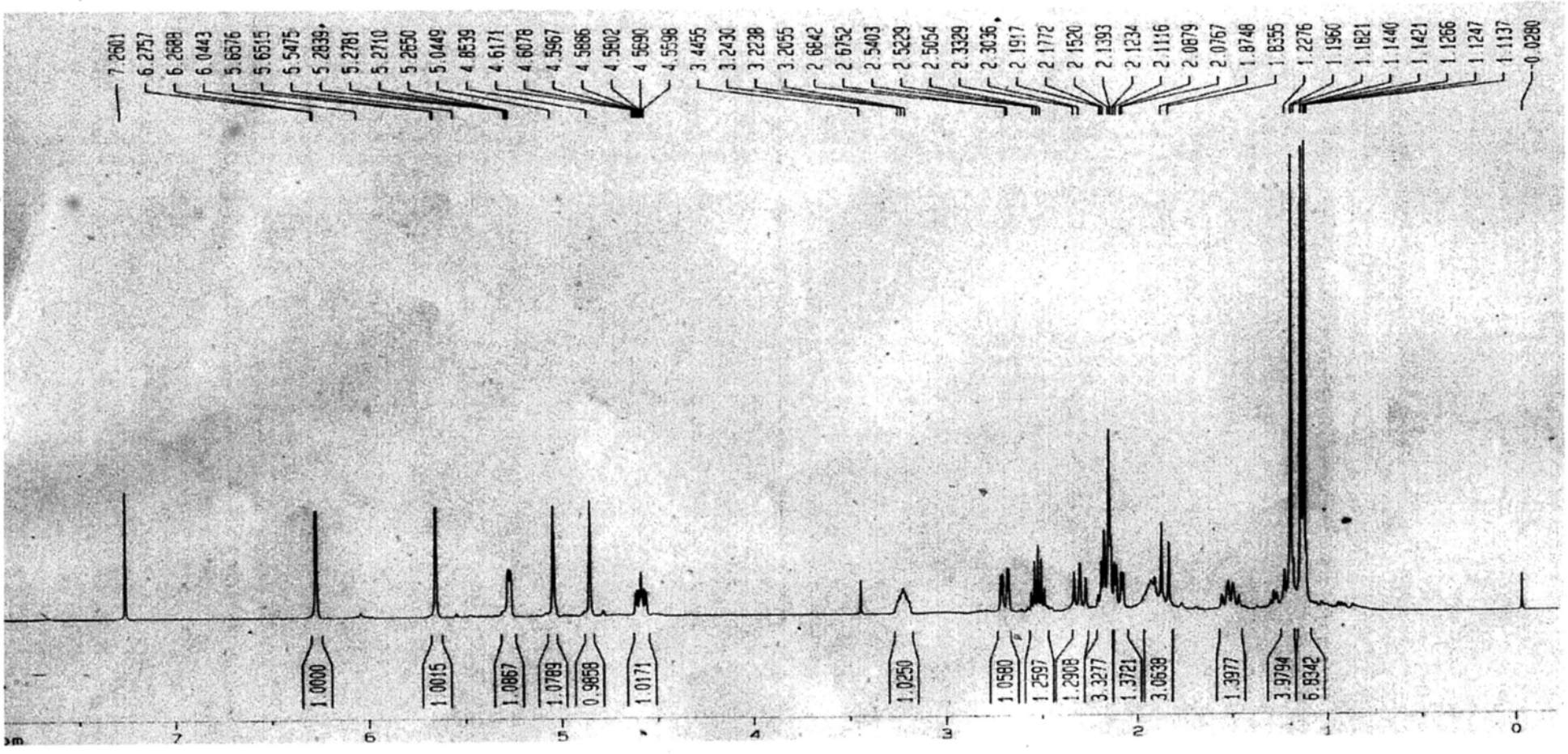

**Appendix 1.2.** $^{13}$C-NMR of 2β-(isobutyryloxy)florilenalin (IF)

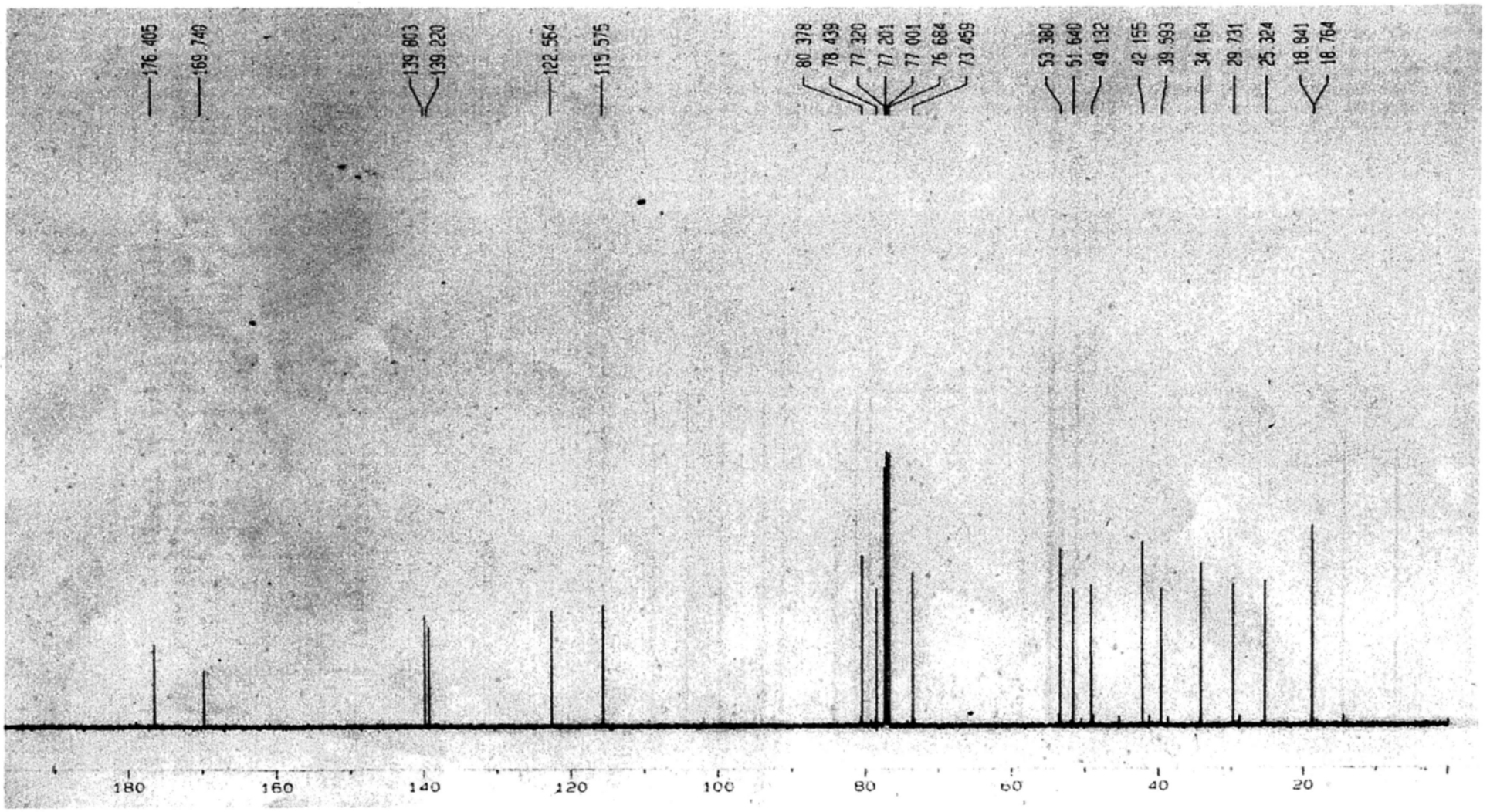

**Appendix 1.3.** DEPT 135 of 2β-(isobutyryloxy)florilenalin (IF)

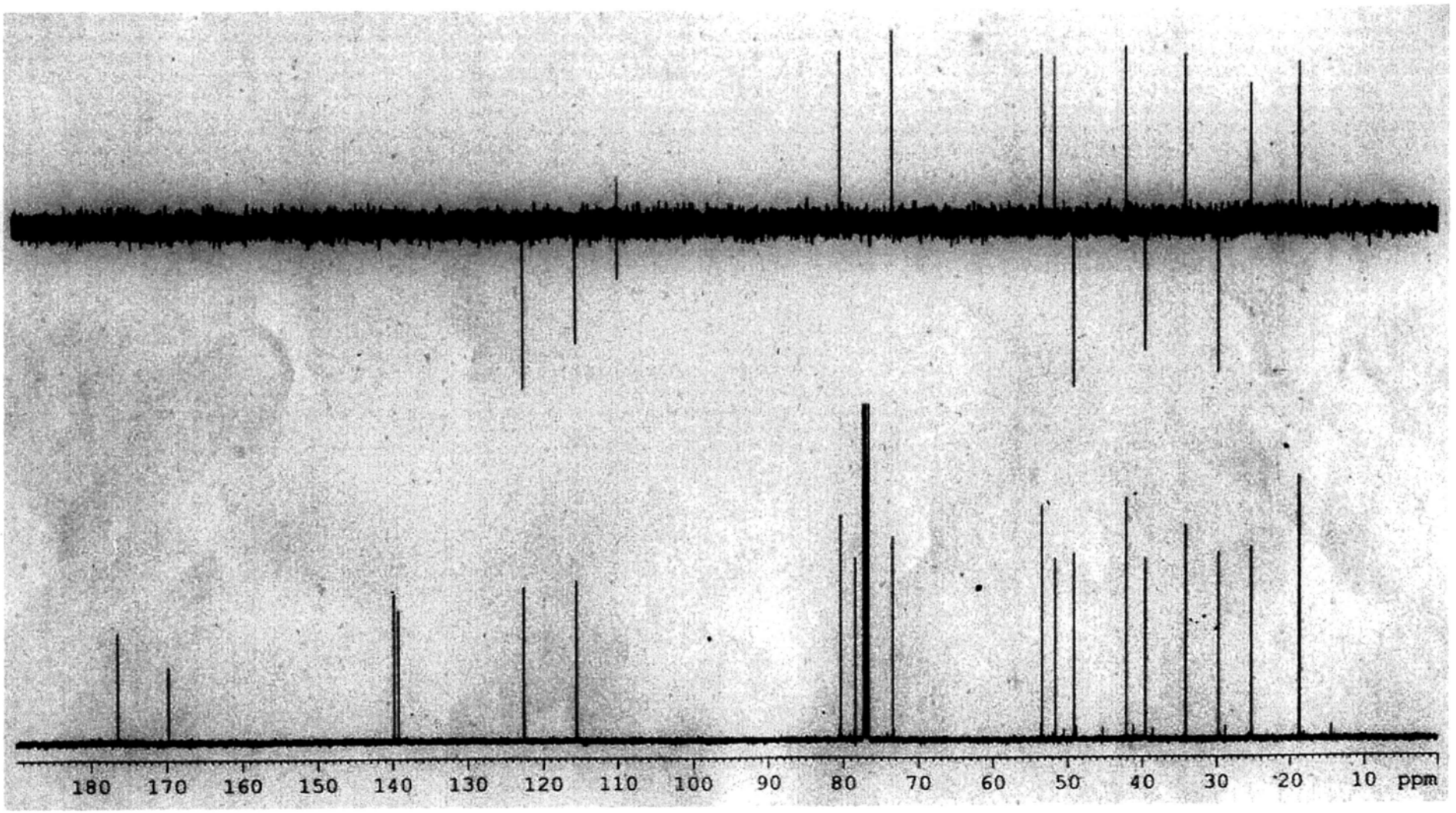

**Appendix 1.4.** EI-MS of 2β-(isobutyryloxy)florilenalin (IF)

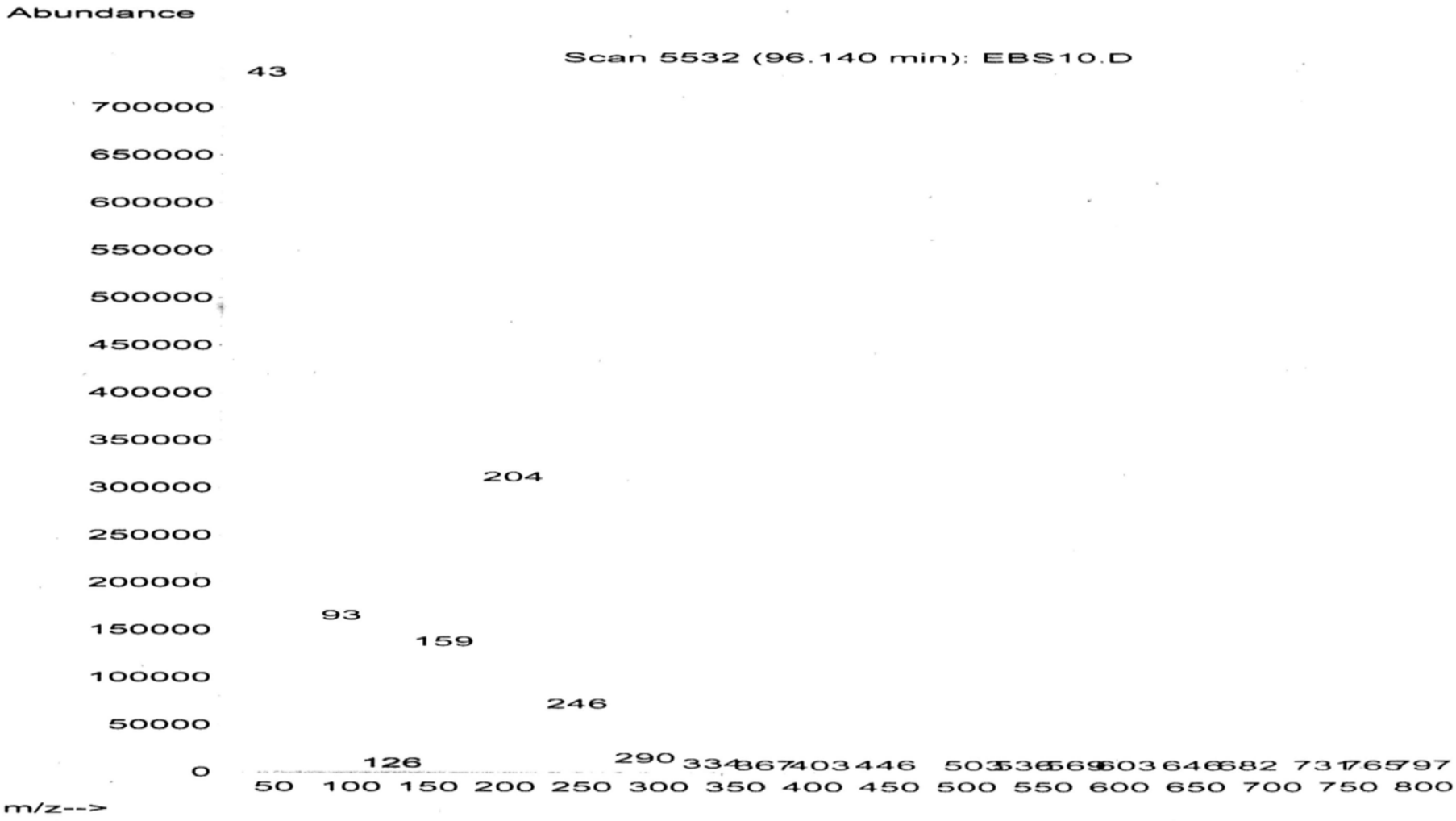

## Appendix 2: Publications

1. **Su Miaoxian**, Wu Xia, Chung Hau Yin, Li Yaolan, Ye Wencai. Antiproliferative activities of five Chinese medicinal herbs and active compounds in *Elephantopus scaber*. *Natural Product Communications* **2009**, *4*, 1025-1030.
2. **Su Miaoxian**, Li Yaolan, Chung Hau Yin, Ye Wencai. 2β-(Isobutyryloxy)florilenalin, a sesquiterpene lactone isolated from the medicinal plant *Centipeda minima*, induces apoptosis in human nasopharyngeal carcinoma CNE cells. *Molecules* **2009**, *14*, 2135-2146.
3. **Su Miaoxian** and Chung Hau Yin. **2008**. Antiproliferation activity in the spice of *Kaempferia galanga* L. The Institute of Food Technologists (IFT) 2008 Annual Meeting & Food Expo$^{SM}$.